NNT : 2015SACLE024

THESE DE DOCTORAT
DE L'UNIVERSITE PARIS-SACLAY,
préparée à L'Université d'Evry-Val-d'Essonne

ÉCOLE DOCTORALE N° ED 580

ÉCOLE DOCTORALE
Sciences et technologies de l'information et de la communication (STIC)

Spécialité Automatique

Par

Sagar AKHEGAONKAR

Development of a Safe and Efficient Driving Assistance System for Electric Vehicles

Thèse présentée et soutenue à Evry, le 27 Novembre 2015 :

Composition du Jury :

Pr. M'SIRDI Nacer	Professeur de l'Université de Marseille, LSIS	Rapporteur
Dr SCIARRETTA Antonio	HDR, Expert de l'IFPEN	Rapporteur
Mr VINCENT Patrick	Expert de RENAULT	Examinateur
Pr. MOUNIER Hugues	Professeur de l'Université d'Orsay, LSS	Examinateur
Dr. HOLZMANN Frédéric	Directeur technique, INTEDIS (Allemagne)	Co-Directeur de thèse
Dr-Ing. GLASER Sébastien	Dr-Ing. TPE, IFSTTAR-VEDECOM	Directeur de thèse
Dr. NOUVELIERE Lydie	MCF de l'Université d'Evry, IBISC	Encadrante de thèse



université PARIS-SACLAY
ÉCOLE DOCTORALE
Sciences et technologies de l'information et de la communication (STIC)

Titre : Développement d'un Système d'Assistance à la Conduite Sûr et Efficient pour le Véhicule Electrique

Mots clés : ADAS, éco-conduite, ECMS, Modélisation & Simulation, ACC, véhicule électrique/hybride,

Résumé : Les progrès dans les domaines des véhicules autonomes, l'hybridation du groupe motopropulseur et les systèmes de transport intelligents (STI) signifient que l'automobile en tant que machine est sur le point d'être réinventée. Les trois domaines technologiques sus-cités ont ouvert des portes sur des avancées possibles au niveau de l'amélioration de la sécurité routière et de l'efficacité énergétique des véhicules qui étaient auparavant limitées en raison de plusieurs facteurs, comme les capacités de détection et de puissance de calcul. Dans ce contexte, un contrôleur de la dynamique longitudinale du véhicule électrique est mis au point et étudié de façon à réaliser un compromis entre sécurité et efficacité du véhicule. Ce système est appelé Smart And Green Adaptive Cruise Control (SAGA). Le dé-veloppement de cette fonction est basée sur l'optimisation de l'énergie ainsi que sur des stratégies de régénération d'énergie en respectant les contraintes des composants du groupe motopropulseur comme la charge de la batterie, la capacité de freinage du moteur et de la situation courante dans le trafic routier. Dans ce processus, des techniques d'optimisation comme la programmation dynamique et la stratégie de minimisation de la consommation d'énergie équivalente (ECMS) sont utilisés. Utilisant de smodèles d'énergie du véhicule et des modèles cinématiques intégrés sur Matlab-Simulink, ce travail de thèse évalue les avantages et les limites de l'utilisation de la fonction SAGA pour diverses topologies de véhicules pour différents scénarios de trafic.

Université Paris-Saclay
Espace Technologique / Immeuble Discovery
Route de l'Orme aux Merisiers RD 128 / 91190 Saint-Aubin, France

université PARIS-SACLAY | ÉCOLE DOCTORALE Sciences et technologies de l'information et de la communication (STIC)

Title : Development of a Safe and Efficient Driving Assistance System for Electric Vehicles

Keywords : ADAS, eco-driving, ECMS, Modelling & Simulation, ACC, electric/hybrid vehicle

Abstract : The progress in the fields of autonomously driven vehicles, powertrain hybridization and Intelligent transportation systems (ITS) means that the automobile as a machine, is on the verge of reinvention. The aforementioned three fields of technologies have opened doors to advanced opportunities in improvement of safety and efficiency of vehicles which were earlier limited due to several factors like sensing capacities and computational power.

In this context, a vehicle longitudinal motion controller is developed and investigated which will actively balance vehicle safety and efficiency. It is named as the Smart and Green Adaptive Cruise Control System (SAGA). Development of this function is based on optimization of energy supply as well as energy regeneration strategies with respect to po--wertrain component constraints like battery charge acceptance, motor braking capacity and traffic situation. In this process, optimization techniques like Dynamic programming and Equivalent Consumption Minimization Strategy (ECMS) are used.

Using vehicle energy and kinematic models built in Matlab-Simulink platform, this dissertation evaluates the advantages and limitations of using SAGA function for various vehicles topologies and in different traffic scenarios.

Université Paris-Saclay
Espace Technologique / Immeuble Discovery
Route de l'Orme aux Merisiers RD 128 / 91190 Saint-Aubin, France

Declaration of Authorship

I, Sagar Akhegaonkar, declare that this thesis titled, "Development of a Safe and Efficient Driving Assistance System for Electric Vehicles" and the work presented in it are my own. I confirm that:

- This work was done wholly or mainly while in candidature for a research degree at this University.
- Where any part of this thesis has previously been submitted for a degree or any other qualification at this University or any other institution, this has been clearly stated.
- Where I have consulted the published work of others, this is always clearly attributed.
- Where I have quoted from the work of others, the source is always given. With the exception of such quotations, this thesis is entirely my own work.
- I have acknowledged all main sources of help.
- Where the thesis is based on work done by myself jointly with others, I have made clear exactly what was done by others and what I have contributed myself.

Signed: _____

Date: _____

"As the saying goes, the Stone Age did not end because we ran out of stones, we transitioned to better solutions. The same opportunity lies before us with energy efficiency and clean energy."

Steven Chu

Acknowledgements

To say that this experience during the last four years has drastically changed my approach towards life would be an understatement. It has taught me to be safe and efficient at the same time, it has taught me to organize matters and optimize processes so that I can achieve a maximum result through minimal effort. Moreover, to secure a deep understanding of past, present and future of global energy/mobility economy is a sort of enlightenment in itself. And for that, I have many people to thank.

First and foremost my professors Dr. Lydie Nouvelière and Dr. Sébastien Glaser. To Lydie I owe my greatest gratitude and appreciation for being an honest critic and at the same time providing encouragement for finding new research horizons. Without her help in academic and administrative fields, this work would have been an impossible task. To Sébastien I thank for his invaluable guidance and visionary ideas which helped form the base of my thesis. It is no easy task to imagine the future of Future! (future of autonomous vehicles).

I wish to express my gratitude to Intedis GmbH & Co. KG for sponsoring my Ph.D work and Dr. Frederic Holzmann for providing me with an opportunity to work at Intedis as a Ph.D student. I wish to extend my appreciation to EU FP7 Programme for funding the eFuture project which allowed me to experience the European ways of doing research. Furthermore, those people of academic and scientific fraternity deserve a special mention who have selflessly made their work publicly available so that people like me could learn from their experiences.

I remain forever indebted to my parents and my sister, it is in them I find my motivation to make this world a better place for everyone. Last but not the least, behind every successful Ph.D man, there is a Ph.D woman. Thank you Dr. Upasana Kulkarni, you truly redefine the challenge called Life.

Contents

Declaration of Authorship i

Abstract iii

Acknowledgements iv

Contents v

List of Figures viii

List of Tables xi

Abbreviations xii

1 Introduction 1
- 1.1 Motivation . . . 1
  - 1.1.1 Safe and efficient mobility . . . 3
  - 1.1.2 Energy consumption . . . 4
  - 1.1.3 Environmental Pollution . . . 5
  - 1.1.4 Driver Comfort . . . 6
  - 1.1.5 Energy efficiency and component life . . . 7
  - 1.1.6 eFuture Project . . . 7
- 1.2 Aim, scope and contribution . . . 8

2 Literature Review 11
- 2.1 Autonomous driving . . . 11
  - 2.1.1 Basic concept . . . 11
  - 2.1.2 Level of Automation . . . 13
  - 2.1.3 Vehicle control . . . 15
    - 2.1.3.1 Lateral mode . . . 15
    - 2.1.3.2 Longitudinal mode . . . 15
  - 2.1.4 Control Architecture . . . 16
    - 2.1.4.1 Sensors . . . 16
    - 2.1.4.2 Data Fusion & Processing . . . 18
    - 2.1.4.3 State of the art (Autonomous vehicles) . . . 19

2.2 Basic powertrain classification . . . 21
2.2.1 Conventional BEV, HEV, PHEV . . . 21
2.3 Energy management strategies . . . 24
2.3.1 Rule based . . . 26
2.3.2 Optimization based strategies . . . 28
2.4 Mobility energy analysis . . . 32
2.4.1 Vehicle energy requirement . . . 32
2.4.2 Energy saving potential analysis . . . 36

3 Simulation Models and Methodology 41
3.1 Component Models . . . 41
3.1.1 IC Engine . . . 41
3.1.2 eMotor . . . 42
3.1.3 Battery (Energy Storage System) . . . 44
3.1.4 Inverter . . . 45
3.1.5 DC/DC converter . . . 45
3.1.6 Power-split device . . . 46
3.1.7 Velocity cycles . . . 46
3.2 Vehicle models . . . 47
3.2.1 Battery electric vehicle . . . 47
3.2.2 Conventional vehicle . . . 49
3.2.3 Hybrid electric (charge sustaining TtR) . . . 50
3.2.4 Plug-in Hybrid electric (charge depleting TtR) . . . 53

4 The Smart and Green ACC function 54
4.1 Introduction . . . 54
4.1.1 Basic concept . . . 56
4.1.2 Constraints of the regeneration system . . . 59
4.1.3 Concept of Safety envelope . . . 63
4.1.4 ISO guidelines . . . 65
4.2 Problem definition . . . 68
4.2.1 Safe headway spacing . . . 68
4.2.2 Minimization of energy consumption . . . 68
4.2.3 Passenger comfort . . . 69
4.3 Possible solutions for the deceleration phases . . . 69
4.3.1 Exclusive motor braking . . . 70
4.3.2 Threshold braking strategy . . . 73
4.3.3 Optimized blended braking . . . 74
4.4 SAGA as an FSRA . . . 75

5 SAGA as an autonomous controller for BEV 78
5.1 BEV component behaviour and energy optimization . . . 78
5.2 Motor operation domains and energy analysis . . . 79
5.3 Dynamic Programming based Acceleration controller for city domain . . . 82
5.3.1 DP problem formulation . . . 84
5.3.2 Deceleration strategy for City domain . . . 87
5.3.3 Results: City domain . . . 90

5.3.4 Modified strategies for City domain . . . 92
5.3.5 Slope and Climate control . . . 97
5.4 SAGA function for BEV: Highway domain . . . 99
5.4.1 SAGA function simulation model . . . 100
5.4.2 SAGA highway domain: Simulation results . . . 101
5.4.3 Energy analysis for typical braking maneuvers . . . 108
5.4.4 Field trial in the eFuture prototype . . . 112
5.4.5 Battery charge acceptance analysis . . . 113

6 SAGA as an autonomous controller for HEV/PHEV 115
6.1 Bi-layer control concept (ECMS+SAGA) . . . 115
6.2 Equivalent Consumption Minimization Strategy (ECMS) . . . 117
6.2.1 ECMS definition through Pontryagin's Minimum Principle . . . 117
6.2.2 ECMS concept definition . . . 120
6.2.3 A-ECMS . . . 125
6.2.4 Simulation Model and Algorithm . . . 127
6.2.5 Engine Starting Penalty . . . 129
6.3 ECMS simulation results for HEV and PHEV . . . 130
6.3.1 Tuning the A-ECMS . . . 131
6.3.2 Results: HEV (charge sustaining) . . . 131
6.3.3 Results: PHEV (Blended operation) . . . 133
6.3.4 Real world cycle evaluation . . . 135

7 Conclusion 138
7.1 Conclusion and summary . . . 138
7.2 Future work possibilities . . . 141
7.3 An architecture for co-operative lateral and longitudinal control of Autonomous vehicles . . . 143

A BEV Powertrain Modelling and Validation 146

Bibliography 154

List of Figures

1.1 State of art ADAS and PMS mode of co-operation . . . 1
1.2 Eco-driving through ADAS, EMS and ITS co-operation . . . 2
1.3 Peak oil curve (Projection for end of oil) . . . 5
1.4 Attribution of GHG emissions . . . 6
1.5 Overview of the eFuture Project . . . 8

2.1 Autonomous driving systems classification based on Level of Automation 14
2.2 A road map for autonomous vehicle development . . . 14
2.3 Sensors for an autonomous driving system . . . 16
2.4 Autonomous driving system architecture . . . 19
2.5 Hybrid vehicle topologies (L:Series, C:Power-split, R:Parallel) . . . 23
2.6 HEV powertrain control/Energy management strategies . . . 26
2.7 Air flow over vehicle body as observed in a wind tunnel . . . 33
2.8 Tyre rolling resistance phenomenon . . . 34
2.9 Gradient force acting on a vehicle . . . 35
2.10 Effect of acceleration (Energy for a 100 m sprint) . . . 36
2.11 Comparison of energy components for city and highway cycles . . . 37
2.12 Comparison of HEV and PHEV as energy savers . . . 39

3.1 Base efficiency engine map for a Saturn 1.9 liter engine in g/kWh . . . 42
3.2 Motor torque-speed-efficiency characteristics . . . 43
3.3 Battery efficiency characteristics over a cycle . . . 45
3.4 Data for inverter efficiency . . . 46
3.5 Worldwide harmonized Light vehicles Test Procedure . . . 47
3.6 Cycle defined with velocity limits . . . 48
3.7 Forward (model 2) and backward (model 1) looking modeling approaches 49
3.8 Schematic model of a conventional vehicle . . . 49
3.9 Intelligent gear selection algorithm . . . 51
3.10 Through the road (TtR) hybrid electric vehicle (7 kWh battery for Charge sustaining) . . . 52

4.1 SAGA: Modes of operation . . . 57
4.2 SAGA: Generic use case . . . 57
4.3 Phases in distance control mode . . . 59
4.4 Maximum deceleration offered by motor (eFuture) . . . 60
4.5 Regenerative charge acceptance characteristics of a NMC battery . . . 62
4.6 A123 cell characteristics for pulse charge acceptance (V_{cell} = 3.8 - 1.6) . . 62
4.7 Comparison of conventional ACC and regenerative braking safety domains 63

4.8 Variation of the safe domain with a deceleration of the lead vehicle 64
4.9 Deceleration limits for LSF system 66
4.10 Jerk limits for LSF system 67
4.11 Reference for deceleration rates 71
4.12 Reference for deceleration rates 71
4.13 Reference for vehicle decelerations at intersections 72
4.14 SAGA as an FSRA 76
4.15 Overall concept application for SAGA function 77

5.1 City and highway domains on a motor map 80
5.2 Some of the possible different velocity trajectories in acceleration phase . 83
5.3 Formulation of a DP algorithm 85
5.4 Calculation of normalized values for E_k as the set of the states e_k^j at the step k, along with its corresponding cost functions $\zeta_k^{i,j}$ starting from the step *k-1* 86
5.5 Optimization results for the acceleration phase using $Q_1 = 1$ and $Q_2 = 1$ 88
5.6 Deceleration maneuver (Entering a low speed zone) 89
5.7 Optimum braking distance estimation 90
5.8 Aggressive driver model 90
5.9 Comparison of optimum velocity trajectory against aggressive driver model with respect to distance 91
5.10 Comparison of optimum velocity trajectory against aggressive driver model with respect to time 92
5.11 Cost function results $(Q_1 = 1, Q_2 = 1)$ 95
5.12 Optimum braking distance 95
5.13 Comparison of new city domain optimization algorithm with the BEV driver model 96
5.14 Tuning the city domain controller for individual preferences 98
5.15 Effect of Climate control on optimization results 99
5.16 SAGA simulation model 100
5.17 Comparison of Green ACC function to conventional ACC 102
5.18 Deceleration maneuver with only motor braking application 103
5.19 SAGA deceleration 130- 50 kph, threshold braking, emergency mode below 1.5 s (Set-up: V_{driver}: 130 kph, T_{driver}: 2s, V_{init}: 100 kph, V_i: 50 kph) 104
5.20 SAGA deceleration 130-80/60 kph, Blended braking control with safety indicator activation at 0.22 106
5.21 SAGA deceleration 130-0 kph, Blended braking control, for various sensing distance in case of a traffic jam 107
5.22 Suddenly decelerating front vehicle maneuver 109
5.23 Energy analysis for braking maneuver 140 - 80 kph 110
5.24 Energy analysis for braking maneuver 140 - 100 kph 111
5.25 eFuture prototype for SAGA function test 112
5.26 eFuture prototype field tests for SAGA function 113
5.27 Current loading on the battery during regenerative braking maneuvers . . 114

6.1 SAGA as applied to a BEV and a HEV/PHEV 116
6.2 SAGA as a supervisor for a bi-layered HEV/PHEV control 117

6.3 Charge and discharge process in a HEV . . . 121
6.4 Approximation of an equivalence factor using energy sweep over the power-split range for a specific cycle . . . 124
6.5 SOC trajectory setups for charge sustaining HEV operation and PHEV blended mode operation . . . 126
6.6 ECMS simulation model . . . 128
6.7 Engine operation points for conventional vehicle over WLTP-class3 cycle (efficiency map in g/kWh) . . . 131
6.8 WLTP class3 cycle engine operating points, conventional ICE (left), TtR ECMS (right) . . . 133
6.9 ECMS controller behavior (charge sustaining HEV, WLTP 116 km, 7 kWh battery) . . . 134
6.10 ECMS controller behavior (blended Plug-in HEV, WLTP 116 km, 13 kWh battery) . . . 135
6.11 ECMS controller behavior on a real world recorded velocity session (A_M) 136

7.1 A generic architecture for a hybrid autonomous vehicle using SAGA function 144

A.1 Vehicle model subsystem (level 2) . . . 147
A.2 BEV energy consumption model (level 1) . . . 148
A.3 Temperature-Power-time characteristics for cooling and heating . . . 150
A.4 BEV model validation results . . . 152
A.5 BEV energy calculation simulation . . . 152

List of Tables

2.1 Cost of ownership comparison between BEV and conventional vehicle at 130,000 km 22

3.1 eFuture prototype parameters 48

4.1 Terminology SAGA generic case 57

5.1 Energy recovery potential for various maneuvers 111

6.1 Tuning the A-ECMS with manual iterations 132
6.2 Fuel consumption comparison for various powertrain configurations 137

A.1 Terminology 149

Abbreviations

ACC	**A**daptive **C**ruise **C**ontrol
AER	**A**ll **E**lectric **R**ange
AECMS	**A**daptive **E**quivalent **C**onsumption **M**inimization **S**trategy
ADAS	**A**dvanced **D**river **A**ssistance **S**ystems
ADV	**A**utonomously **D**riven **V**ehicles
BEV	**B**attery **E**lectric **V**ehicles
CDCS	**C**harge **S**ustaining **C**harge **D**epleting
CACC	**C**o-operative **A**daptive **C**ruise **C**ontrol
CS	**C**harge **S**ustaining
DSRC	**D**edicated **S**hort **R**ange **C**ommunication
DP	**D**ynamic **P**rogramming
EDAS	**E**co **D**river **A**ssistance **S**ystems
ECMS	**E**quivalent **C**onsumption **M**inimization **S**trategy
EM	**E**lectric **M**otor
EMS	**E**nergy **M**anagement **S**ystem
ESS	**E**nergy **S**torage **S**ystem
FSRA	**F**ull **S**peed **R**ange **ACC**
GACC	**G**reen **A**daptive **C**ruise **C**ontrol
HEV	**H**ybrid **E**lectric **V**ehicle
IC	**I**nternal **C**ombustion
ICT	**I**nformation **C**ommunication **T**echnology
ITS	**I**ntelligent **T**ransportation **S**ystems
KE	**K**inetic **E**nergy
LSF	**L**ow **S**peed **F**ollowing
LIDAR	**LI**ght **D**etection **A**nd **R**anging

NO	**N**itrogen **O**xide
NMC	**N**ickel **M**anganese **C**obalt
NEDC	**N**ew **E**uropean **D**riving **C**ycle
PMP	**P**ontryagin's **M**inimum **P**rinciple
PHEV	**P**lug-in **H**ybrid **E**lectric **V**ehicle
RADAR	**RA**dio **D**etection **A**nd **R**anging
RB	**R**ule **B**ased
SAGA	**S**mart **A**nd **G**reen **ACC**
SOC	**S**tate **O**f **C**harge
SI	**S**afety **I**ndicator
TtR	**T**hrough **t**he **R**oad
V2V	**V**ehicle **to V**ehicle
V2I	**V**ehicle **to I**nfrastucture
WLTP	**W**orldwide harmonized **L**ight vehicle **T**est **P**rocedures

For a clean and sustainable Earth for generations to come

Chapter 1

Introduction

1.1 Motivation

Minimum energy expense and maximum safety with comfort characterizes the definition of ideal human mobility. Advanced driver assistance systems (ADAS) have been traditionally associated with driver/passenger comfort and safety enhancement. On the other hand, the energy efficiency part, which is significant with respect to CO_2 emissions and carbon footprint of mobility has been largely addressed through powertrain or energy management systems (PMS or EMS) and not through ADAS. Hence, as shown

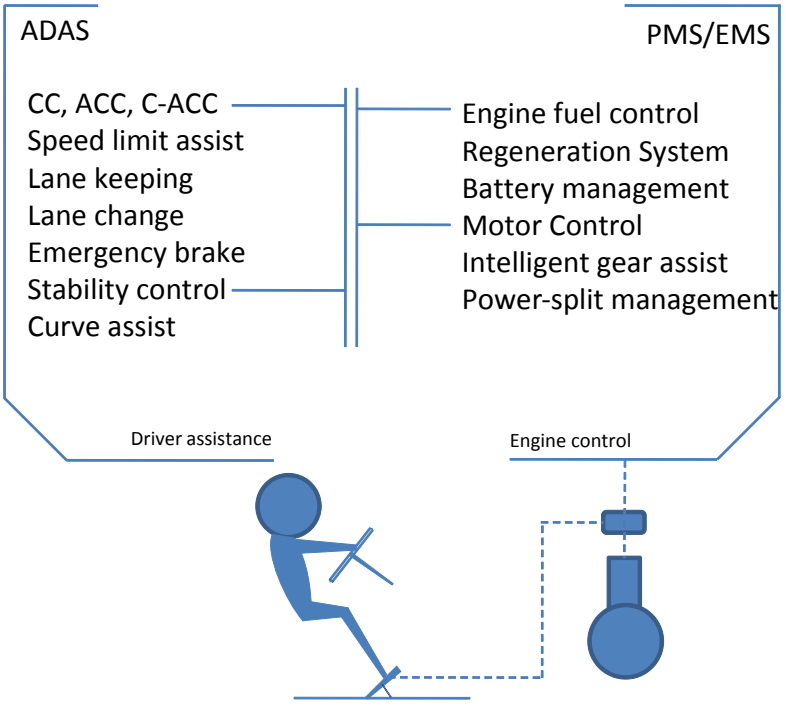


FIGURE 1.1: State of art ADAS and PMS mode of co-operation

in Figure 1.1, in the past, a clear distinction has emerged in the development of these two systems, namely, ADAS and EMS where it can be stated that the co-operation or communication between these systems has been present only on a platonic level (e.g. ACC) or in most cases, not at all (e.g. Lane keeping).

As of today, the "Automobile"as a machine is on the verge of reinventing itself and its conversion into a fully automated mobile-robot may happen sooner than projected. The advent of autonomously driving vehicles (ADVs) is evident through the functional prototypes demonstrated in [LA+11] and [BM+12]. In an ADV, the architecture has to support simultaneous lateral and longitudinal autonomous control. Hence, it may be stated that the active safety systems (integrated into motion control) must co-operate with the powertrain control systems. In fact, the concept of ADV, where the driver himself is replaced renders the original definition of driving assistance obsolete. Therefore, a completely new and expanded architecture emerges where the advanced driving assistance systems fully co-operate with the powertrain management systems to generate a safe motion control vector for the vehicle as shown in Figure 1.2.

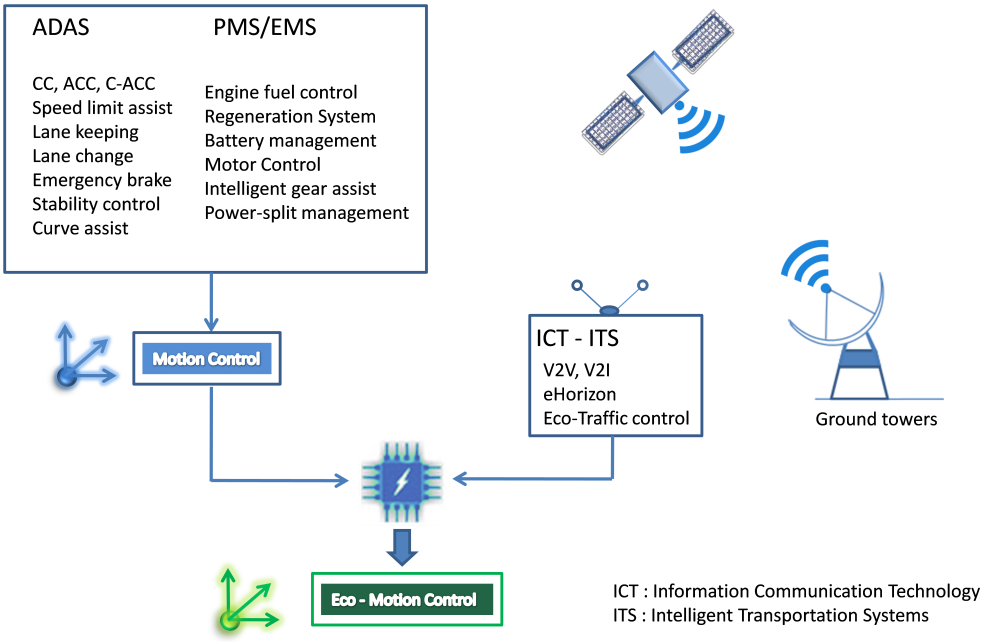


FIGURE 1.2: Eco-driving through ADAS, EMS and ITS co-operation

In parallel, there has been a high level penetration of the Information and communication technologies in the automotive field. This has led to development of automotive specific data exchange platforms like vehicle to vehicle (V2V) and vehicle to infrastructure (V2I). Furthermore, it enables electronic mapping and navigational guidance through

the eHorizon[1] and Traffic control algorithms. This has resulted into advancement of a new approach towards transportation management coined as intelligent transportation systems (ITS). ITS facilitates the supply of relevant information to the vehicle motion control system so that intelligent decisions regarding safety and efficiency can be computed and implemented in real time. From the scenario described above, it is clear that the ADAS of the future presents higher capabilities and more advanced characteristics than those implemented today. Hence it is important to revisit the defining properties of ADAS in order to establish the new capabilities, requirements and limitations for the ADAS of future.

1.1.1 Safe and efficient mobility

The new generation of ADAS is not only expected to improve safety but also overall efficiency. While driver and pedestrian safety form an important part of human mobility, it is also imperative to balance it with environmental safety. Thus, the newly coined term "Eco-driving" comes into existence. Hence, ADAS which have a capability of Eco-driving are classified as eco driving assistance systems (EDAS). Research projects like eCoMove [ecob] and EcoDriver [ecoa] have focused their efforts on coaching the driver to drive as efficiently as possible. However, for many individuals, driving style closely resembles their personality and constant advice on driving style may often become irritating. The modern car is being loaded with so much technology that, information, more than a human brain can process at a time, is being presented to it every instant through the human machine interface. This might, on the contrary lead to reduced safety. In order to balance safety and efficiency a more logical solution may be to eliminate the driver from the equation and load him with an easy supervisory task while the autonomous car controls itself laterally and longitudinally.

Theoretically, autonomous driving presents several advantages over human driving. For example, the control hardware will never experience fatigue or will not be distracted from the given tasks. However, the safety aspect is not the most significant improvement that autonomous driving offers. Embedded processors are better suited for processing the relevant information related to future driving conditions and compute intelligent decisions quickly without compromising on the given driving task. This is something which is not possible for a human driver given the complexity of data and multitasking requirements demanded from the driver, while he is already occupied with basic driving task. Moreover, there are certain Eco-driving maneuvers like intelligent traffic signal to vehicle communication, efficient velocity trajectory following, efficient acceleration control,

[1] eHorizon is a system which combines data from sensors with on-board digital maps to provide information about short term future road conditions like speed limits and road geometry even before they appear on the visual horizon.

intelligent intersection management etc. that are better managed by the autonomous controller than by human intervention.

Although most research related to the EDAS till date has been concentrated in area of conventional internal combustion (IC) engine vehicles, the development of hybrid and electric vehicles has added another dimension to the capabilities of EDAS functions. With an efficiency range of about 5 – 35% (as approximated from the engine efficiency map 3.1), the IC engine seems to be the main culprit regarding poor efficiency of vehicles. Hybridization allows for part of the power requirement to be supplied from electric source which is clean and distinctly efficient as compared to IC engine. Therefore, in any development of new generation EDAS functions, it becomes necessary to integrate the hybrid powertrain controller or energy management systems together with motion control systems. Moreover, the tradition of designing the EDAS as a separate system needs to be modified. In order to ensure that the EDAS uses relevant components of the powertrain efficiently, EDAS and these components have to be tailored with respect to each other's requirements. An example of this would be designing the battery and the battery management system (BMS) such that the current acceptance characteristics of the battery packs suits the "efficient and exclusive (only/fully) motor braking characteristics" of the regenerative braking system in order to recuperate maximum energy. Furthermore, the EDAS should take into consideration the limitations of battery pack, so as not to damage the internal chemistry and result in a premature replacement of the pack.

1.1.2 Energy consumption

In the modern world, energy resources of a nation have become the direct measure of its population lifestyle. This was evident in the 18th century when the discovery and industrialization of oil production transformed every aspect of civilized life, especially transportation. Entering the 21st century, oil forms the base of socio-economic-political structure of every nation and hence is, financially, the single most important natural resource. However there are already talks of peak oil in the market which means that oil production in most oil wells has reached its peak point and hence forth await decline in oil supply. The truth in this theory is quite controversial considering that creating an artificial low in supply increases the demand and hence the oil rate. It was in 1956 that geoscientist M. Hubbert presented the philosophy of bell shaped oil discovery and production curve as in Figure 1.3 and predicted that the U.S. oil peak will occur in 1971 [Def08].

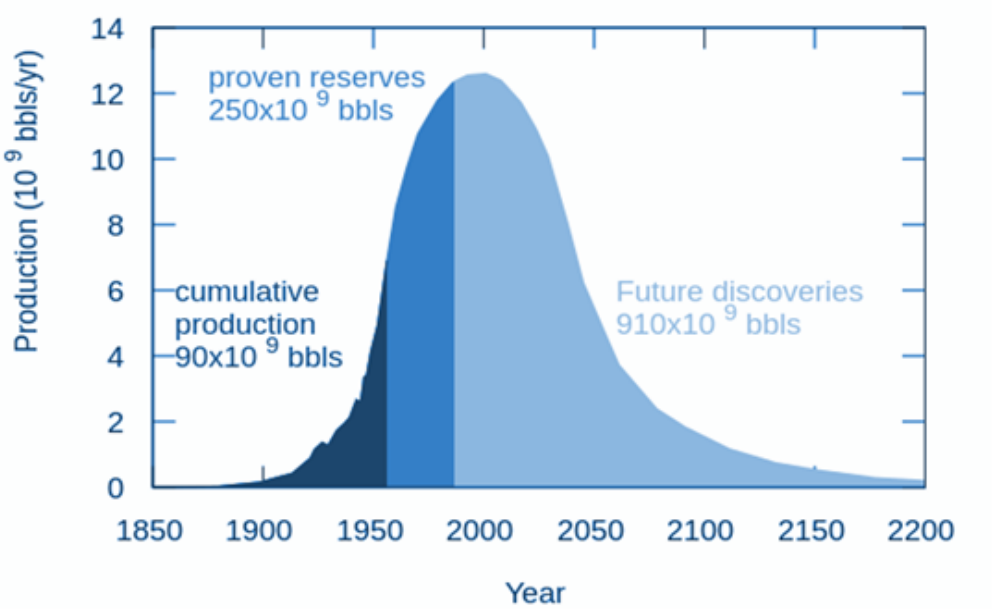


FIGURE 1.3: Peak oil curve (Projection for end of oil)

It was observed that he was right and thereafter several analysts have predicted a world oil peak in early 21st century which has led to belief of oil crisis or even end of oil economy within next 50 years. On the other hand global oil demand has kept on increasing and it is projected to increase 38% till 2030 [IEO14]. In 2006, the European Commission drafted an action plan with target to decrease energy consumption by 20% till 2020 [KR08].

In such situation it is only imperative that the supposedly remaining oil must be consumed smartly and as efficiently as possible. This dictates one of the most significant requirements to the future EDAS.

1.1.3 Environmental Pollution

While oil crisis presents a socio-economic-political chaos, unregulated oil burning has a more dangerous effect. Theoretically, burning fossil fuels should produce only carbon di oxide and water. Unfortunately IC engine emissions contain several by products such as carbon mono oxide, nitrogen oxides, and unburned hydrocarbons in addition to carbon di oxide all of which cause significant environmental damage and are unhealthy for human, animal and plant life. CO_2 is the main source of green house effect which is a phenomenon where excessive green house gas (GHG) traps heat from sun and causes artificial imbalance in natural entropy. It is credited with sudden temperature rise in recent years, melting of polar ice, several hurricanes, heat waves and other natural disasters. As observed in Figure 1.4 [GHG13] [GHG11], in the European Union (EU)

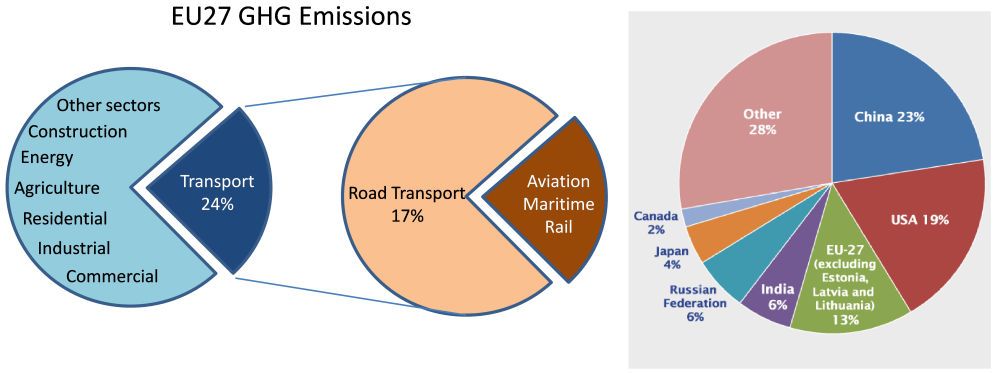


FIGURE 1.4: Attribution of GHG emissions

alone, 24% of CO_2 generation is attributed to transportation sector. Out of this, 17% is contributed by road transport. Data suggests that the EU and North America alone contribute the world's 32% CO_2 production.

Incidentally, the road infrastructure of these two continents presents most suitable conditions to implement autonomous driving vehicles, V2I and EDAS. In [KR08], a recently compiled study from EU commission concludes that applying ITS more widely in transportation sector will help deliver significant energy efficiency gains and cut global greenhouse gas emissions by up to 15% every year by 2020.

1.1.4 Driver Comfort

Depending on the traffic situation, at times, driving may be perceived as pleasant experience. Otherwise, in congestion or long monotonous trips it may become source of fatigue and irritation. In such conditions, autonomous driving offers to take care of the complex driving tasks and provide the driver a comfortable driving experience. Not only does this reduce the probability of accidents but also the physical strain on the driver in addition to ensuring efficient powertrain operation. Furthermore the EDAS must also take into account the limitations of longitudinal and lateral acceleration limits as well as the jerk limits thereby ensuring a smooth trip for the driver and passengers. Commercially available intelligent systems like highly automated ACCs are regulated by international standards like [ACC10] to take into consideration driver and passenger comfort characteristics such as acceleration/deceleration and jerk limitations. Another example is the Mercedes-Benz Intelligent Drive [MBI] which goes one step further to ensure driver comfort with extensive vehicle system automation ranging from lighting systems to active chassis control.

1.1.5 Energy efficiency and component life

Even with additional information about beyond-horizon traffic and road conditions, the effectiveness of EDAS is mainly characterized by the powertrain. A conventional IC engine powertrain offers far less flexibility to effectively use the ITS available data than the hybrid electric or even the pure electric powertrain. The main reason for this is that hybridization not only offers access to clean and efficient energy but also provides regeneration of the excess spent energy. However, the single most important component in the hybrid system is the battery which is not only prohibitively costly, but also very sensitive to operational deviations. In [GRO12], tests suggest that aging process of the lithium-ion battery is closely related to the loss of cyclable lithium. The loss of cyclable lithium is attributed to very high charge or discharge current which means that very high acceleration or high power demand from battery may damage it. Therefore, the EDAS must control the powertrain to operate within the allowable limits of such sensitive and expensive components.

New generation lithium batteries allow for a high charge acceptance without an irreparable damage to their chemistry. It is normally defined in terms of time constraints as a 10 s or 15 s regeneration pulse [GAI09]. This phenomenon limits the time and in turn the amount of energy that can be harvested during the regenerative braking. Therefore, it is matter of complex optimization between saving regenerative energy and conserving the battery life. The modern EDAS has to take into consideration several factors to balance the component life and still operate as efficiently as possible while maintaining driver comfort.

1.1.6 eFuture Project

The eFuture project [efu], funded by the European Union under the 7th Framework Program (FP7) was implemented during 3 years till September 2013. It was coordinated by Intedis GmBh & Co. KG with 5 partners namely, Hella KGaA Hueck & Co., Tata Motors European Technical Centre (TMETC), Miljøbil Greenland, French Institute of Science and Technology for Transport, Development and Networks (IFSTTAR) and Würzburg Institute for Traffic Sciences.

The aim of eFuture was to prepare the next generation of electric vehicle by creating a platform which minimizes its energy needs without compromising safety. A new architecture specifically adapted for this purpose of optimization between safety and energy efficiency was designed. It is based on the concept of decision units where dedicated

sub systems process the real-time incoming data to control various actuators depending on the optimization strategy. In this context, the ADAS systems were reworked to accommodate the impact of optimization strategies on the driver.

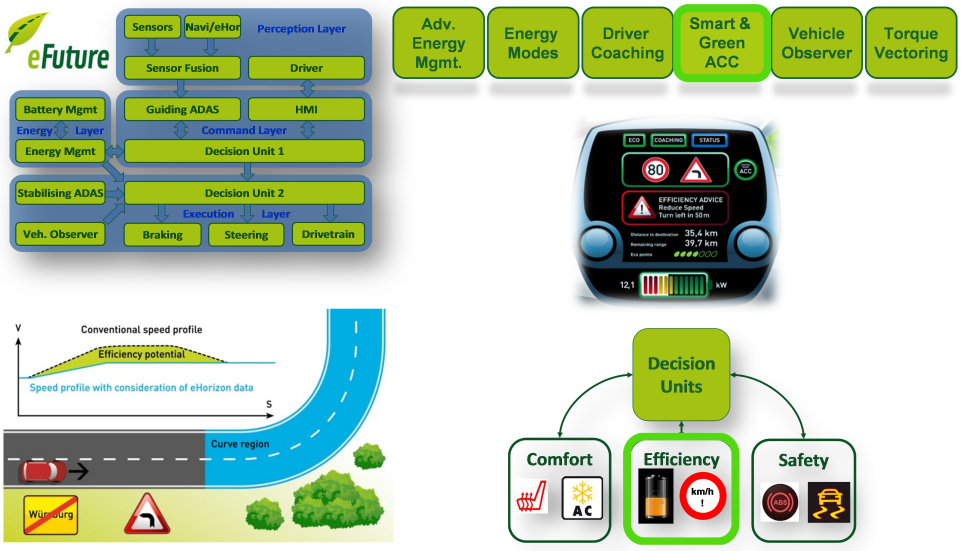


FIGURE 1.5: Overview of the eFuture Project

Figure 1.5 presents an overview of the fundamental concept in the eFuture project. The sensors, actuators and decision units are structured as a layered architecture in addition to energy management and ADAS systems. The smart and green adaptive cruise control (SAGA) forms an inherent part of the eFuture concept. It is investigated as a core subject in this thesis.

1.2 Aim, scope and contribution

The aim of this thesis work was to develop a safe and efficient driving assistance system with focus on electric vehicles. With the term "Safe and Efficient", the emphasis is on the idea that such a driving assistance system will strive to achieve best possible energy efficiency without compromising the present level of safety currently offered by standard driving assistance systems as defined in [ACC10]. In the updated terminology, an ADAS with eco-driving capabilities is termed as an EDAS.

In this context, it must be taken into account that eco-driving is not just an attribute of EDAS but can only be implemented through extensive powertrain modification, availability of near and beyond horizon data and vehicle automation for lateral and longitudinal control. Thus, even if the aim of this thesis is development of an EDAS, the scope extends well beyond normal motion control domain of standard driving assistance

systems like Adaptive Cruise Control. Thereby, not only the kinematic analysis is addressed but also the energy efficiency behavior of the vehicle as a whole is investigated to develop a complete autonomous/automated vehicle longitudinal motion controller.

Such an intelligent vehicle longitudinal motion controller would have to be in essence an ACC and hence, the controller is named as Smart and Green Adaptive Cruise Controller (SAGA). The SAGA concept is a generic idea based on above described aspects. This generic concept is then methodically adapted to various vehicle powertrain topologies to finally develop a tailored system which takes into account the different component setups and their respective operational behaviors.

The SAGA concept blurs the line between the energy management system (EMS) and the ADAS to combine them into one. Normal EMS operates to optimally control the powertrain and supply the requested power as efficiently as possible. On the other hand, ADAS like an ACC, will generate vehicle motion commands and in turn, power demand which is then supplied by the powertrain at whichever efficiency present at that operation point of the powertrain.

In contrast to the normal ACC and EMS operation, the SAGA concept generates optimal motion commands which take into consideration beforehand, the best possible efficiencies offered by the powertrain and thereby enhancing the operational system efficiency. In addition to this, the SAGA function optimizes the regenerative braking to extract maximum possible energy from deceleration maneuvers without compromising the safety factor.

In this thesis, the application of the SAGA function to a battery electric vehicle (BEV), a pure hybrid and a Plug-in hybrid is investigated through a complete kinematic and energy analysis of these vehicle topologies, by modeling and simulating them on the Matlab Simulink platform.

The following papers are a part of work done in this thesis.

Sagar Akhegaonkar, Lydie Nouvelière, Roman Potarusov, Volker Scheuch, Frederic Holzmann, Sebastien Glaser, *"Modeling and Simulation of Battery Electric Vehicle to Develop an Energy Optimization Algorithm"* AVEC'12 The 11th International Symposium on Advanced Vehicle Control September 9-12, 2012, Seoul, Korea

Sagar Akhegaonkar, Sebastien Glaser, Lydie Nouveliere, Frederic Holzmann, *"Smart and Green ACC series: A city and highway specific approach towards a safe and efficient eDAS"*, EVS27, November 17-20, 2013, Barcelona, Spain

Sagar Akhegaonkar, Sebastien Glaser, Lydie Nouveliere, Frederic Holzmann, *"Smart and Green ACC: As Applied to a Through the Road Hybrid Electric Vehicle"*, AMAA 2014, 23-24 June 2014, Berlin, Germany

Sagar Akhegaonkar, Lydie Nouveliere, Sebastien Glaser, Frederic Holzmann, *"Smart and Green Autonomous Vehicle Controller: Enhancement of Regeneration and Powertrain Strategy"*, AVEC'14 The 12th International Symposium on Advanced Vehicle Control, 22-26 September, 2014, Tokyo, Japan

Sebastien Glaser, Sagar Akhegaonkar, Olivier Orfila, Lydie Nouveliere, Frederic Holzmann, *"Smart and Green ACC, Safety and efficiency for a longitudinal driving assistance"*, AMAA'13, June 2013, Berlin, Germany

S. Glaser, O. Orfila, L. NOUVELIERE, Roman Potarusov, Sagar Akhegaonkar, Frédéric Holzmann, Volker Scheuch, *"Smart and Green ACC, adaptation of the ACC strategy for electric vehicle with regenerative capacity"*, Intelligent Vehicle Symposium IV'13, Brisbane, Australia, June 2013

Sagar Akhegaonkar, Sebastien Glaser, Lydie Nouveliere, Frederic Holzmann, *"Smart and Green ACC: Energy and Safety Optimization Strategies for EVs"*, IEEE Transactions on Systems, Man and Cybernetics: Systems, Status: Submitted under review (SMCA-14-07-0341)

Chapter 2

Literature Review

As discussed earlier, the idea of a smart and green adaptive cruise control originates from various developments in the field of autonomous vehicles, powertrain electrification and intelligent transportation systems. In this chapter, a brief state of the art for these fields is presented. Additionally, a comprehensive overview of vehicle energy requirement and energy saving potential is discussed. The chapter also dwells upon the necessity and feasibility of an intelligent and efficient autonomous vehicle longitudinal motion controller.

2.1 Autonomous driving

2.1.1 Basic concept

Depending on the traffic situation, at times, driving may be a pleasurable experience. Otherwise, in congestion or long monotonous trips it may become source of fatigue and irritation. According to the 2013 European accident and safety report [vol13], every year about 1.2 million individuals perish in traffic accidents and over 90% of accidents are caused due to human error. This figure could be significantly reduced if only the human driver is replaced by a control system which is free from the inherent human biological limitations like drowsiness, fatigue and inability to focus on a task for prolonged period of time.

Autonomously driven vehicles is a very old concept. In 1939-57, the Central power and light company ran an advertisement campaign which urged people to use its electricity and one day perhaps run autonomously driven vehicles with it. The eureka PROMETHEUS project (PROgraMme for a European Traffic of Highest Efficiency and Unprecedented Safety, 1987-1995) [eur] was one of the early demonstrators of the fully

automated road vehicle. Since then, significant advancement in on board computing capacity has enabled real time image processing such as object/edge detection, recognition, classification, and tracking using vehicle mounted cameras. Combined with long and short range sensor data, a fairly satisfactory three dimensional virtual model of the real surrounding environment can be generated and updated in real time. This presents a possibility to apply automated lateral and longitudinal control for a road vehicle [LA+11], [BM+12].

In theory at least, such an automated system promises to increase safety levels and passenger comfort. Therefore, the preliminary research efforts are concentrated to achieve a high degree of confidence in lateral control of the vehicle. However, the automation of vehicles offers much more than just safety and comfort. Autonomously driven vehicles are uniquely capable to implement a perfect eco-driving system. To prove this point, one must first have a look at the golden rules of eco-driving [BZP13].

1. Ensure proper gear selection: So that the IC engine operates in the most efficient region
2. Shift into a higher gear early: This reduces the engine rpm and returns the operating point into more efficient region
3. Leave vehicle in gear when braking: This will run the engine with vehicle momentum thus avoid engine idling fuel consumption
4. Maintain a steady speed at highest possible gear: Gear ratios are designed to ensure efficient engine operation at cruising speeds
5. Look ahead and anticipate traffic flow: Sudden braking and acceleration increases fuel consumption
6. Switch off engine at short stops: This reduces engine idling fuel consumption
7. Check and adjust tire pressure regularly: Tire pressure has a direct effect on wheel/Tire resistance
8. Make use of in-car fuel saving devices such as on-board computers and dynamic navigation to avoid traffic jams: Modern navigation devices do provide this service at a premium

For most drivers, the task of basic driving is itself complex enough. In such a situation, if the driver is expected to implement the above described rules for eco-driving simultaneously, it will be very stressful for him/her and on the contrary might lead to reduced safety and unwanted distraction from the main task. On the other hand an autonomous

vehicle which is controlled with microcontroller has enough processing capability to perform the basic driving task and in parallel, implement the eco-driving concept without compromising safety.

Furthermore, it would be worth mentioning the limited ability of human drivers to effectively use the information provided by the electronic horizon (eHorizon) mapping and V2V, V2I communications. For example, consider a situation where the human driver is provided with information on the HMI (Human Machine Interface) regarding a traffic signal 1 km ahead which would turn green in 30 sec. For the human driver, it would be difficult to utilize this information effectively, but the microcontroller based eco-driving system can exactly compute the best possible velocity trajectory to be implemented so that least amount of energy is consumed and the vehicle passes the signal when it is green. While the human driver would be least interested in investing the brain power in such a task where the return on investment would be some watt-hours (Wh) of energy, the autonomous vehicle controller would repeatedly perform the same task without fatigue or loss of interest and more effectively as compared to the human driver.

Therefore, it can be stated that autonomous driving can have significant impact not only in safety and comfort areas but also in vehicle efficiency and eco-driving. Hence, this thesis investigates the effect of autonomous longitudinal motion control as applied to various new powertrain topologies by kinematic and energy analysis through simulation.

2.1.2 Level of Automation

Development of a complete autonomous vehicle is a step by step process. In order that the transition from a human driven vehicle to an autonomously driven vehicle is smoothly completed, it is necessary to gradually introduce the automated systems into road vehicles from low to high level. In this context the autonomous vehicle systems are classified according to their properties and the level of automation they offer. Different institutions like National Highway Traffic Safety Administration (NHTSA) or the Verband der Automobilindustrie (VDA) attempt to standardize such a classification. The basic idea is presented in Figure 2.1, it is based on [vda] and in line with new SAE J3016 standard [SAE14] .

A basic guideline for the classification is the level of involvement of driver or vehicle controller. At present vehicles with assisted systems (ACC, lane keeping, lane change) are available in the market. The development prototypes such as the Google driverless car, Mercedes Bertha [DAB14] and Vislab Braive [BM+12] must be classified as partly automated vehicles as they still need driver supervision. While the target of the fully automated car would be to drive itself without any driver supervision, a driver needs

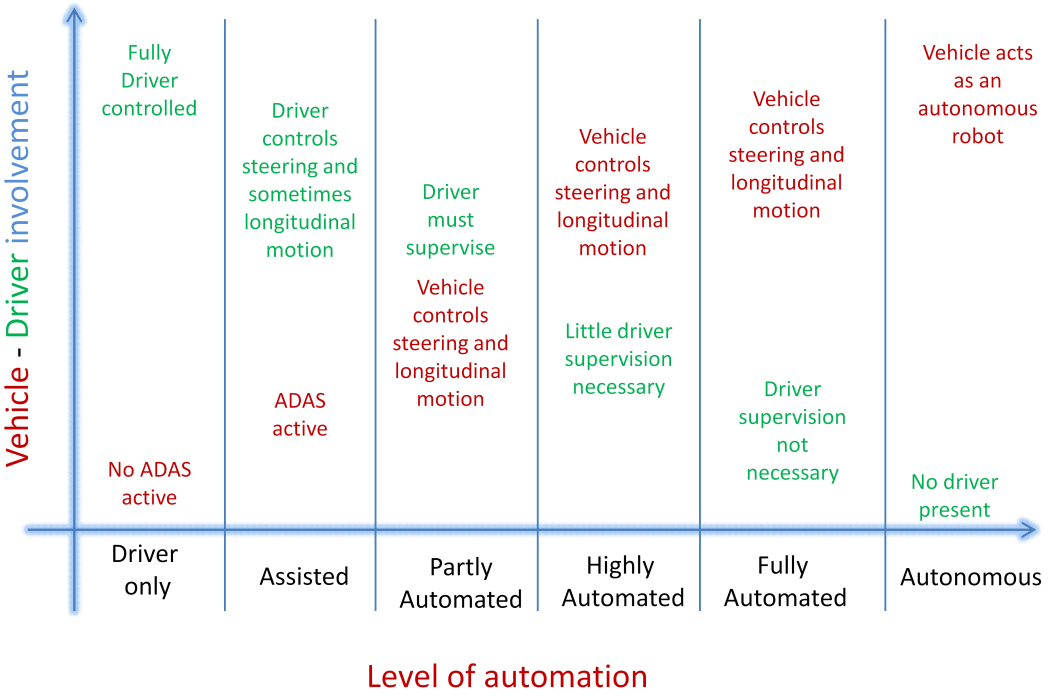


FIGURE 2.1: Autonomous driving systems classification based on Level of Automation

to be present to intervene if the vehicle requests it. There is a clear difference between fully automated and the fully autonomous vehicle. In a fully autonomous vehicle there is no need of driver in other words it will be a driverless car in its true sense.

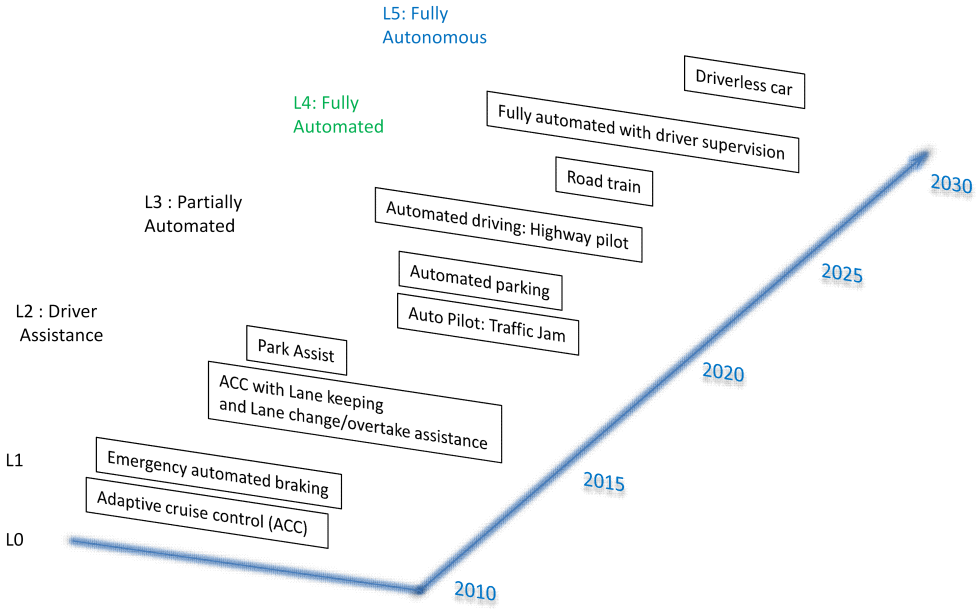


FIGURE 2.2: A road map for autonomous vehicle development

Figure 2.2 represents a implementation road map for the autonomously driven vehicles.

While there are several successful demonstrations through different EU projects e.g. Prevent or Adaptive for highway pilot, Volvo SATRE for road trains and the DARPA grand challenge 2007 for the driverless vehicle, the actual implementation of the autonomous vehicle on the public roads depends on infrastructure standardization and adaptation of existing policies accordingly. Hence, the IHS 2014 report projects the final implementation close to 2030.

2.1.3 Vehicle control

The motion control of an autonomous vehicle can be described as a combination of lateral and longitudinal directional control. Essentially, the main idea underlying autonomous vehicle motion control is to define short missions to displace the vehicle from one defined GPS point to the next.

2.1.3.1 Lateral mode

During the vehicle displacement, it is ensured that the vehicle remains inside the specific tolerance area defined by the road lane markings. The road lane markings are detected using vehicle mounted multiple camera systems which at times may have a field of view of almost 360°. Using real time images captured in front and/or rear view, a spline/curve fitting algorithm is used to determine the oncoming road curvature [Klu94], [DZ87]. A lateral control is achieved using feedback from external cameras and internal inertial measurement system combined with the wheel speed and steering angle data fusion.

It must be noted that in comparison to the longitudinal vehicle motion, the lateral vehicle motion requires negligible amount of fuel energy. Since lateral vehicle motion does not make a large impact on the total energy consumption of the vehicle, this thesis ignores lateral vehicle motion and concentrates on energy and safety characteristics of longitudinal vehicle motion only.

2.1.3.2 Longitudinal mode

The longitudinal motion control in an autonomous vehicle may be simply described as an intelligent extension of the standard adaptive cruise control (ACC), wherein, the extension being the camera and map based speed limit detection. In more advanced cases the speed limit detection may be supplied using V2V, V2I and dedicated short range communication (DSRC) systems.

The basic concept for longitudinal vehicle motion control is to follow the GPS guide points at the velocity permissible with respect to speed limits and obstacles. For this purpose the autonomous vehicle uses multiple long and short range RADAR (Radio detection and ranging) and LIDAR (Light detection and ranging) sensors. These sensors can provide data regarding the distance, speed and angle of the obstacle ahead with millimeter accuracy. If case of a clear front road, the vehicle must follow the legal speed limits. If there is another vehicle in front, then the ego vehicle must follow the front vehicle with a minimum safe distance. This is known as headway spacing control.

It is important to note that almost all of the energy spent to displace the vehicle can be attributed to the longitudinal motion of the vehicle. Therefore, autonomous vehicle longitudinal control acts as a base upon which this thesis is developed. A detailed section dedicated to it is found later where the concept of SAGA function is developed based on longitudinal control of an autonomous vehicle.

2.1.4 Control Architecture

2.1.4.1 Sensors

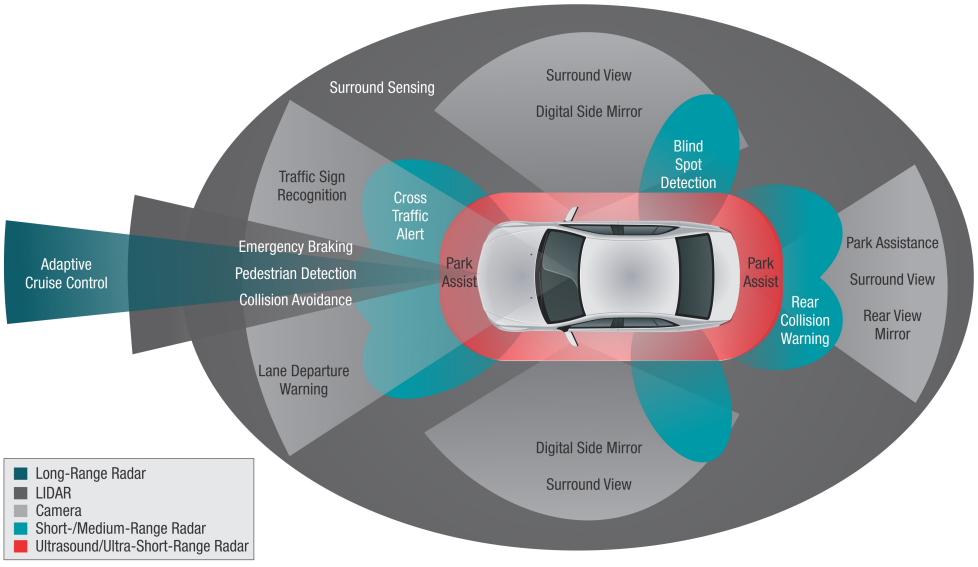


FIGURE 2.3: Sensors for an autonomous driving system

To develop a detailed model of the vehicle surrounding environment various setups of sensors may be deployed as shown in Figure 2.3 [SE] . One such example would be the Vislab BRAiVE prototype vehicle [BM+12] where to achieve a 360 deg sensing it uses 10 cameras, 4 laser scanners, 16 laser beams, 1 RADAR, GPS, IMU (Inertial Measurement Unit) and various other small sensors. Some other prototypes may use

a different combination of sensors to generate a satisfactory sensory system. In the following, important sensors are described to provide a brief understanding of the overall system.

RADAR

It is an acronym for Radio Detection and Ranging. As the name suggest the RADAR uses radio waves to detect and track objects. The latest models of this device are small enough to be integrated into the automotive bumper assembly. It can measure direct distance and speed of an obstacle. Such a system is fairly unaffected by bad weather conditions and pollution or by light or glare. They are comparatively inexpensive compared to other sensors and offer a wide range of detection capability.

The on-board automotive applications RADAR sensors can be classified as long range RADAR (LRR) and short range RADAR (SRR). Short range RADAR are typically operated at 24 Ghz and provide a high resolution distance measurement with a range up to 40 m and observation angle of upto 60° which is quite wide by RADAR standards. Such devices are mainly used for blind spot detection, lane change system, parking maneuver, rear crash collision warning and for some short range (urban) ACC support. The long range RADAR operates at 76 Ghz with detection range up to 120-200 m. At this distance the required field of view to cover the front and adjacent lane is about 8° to 16°. They are typically used as sensors for ACC application.

Since RADAR uses radio spectrum there are certain frequency and power limitations which are specified for these systems. With increasing implementation of autonomous vehicles it is possible that these systems will interfere with each other. Therefore, although RADAR algorithm at present is not complicated, it may become complex in order to integrate new methods for vehicle to have a specific RADAR stamps for better recognition. This may present new challenges not only with respect to system complexities but also cost.

LIDAR

LIDAR may be interpreted as LIght Detection And Ranging or Laser Imaging Detection And Ranging. The advantage of LIDAR over RADAR is that in RADAR detection, non metallic objects produce weaker reflection while certain material produce none, such objects are surely detected using LIDAR. The basic concept is to fire laser beams and measure time for the reflected beam to return. The device can fire upto 150,000 pulses per second with a wavelength of 850-905 nm. The field of view is about 1° to 16° and multiple overlapping beams (16 of them) are used. The range is about 120-200 m.

An advanced LIDAR active scanning uses a 64 beam 360° FOV (Field Of View) system typically applied in case of autonomous driving prototypes for 3D mapping applications. These systems are prohibitively expensive and presently may cost more than the vehicle itself. They have extremely high complexity of operation algorithms and may be ineffective in bad weather like snow or spray.

Camera Systems

Cameras serve as the eyes of the autonomous vehicle. Camera systems may be monocular or stereo depending on the need of application. While mono systems may be fast and computationally less demanding, stereo systems provide 3D imaging useful to track object movement and determine distance.

One of the main application of camera vision is lane marking detection and lane tracking. Although the mono camera is sufficient for this, reliable detection is still not possible due to shadows, image contrast, wearied and occluded lane markings and inconsistent lighting conditions. Night operation is possible under headlight light but is less efficient compared to day. Using camera to capture front and rear FOV and applying spline fitting algorithms it is possible to determine the oncoming road curvature and track ego vehicle motion.

Vision systems can be programmed to recognize the rear part of a vehicle considering that vehicle have distinctive features such as rectangular shape, rear windscreen, license plate etc. Using stereo camera it is possible to determine distance, speed and track the front vehicle. Thereby it is useful to position and track the front vehicle in order to implement lane change and overtaking maneuvers as well as collision warning and mitigation. Using a similar idea but more complex detection and tracking algorithms it is also possible to track pedestrians and other roadside objects which may potentially intersect with the vehicle planned trajectory.

Cameras are also useful for traffic sign recognition, although in future it would be preferable to combine this along with a V2I or DSRC signal which would communicate important intersection and speed limit changes well before they are actually encountered.

2.1.4.2 Data Fusion & Processing

It is clear that every sensor has its advantages and disadvantages. While the camera and LIDAR are not very effective during bad weather the RADAR is minimally affected by it. On the other hand RADAR cannot sense certain materials which are better identified through LIDAR. Similarly RADAR can effectively compliment the lateral accuracy of vision systems by adding the longitudinal dimension data to it. Therefore all the data

from sensors are fused together to form a reliable sense of surrounding environment. The sensors form only the input layer of the overall autonomous vehicle control structure. Powerful processors are required in order to actually interpret the incoming data, make sense out of it and issue control commands to the actuators. Figure 2.4 presents a schematic diagram to give an understanding of the underlying architecture, it is based on [LH+08].

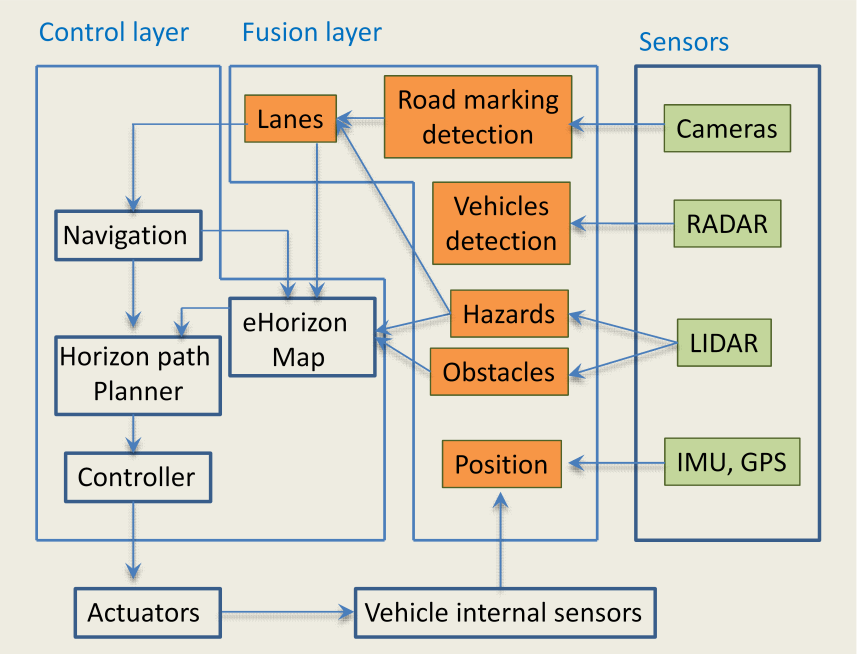


FIGURE 2.4: Autonomous driving system architecture

A large amount of data is generated every second from the sensors depending on the configuration. For example, a setup using 750x480 camera resolution generates about 39 MB/s data feed [LH+08]. This data needs to be processed fast to make real time control possible. Initially, the autonomous vehicle prototypes used large and heavy hardware which is now being replaced by FPGA (Field Programmable Gate Arrays) in final stages which pack large computational power in small packages and are especially useful for image processing.

2.1.4.3 State of the art (Autonomous vehicles)

Development of the autonomously driven vehicles has come a long way since its inception in the 80s. Among several other development programmes, two projects are credited with distinguished success in achieving substantial progress in the autonomously driven vehicle development. In the following, further details of the Eureka Prometheus and DARPA Grand Challenge programmes are elaborated.

Eureka Prometheus

The eureka PROMETHEUS Project (PROgraMme for a European Traffic of Highest Efficiency and Unprecedented Safety, 1987-1995) can be recognized as a pioneer project in the field of autonomous driving. With almost 750 million € in funding over 96 months it was the largest Pan-european project with involvement of several universities and OEMs. Most notable performers were Daimler-Benz AG and Bundeswehr University Munich. It must be noted that this project was carried out in a timeline where high capacity processors and computer vision were in nascent stage of development. In 1994 the project successfully demonstrated twin robot vehicles VaMP and VITA-2 which drove more than one thousand kilometers on a Paris multi-lane highway in standard heavy traffic at speeds up to 130 km/h. Later in 95', using saccadic (quick changing) computer vision and transputers (parallel computing microprocessors) a re-engineered S-Class Mercedes Benz prototype demonstrated autonomous control in its trip from Munich to Copenhagen and back, over 1000 miles where speeds of 175 km/h were achieved and 158 km were driven continuously in autonomous mode.

DARPA Grand Challenge

Three autonomous vehicle competitions were organized by DARPA (Defense Advanced Research Projects Agency) in year 2005, 06' and 07. Several teams comprising of universities and private sector demonstrated their prototypes to compete in the DARPA defined routes. The state of art autonomous driving was present with performance improving each year.

In 2007, six teams finished a 96 km course with difficult terrains and obstacles with their vehicles without any human driver present. Although the average speed of best performer was about 22.5 km/h with a finish time of about 4 hours, it was established that with controlled environmental disturbances (no sudden pedestrians etc), autonomous driving is in a quite advanced stage of development and implementable soon.

Google Driverless Vehicle

Internet search company Google can be recognized as pioneers of modern day autonomous vehicle. Google modified a Toyota Prius with additional equipment like cameras, RADAR, 64 beam laser system along with high definition inch-precision maps.

As of June 2015, it was claimed that Google driverless vehicles had clocked almost 1.6 million km in testing.

2.2 Basic powertrain classification

2.2.1 Conventional BEV, HEV, PHEV

Based on their powertrains, vehicles can be classified as conventional IC engine propelled, pure battery i.e. fully electrified vehicle and a mix of fuel and electricity defines the hybrid vehicles. A hybrid vehicle can be further classified as a pure hybrid or an externally chargeable Plug-In hybrid electric vehicle. Considering that IC engine based conventional vehicle is a well known concept, this subsection concentrates on the other relatively modern vehicle concepts.

BEV

Battery electric vehicles run only on electric energy stored in the battery packs. Since there is no oil burned the BEV are designated as Zero Emission Vehicles (ZEVs). Although BEV may be seen as a solution to the problem of air pollution and global warming, compared to fuel energy density (16 km/kg approx.), the most advanced battery pack fairs only with about 0.7 km/kg energy density. This means that even if the BEV has an operational efficiency of about 70-80% it always will have a limited driving range and may not be a complete replacement for the present day conventional vehicles because of its large recharge duration (approx 8 hours). The state of the art Lithium ion based batteries used for BEV propulsion are expensive (about $650/kWh) [S+10] although they are projected to be halved by 2020. They form the most expensive and sensitive component in a BEV. The batteries have a specific life cycle e.g. about 400-600 (Li-Polymer) [bata] after which they need to be replaced.

Apart from the ability to regenerate energy through electric braking, the advantage of BEV is that it is the most clean form of mobility if it is ensured that the electricity it uses, is from the renewable and non polluting sources. Else, it is just a question of substituting the emissions required to produce the electricity (at power plants) which propels the clean BEV. The Table 2.1 presents the comparison of cost of ownership economics for a BEV against the a conventional vehicle. For this purpose, one relevant candidate from each category is chosen, namely the Nissan Leaf as BEV and Volswagen Golf diesel as a conventional vehicle. The approximate time or mileage for battery replacement is based on [batb] where a Leaf customer has reported actual battery performance depletion at about 122000 km which means he will need a new battery. The price for new battery is based on [batd] and [batc] taking into consideration the european and American price parity ratio. The cost comparison is done at 130000 km which is where one must change the battery and an owner might think of reselling the car.

TABLE 2.1: Cost of ownership comparison between BEV and conventional vehicle at 130,000 km

Cost comparison @1,30,000 km	**Diesel car (e.g. VW Golf)**	**Nissan Leaf**
Capital cost	25,000/- € (approx)	35,000/- € with battery
Fuel/electricity costs @130,000 km	9,100/- € @ 1.4€/l diesel and 5 l/100km	4,900/- € 0.25€/kWh & 160 km/charge + infrastructure usage for quick charge = 5,500/- € approx
Maintenance costs	Marginally high	Marginally low
Battery change @130,000 km approx.	0/- €	6,000/- € approx. with refitting cost
Comparative costs	34,100/- €	45,900/- €

It is clear that for the end user, even after considering the extra maintenance for IC engine, cost of ownership for BEV is considerably higher than that of conventional IC engine vehicle. Apart from this one has to take into consideration that a BEV cannot be used on long distance trips except ones with huge batteries which makes the basic car cost prohibitively expensive.

HEV

On the other hand the hybrid electric vehicle (HEV) offers possibility to use both IC engine propulsion and electric drive. However, adding both system together in one car dramatically increases the weight and complexity of the vehicle. In increasing order of electrification HEV can be classified as micro, mild, full hybrid or a further step at Range extended full hybrid which has a very small IC engine enough to extend the limited range of the BEV.

Based on the way the powertrain components are mechanically connected, HEV can be classified as Series, Parallel or Power-split hybrids as seen in Figure 2.5. The following section presents specifics and highlights the advantages and disadvantages of the various hybrid topologies.

Series hybrid powertrain

The Series topology is named as such because all the powertrain components are connected in series. As seen in Figure 2.5 (left) the IC engine is mechanically connected to the generator which is then electrically connected to motor and both share a connection to battery to store or demand energy as required. The highlight of this type of system is that the IC engine is mechanically completely isolated from the wheels. This means that the power supply from IC engine is not directly dependent on the transient and frequent deviating demand from the velocity cycle. The generator-motor-battery system acts as

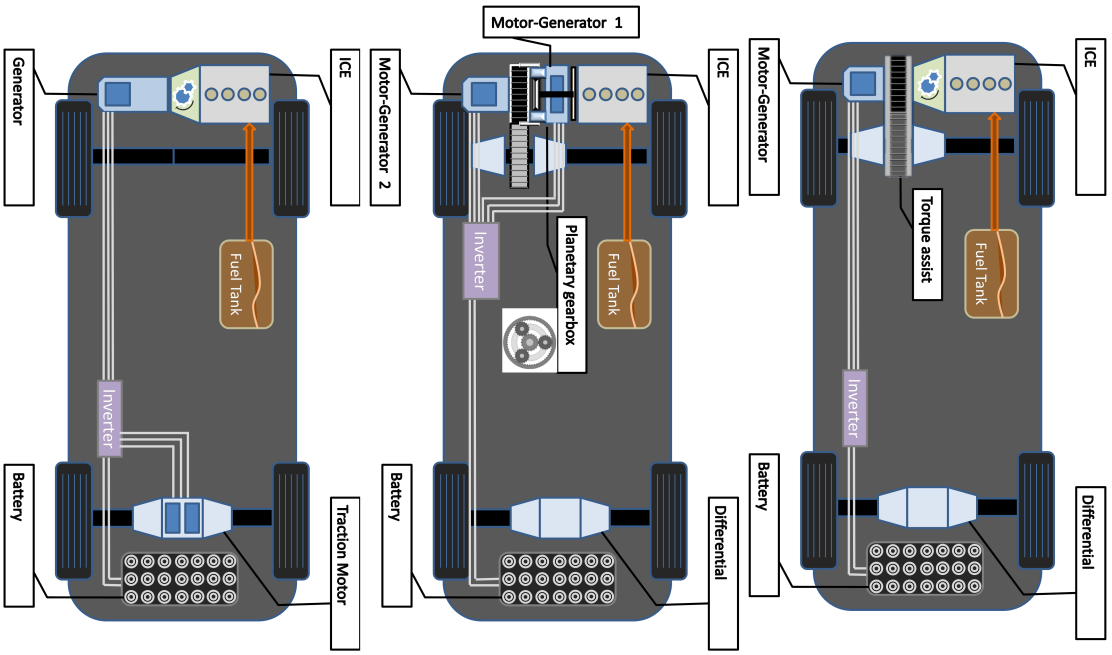


FIGURE 2.5: Hybrid vehicle topologies (L:Series, C:Power-split, R:Parallel)

an virtual e-gearbox (engine can run freely independent of vehicle velocity) and allows for flexible engine operation, thereby the engine can operate in the most efficient area of its fuel consumption map. A simple topology design means that the control algorithm is not complex and also allows simple packaging.

However, since the only direct propulsion component is its electric motor, the motor has to be designed for maximum power requirement attribute. Also, there are four power converters involved in the process (engine, generator, motor, battery) which leads to lowering the overall efficiency of the powertrain although it will always be more than that of conventional vehicle. Due to this the series topology is more suitable for urban driving than highway. The Fisker Karma is an example of series hybrid powertrain.

Parallel hybrid powertrain

The parallel topology Figure 2.5 (right) allows for the motor and IC engine to supply torque together. Thereby the main idea is to have the IC engine mechanically connected to the wheels and have an electric motor in parallel to add or consume excess torque so that the engine always remains in best efficiency region. Since torques can be added it is possible to reduce the size engine, motor and battery compared to series topology. This reduces weight and also direct mechanical coupling eliminates the conversion losses. Because of smaller size the motor may be packed directly in the transmission leading to a compact package. The parallel topology is better suited to highway conditions. On the downside since the IC engine is mechanically coupled to the wheels, the control algorithm

cannot always choose the best operating points for engine as in series operation. Honda's Insight, Civic, and Accord hybrids are examples of production parallel hybrids.

Power-split (Series-Parallel) hybrid

Power split hybrid topology may be simply described as a combination of series and parallel hybrids which offers to combine the advantages of both the topologies. Such a configuration is made possible by using a torque/power split device as seen in Figure 2.5 (center). It is a planetary gearbox as shown with its sun gear connected to IC engine, planets connected to motor-generator and the ring gear connected to the propulsion motor which is directly coupled to the wheel output. A different type of connection combination is also possible. The idea is to adjust the speed of engine using the motor-generator and adjust torque using propulsion motor, thus adjusting the operating point of engine in the efficient region.

Using such a configuration requires a highly complex control algorithm. Because the three components are mechanically connected through the planetary gearbox the control algorithm has an inherent limitation in controlling the speeds of components. For e.g. during low speeds where it is beneficial to keep the engine off, the engine has to be forcibly turned on at around 40 mph (in Prius) since the generator would exceed its maximum allowable speed if the engine is not forced on. This type of connection means that failure of even one component stalls the vehicle completely.

2.3 Energy management strategies

Due to ever increasing electrical energy component in modern vehicle, often there is a confusion between actual Energy Management Systems (EMS) and electrical load management systems. Furthermore, considering that in a BEV there is no thermal energy source, the electrical load management systems is assumed to be the energy management system. However, such a conception is flawed. While scope of electric load management covers distribution of power over the internal powernet, the energy management system's scope extends beyond that towards minimizing the power requirement for vehicle mobility and thereby ensuring highest possible operational efficiency and reduction in harmful emissions. The following section is briefly dedicated towards covering various energy management systems and strategies.

BEV

From operational point of view, the BEV can be simply viewed as a motor controller. Since there is only one source of energy supply (i.e. battery), the energy demand is

supplied by a single source and hence it seems it would be pointless to have any complex energy management system for a BEV. Apart from this, the BEV components have considerably good efficiency performance, for e.g. the motor is tuned to mostly operate in the region from 75% to 95%, modern Lithium based batteries offer more than 95% whereas the energy conditioners like inverters and DC/DC converters offer about 97% which means that with regenerative braking overall systems offers about 70-80% efficiency.

While the above may be true, it must be considered that the driving range of a BEV is severely limited and a battery recharge may require at times about 8 hours. Also, to achieve the above stated figures the BEV must be operated in a defined region of operational parameters. For e.g. it is very tempting for a driver to have a high acceleration from standstill. However, in such a maneuver since high power is required, the efficiency of each component drops dramatically in addition to a possibly irreversible damage to the battery chemistry. Again, due to driving range limitation, to increase driving range, it is better to have lower acceleration and maintain medium average speed. A lot of energy saving potential lies in the regenerative braking maneuvers. However, it is limited due to certain bottleneck components such as the battery. Using certain information from the intelligent transportation systems, it is possible to circumvent such bottlenecks.

Hence, classical optimization theories are not applicable for BEV. The energy management system for a BEV is based on various operational characteristics of the vehicle described above. An EMS for BEV based on these points is discussed later.

HEV

Hybrid electric vehicle consist of two or more different energy sources. These energy sources may be different not only with respect to the type of energy they supply, but also the characteristics such as energy density, power density etc. Hence, to fulfill the mobility attributes of the vehicle such as drivability and fuel economy these power sources must be designed to requirement and must be managed properly. Depending on type and topology of the powertrain systems various classical optimization systems may be applied. However, not all are implementable in real time. The main aim of the control strategies are as follows

1. To operate the powertrain at the best possible efficiencies
2. To decide how much power to be supplied from which power source
3. To regulate the state of charge of the battery
4. Provide a robust control without failure

In Figure 2.6, HEV control strategies are classified as rule based (RB) or Optimization based. Such a classification is based on [BG+10], [Sal07]. With reference to Figure 2.6, the research and development in the HEV control strategies is briefly described in the following.

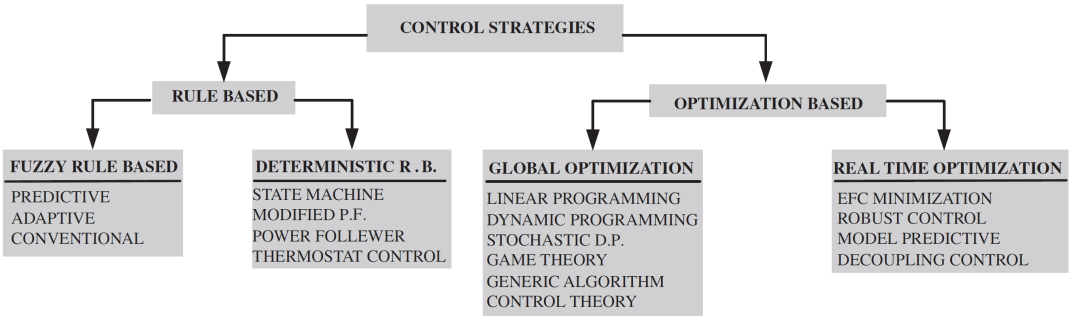


FIGURE 2.6: HEV powertrain control/Energy management strategies

2.3.1 Rule based

These strategies run on fixed rules. Such rules may be designed or derived depending on heuristics, intuition, human experience, fact based reasoning, modeling and simulation and generally without a priori knowledge of predefined driving cycles. Because these strategies are specifically rule based, they are easy to program and execute. They are robust and flexible towards noise in input data. Hence, such strategies are real time implementable. The only disadvantage with these strategies is that they do not try to optimize the given system component operation and hence even if they gain in robustness they lose a major portion in energy optimization. However in a situation where the hybrid vehicles are in initial stage of commercialization and processing hardware capacity is relatively limited by cost, reliability has more weightage than extra efficiency. Most hybrid electric vehicles available in market run on rule based strategies.

The idea behind operating the powertrain at best efficiency is based on controlling the operating point of the main energy source i.e. the IC engine as close as possible to the best efficiency region. Such a concept is coined as "Load leveling" where the engine load is manipulated by the electric motor and generator to operate the engine at the best efficiency torque and speed point. The rule based strategies are further classified into fuzzy rule based and deterministic rule based methods and are described briefly in the following.

Deterministic rule based methods

Heuristics based on power flow analysis of the hybrid powertrain, engine efficiency maps, and fact based reasoning is used to determine the rules for such strategies, hence the

name. One such strategy is the Thermostat (on/off) control strategy. It is a primitive method where the battery SOC is maintained within a specific range by switching the engine on and off. It is applicable for a series hybrid city bus running on prescheduled routes [NSW09].

A more complicated strategy is the "power follower control" where IC engine is supported by the EM (Electric Motor). Below a certain speed (low efficient region for engine) only EM is used. If demanded power exceeds maximum engine power, the EM supports to supply the excess power. Engine is shut off if power demand falls below a limit. In case of low battery SOC engine has to provide additional power to recharge the batteries. With such a strategy, a rough control over efficient engine operation is managed but there is no optimization. Since it is robust, the control strategies of Toyota Prius and Honda Insight are developed based on power follower control [BCM99]. This strategy is further developed as a "modified power follower" [JWR00] where an adaptive rule based EMS is proposed. The main goal of this approach is to optimize the energy usage and emission by calculating a cost function representing overall fuel consumption and emissions at candidate operating sample points.

Fuzzy rule based methods

Considering that operation of a hybrid drivetrain resembles that of a multidomain (thermal and electric), non linear and a time-varying system fuzzy logic seems to be an attractive solution for its control problem. This type of control system may be viewed as an extension of the deterministic rules based control where the decision making property of fuzzy logic can be used to realize a real time and sub-optimal powersplit. The advantage of using fuzzy rule-based controller is that they are tolerant towards imprecise input measurements and component variations and also, they can be easily adapted and tuned according to system if necessary.

Conventional fuzzy strategies (based on fuzzy rule methods) make use of classical fuzzy attribute rule tables which are designed based on efficiency maps and various driveline performance test results. For e.g. in [LS98] the authors attempt to design a fuzzy logic based control strategy to minimize NO_x emissions while sustaining the battery charge and supplying the driver requested torque. In order to design the fuzzy rules, a dynamo test had been carried out, where power converter's torques and overall NO_x emissions were measured. In [BWGR00] conventional fuzzy logic is applied to design a load leveling strategy for HEV. In this system, the fuzzy logic forces the IC engine to operate at or near its best efficiency point at all times. Using fuzzy logic it is possible to evaluate several conditions (requested torque, driveline efficiency map, emission map, battery SOC etc) to make a pre-programmed decision. Since the number of processing steps are limited, it is easily possible to program and execute such a logic

on a microcontroller. On the other hand, a complete system optimization is not possible using fuzzy rule based control.

In [RWRG03], the fuzzy logic control is extended to be **adaptive** to certain situations. It is observed that not all efficient engine operation points offer low emissions. An ideal operating point can be calculated by optimization of a criterion of which weighted fuel (efficiency) and emissions are contending parameters. Tuning the corresponding weights, the relative importance between efficiency and different emissions can be modified due to requirements in various operating conditions. In areas with critical air pollution, operating points with high emission are penalized, whereas at other times engine efficiency is given precedence.

Another variation of fuzzy logic is described in [RWRG03] where the logic takes into account future event data. Such a system is classified as **Fuzzy predictive strategy**. It takes into account data such as horizon traffic situation in case one is entering a city from highway or road elevation etc. Depending on this information the strategy decides when it is best time to use more battery power or charge the batteries for anticipated traffic.

2.3.2 Optimization based strategies

These strategies involve non-casual optimization of powertrain performance. The optimal reference torques for power converters and optimal gear ratios are calculated by minimization of a cost function generally representing the fuel consumption or emissions. Optimization is performed taking into consideration a fixed driving cycle. Iteration to find the best possible results are performed which eventually yields to a global minimum. This however requires the knowledge of past and future events which is not actually possible in reality. Hence, non-casual approaches cannot be applied in real time systems. They are however a basis for designing rules for deterministic rule based strategies or fuzzy logic control strategies.

Non-casual approaches can be adapted by assuming certain future event conditions based on past events. In such a case a real time optimization based control strategy is realizable where an instantaneous cost function is defined based on equivalent fuel consumption to ensure overall fuel consumption minimization and self-sustainability of electrical path. Although such an approach is suboptimal it comes very close to the performance of optimal systems and is real time implementable unlike non-casual optimization strategies. Such an approach is discussed further later in this thesis, the original literature can be found in [PDG+02].

Global Optimization: Non-casual strategies

There are several approaches to achieve the global minimum based on a cost function representing the system efficiency and emissions over a fixed drive cycle. However the problem with non-casual approaches is that they are computationally intensive and require a highly defined drive cycle information. However, in reality no drive cycle is accurately followed. Nonetheless, these approaches serve as an analysis tool to assess and tune other strategies. In the following section, some of the non-casual approaches are briefly described.

In [TB00] the concept of **Linear Programming** by application of convex optimization to the control problem of hybrid powertrains is discussed. The system (series hybrid) is formulated for optimizing the efficiency as a nonlinear convex optimization problem that is finally approximated by a large linear program. In this approach, the instantaneous fuel consumption is assumed to be an increasing convex function of engine power output. The problem is to minimize the overall fuel consumption subject to constraints on the engine, battery, braking power levels, and battery energy. Formulation of fuel minimization problem as linear programming simplifies finding a global optimum however the fact that such an approach may not be adaptable to a more sophisticated hybrid topology limits its applications.

Using the **Control theory approach** in [DLGR04], optimal control theory was directly applied to find a global optimal solution for the energy management problem in a parallel torque addition topology where the reduction gear is located between the engine and EM. Considering the topology construction, the system is defined in mathematical equations using engine torque, speed and component efficiencies. Since the torque and speed are given by the speed cycle, the whole system equation of the instantaneous IC engine fuel consumption may be defined using only two variables i.e. torque and gear number. The battery is modeled as a dynamic system with SOC as output. The constraints are embedded by introducing Lagrangian parameters and optimality conditions are given by first and second order derivatives with respect to control and the introduced Lagrangian parameters. A quasi-analytical solution has been found after some manipulations. In comparison with other approaches to find a globally optimized solution, the analytical nature of this method makes it a superior one. However, variation of drivetrain structure makes it more complicated to find an analytical solution, compared with numerical and iterative-based methods.

Dynamic programming [Bel54], is a very flexible global minimization problem solving technique which can be easily adapted to solve variety of problems. Since it is such a powerful tool to solve general dynamic optimization problems and it can easily handle the constraints and non linearity of the problem, it seems to be a reasonable approach

to obtain a globally optimal solution for the power split decisions in HEV. The basic idea underlying application of dynamic programming to HEV involves discretizing the velocity cycle into N steps. This means that the velocity cycle must be known a priori. Furthermore, a cost function is developed which consists of entities which need to be minimized over the cycle for e.g. fuel cost or emissions. At every step the state of the vehicle is defined by variables e.g. speed, torque etc. The local value of cost function to move from present step to next one is dependent on the state variables. The aim is to minimize cost at each local step so that the summation of all these minimum local cost would yield to a global minimum. Dynamic programming may be performed backwards or forward with respect to a drive cycle. In [LPGK03], dynamic programming is used to find the global minimum for a hybrid electric truck. The main problem with this technique is the high computational requirement. Since it needs to know the velocity cycle a priori it cannot be implemented in real time.

In [LPG04], the problem of optimization for a HEV is handled using **Stochastic dynamic programming** by formulating the energy management as an infinite-horizon stochastic dynamic optimization problem. In this approach, the power management strategy is optimized over a family of random driving cycles in an average sense. In order to obtain a time-invariant control strategy, an infinite-horizon optimization problem is formulated and solved by using stochastic DP. Although this approach is not a real-time solution by nature, but since a family of random driving cycles is used to find an optimal solution, the control law derived from SDP may be directly used in real-time implementation.

Genetic Algorithms is another approach which can be effectively used to solve non linear constrained problems as described in [Sal07]. It involved chromosomes consisting of genes representing static threshold such as highest and lowest desired battery SOC vehicle speed below which engine is shut off etc. with variation within a scheduled window as wide as possible. An objective function F takes into consideration fuel consumption and emissions. The fitness of corresponding chromosome is evaluated based on a fitness function. A tournament type selection (for example: best three from the set of samples) is employed as the selection function. Moreover, the genetic operators employed are the heuristic crossover that takes two parents and performs an extrapolation along the line formed by the parents outward in the direction of the better parent. The genetic algorithm approach is very useful for complex nonlinear optimization problems since it leads to a more accurate exploration of the solution space than a conventional gradient-based procedure. Nevertheless, it does not give the necessary view to the designer of the power train, unlike an analytical approach.

Real-Time Optimization

The global optimization strategies cannot be applied in real time and the rule based strategies apply a very rough control over the HEV system. With advancement in the processing capacity it is now possible to apply sub-optimal real time strategies to HEV which have a satisfactory performance as compared to non-casual optimization strategies. These approaches are summarized in the following.

The introduction of equivalent consumption minimization strategy (ECMS) [PDG+02], opened new possibilities for application of optimal control theory for real time power management in HEV. It is based on estimation of equivalent fuel consumption i.e. the fuel which will be spent in future to recharge the present discharging batteries or the fuel which will be saved in the future by discharging the present charging batteries. Apart from being implementable in real time ECMS is easily adaptable to different HEV configuration and also to PHEV with certain modifications in the strategy. ECMS is initially optimized offline using standard velocity cycles, however such a strategy does not perform well in real time. Hence, in [MRGS05], adaptive ECMS is developed which adapts the control variable according to changes in the control system.

In [PKR05] and [DGR02] a new approach is proposed with a control strategy to ensure acceptable drivability of the vehicle, in addition to driver power demand and battery SOC. Here the criterium for good drivability is smooth gear shifting and minimizing excessive driveline vibration. It involves a **decoupling control strategy** where the controller's output is composed of three components. The first component is dedicated to the satisfaction of the driver power request and is designed using an ECMS. The second component is devoted to the control of battery SOC. The third component is used in ensuring drivability and is obtained by using a gain scheduled infinite horizon linear quadratic regulator in which the performance index is defined as the difference between engine speed and turbine speed of the torque converter. Including more control objectives such as smooth gear shifting in the optimization problem can be regarded as a breakthrough; however, it is still in the early stages of development.

Some other real time optimization strategies include Robust control approach [PSRS03] where a feedback controller is used to minimize the fuel consumption of a PHEV and **Optimal predictive control** [CCS08] which uses a look ahead window to evaluate a fuel consumption cost function and develop a real time predictive optimal control law based on preview driving patterns and terrain information giving a superior fuel economy as compared to instantaneous one.

2.4 Mobility energy analysis

In order to design an efficient driving assistance system, it is necessary to evaluate the mobility energy requirement of the vehicle. In the following sub-sections, the vehicle energy requirements are discussed in brief along with possible energy reduction potentials.

2.4.1 Vehicle energy requirement

The main aim of any vehicle is mobility and the energy required to move any mass from one point to another can be expressed as the product of required force and covered distance,

$$\begin{aligned} E &= F \times d \\ &= F \times v \times t \\ &= P \times t \end{aligned} \tag{2.1}$$

where, E is required energy, v is vehicle velocity, P is power and t is the required time.

In an ideal environment like space, the force acting on the vehicle would be fairly simple to analyze. However, in earth's atmosphere there are various forces acting on the vehicle which need to be overcome in order to move the vehicle. These forces and the energy spent to overcome them are expressed below.

Acceleration Energy

The vehicle must be accelerated to obtain the desired velocity, in order to do so, certain amount of energy has to be supplied to the vehicle. The acceleration energy can be best explained by Newton's law of Motion where the force required to propel the vehicle is,

$$F = m \times a \tag{2.2}$$

where,
F = Force applied (N)
m = Mass of the body (kg)
a = Acceleration achieved by the body (m/s^2)

Air Drag Energy



FIGURE 2.7: Air flow over vehicle body as observed in a wind tunnel

The atmosphere of earth is filled with many gases in different proportion. Air is nothing but a term used to define these gases collectively. These gases have their own masses which can be observed from the term density of air i.e. 1.2 kg/m^3 (at 20°C). When a vehicle moves forward it must displace the air in its path to occupy that space in front of it. Since air has mass and therefore inertia of its own, the vehicle must apply some amount of force to displace the air in front of it. This force is dependent on the air density, air velocity, vehicle velocity and vehicle front area. As seen in the Figure 2.7 [air], a vehicle is tested for air drag forces in a wind tunnel. The air impacts on the front end of the vehicle. Force measuring load cells are placed at the wheels of the vehicle, the forces registered during this test are the air drag forces. The air drag energy can be calculated with the following formula.

$$E_{drag} = \int P_{drag}\, dt$$

$$P_{drag} = F_{drag} \times v \tag{2.3}$$

$$F_{drag} = \frac{C_w \times \rho \times A \times v^2}{2}$$

where,
E_{drag} = Air drag energy (J)
P_{drag} = Air drag Power (W)
F_{drag} = Air drag Force (N)
C_w = Coefficient of air drag
ρ = Density of air (kg/m^3)
v = Velocity (m/s)

Wheel - Road Resistance Energy

As the name suggests, this energy is spent to overcome the resistance due to rolling of the wheels. Automotive tires are made of rubber and other supplementary compounds to add strength and durability. Since their main function is to isolate the vehicle from the irregularities of road surface, they are characteristically flexible. When the wheel is spun at a high velocity, the centrifugal force acts at its periphery and causes the tire to expand. When the tire is on the road surface, it is deformed as shown in the Figure 2.8 [Whe] . The length a-b along the circumference of the tire is more than the actual deformed length a-b which forms the secant. This means that the already expanded tire is compressed to the length of the secant in the patch a-b. When the tire rolls on the road surface different patches along the tire surface hit the road and get compressed after passing through point 'a' till point 'b'. After point 'b' the tire is again allowed to expand to the original size. This creates a lot of vibration along the surface of tire at high velocities and micro slippage along the patch a-b.

Flexible materials absorb energy when they are stretched and release energy when they bounce back. However while doing this, they are affected by a typical phenomenon called Hysteresis. Hysteresis is defined as "A characteristic of a deformable material such that the energy of deformation is greater than the energy of recovery."The rubber compound in a tire exhibits hysteresis. As the tire rotates under the weight of the vehicle, it experiences repeated cycles of deformation and recovery, and it dissipates the hysteresis energy loss as heat. Hysteresis is the main cause of energy loss associated with rolling resistance and is attributed to the visco-elastic characteristics of the rubber [ftNTES06].

Rolling Resistance is standardised with the coefficient of rolling resistance f_r.

$$f_r = \frac{Resistance\ force\ offered\ by\ road\ against\ tyre\ rolling}{Total\ mass\ of\ the\ vehicle} \tag{2.4}$$

The Energy required for rolling resistance is given by the formula.

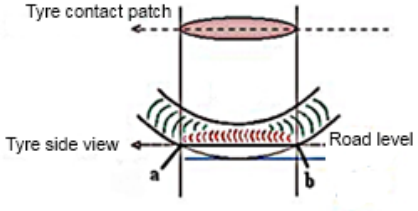


FIGURE 2.8: Tyre rolling resistance phenomenon

$$E_{roll} = \int P_{roll}\, dt$$

$$P_{roll} = F_{roll} \times v \tag{2.5}$$

$$F_{roll} = M \times g \times f_r$$

where,
E_{roll} = Rolling resistance energy (J)
P_{roll} = Rolling resistance Power (W)
F_{roll} = Rolling resistance Force (N)
M = Total mass of vehicle (N)
g = Gravitational acceleration (m/s^2)
v = Velocity (m/s)

Gradient Energy

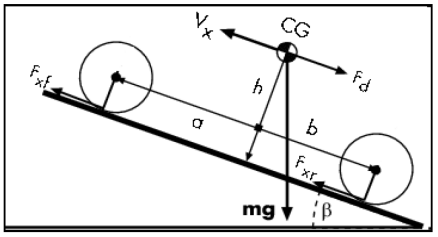


FIGURE 2.9: Gradient force acting on a vehicle

The energy requirement to overcome road slope can be better explained with help of the Figure 2.9. When the vehicle is on a horizontal road surface, the weight of the vehicle (Mass× Gravity), acts in the direction normal to the road surface. However when the vehicle encounters a slope a part of this weight starts acting in the backward or forward direction depending on the slope and slope angle. It can be seen in the Figure 2.9 that for a slope of angle β, a force F_d acts in the backward direction. The magnitude of the force due to slope is given by the following formula which can be further extended to find the energy requirement.

$$F_{gradient} = M \times g \times \sin\beta \tag{2.6}$$

2.4.2 Energy saving potential analysis

The aim of mobility is to move from one point to another. This process can be accomplished with several variable process parameters for e.g. acceleration, velocity, stop and go events frequency, travel path etc. Hence, the same mission from point A to B may have different energy consumption associated with it depending on the mission parameters stated above. In this subsection, the potential of these parameters to reduce the energy consumption is analyzed.

Acceleration

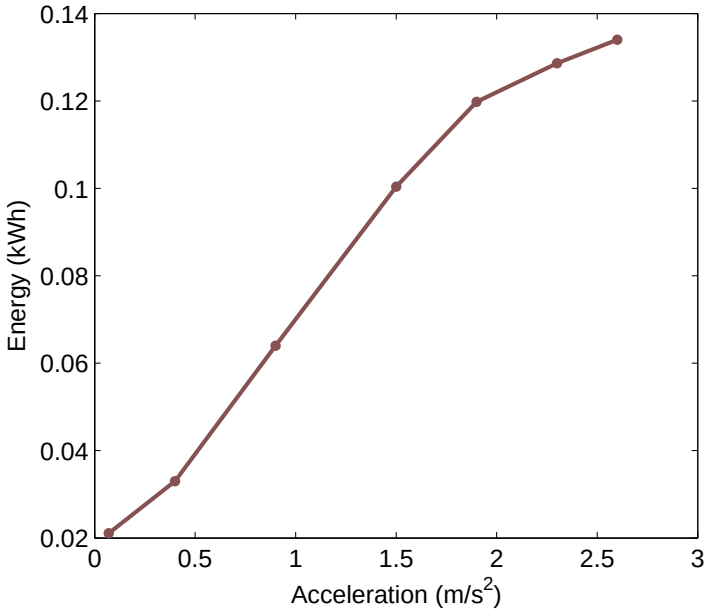


FIGURE 2.10: Effect of acceleration (Energy for a 100 m sprint)

Theoretically, as observed from equation 2.2, the higher the acceleration, the more the energy required to achieve it. In the Figure 2.10, a BEV model is simulated to perform 100 m sprints with different acceleration values. It is seen that if the same 100 m are covered with higher acceleration value, more energy is taken out from the energy storage (e.g. battery) and transferred into the vehicle mass as kinetic energy. Acceleration energy is stored into vehicle as momentum/ kinetic energy which is dissipated through road resistance, air drag, gradient energy requirements, and braking. Then, in a city driving scenario which is characterized by frequent standstill to velocity limit acceleration transitions and vice versa, high acceleration leads to a high average velocity which means more air drag. Also, a vehicle which undergoes high acceleration stores a large quantum of its battery energy into the vehicle as momentum. In such a situation, if the vehicle must brake then the stored momentum will be wasted as heat or regeneration system component losses. According to this philosophy, a very low acceleration value will lead

to maximum energy savings. However, it will also lead to long time duration to cover the same distance. Hence, taking into consideration the powertrain efficiency behavior in the city traffic, there must be certain optimum velocity trajectory defined by specific acceleration values which optimizes the energy and time requirements.

BEV is propelled with electric motor which has a virtually no lag between power demand and delivery like in case of IC engine propelled vehicles. Additionally electric motors are able to supply peak torque at the start of their operating range. This quick and high torque motor behavior might psychologically provoke the driver to accelerate with higher values especially from standstill. Not only is this maneuver inefficient in terms of system efficiency but also detrimental to battery chemistry. Hence, acceleration must be limited to certain optimum values to save energy and increase battery life.

Air drag energy component

One way to reduce the air drag energy component is through the physical vehicle form. Reducing the coefficient of drag C_w can have dramatic effect on energy consumption as shown in [Akh11]. Another factor affecting the air drag energy component is the vehicle velocity itself, considering that there is a square of velocity in the air drag force expression 2.3. In an approximate comparison of various energy components in city and highway cycles as in Figure 2.11, it is apparent that air drag component does not make for a major portion of energy in city cycles.

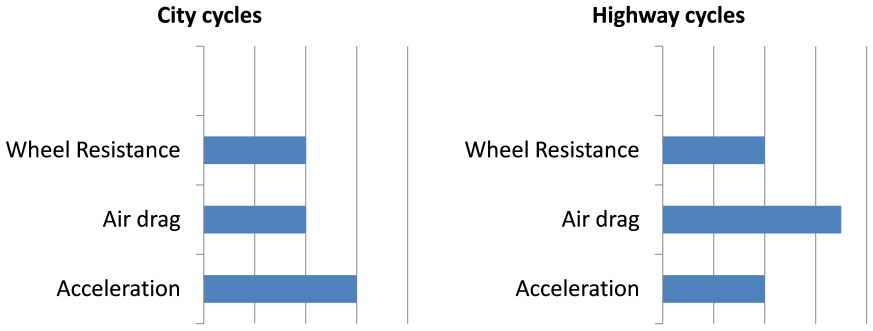


FIGURE 2.11: Comparison of energy components for city and highway cycles

This is owing to the low speed limits (30-50 kph) in the city traffic conditions. Hence, in city traffic it doesn't make sense to reduce velocity in order to save on the air drag component. However, in the highway traffic where speed limits go as high as 130 kph, air drag makes up for the majority of the energy consumption. Reducing the velocity will indeed save a major portion of energy but in the process will add up to the total time of travel. Therefore, it is necessary to find an optimum between energy saving and time to destination.

Wheel Resistance component

Wheel resistance is an energy component which is directly proportional to the distance traveled and hence the only way to reduce it is by using a suitable tire material. The benefits of using a low resistance tire are simulated in [Akh11]. There are certain tires which offer low resistance coefficient however it must be considered whether such tires may compromise on safety or durability.

Gradient Energy

There is no energy saving potential in the gradient energy as such. However, it does form an important part of energy management strategy. Downhill slopes offers opportunity to regenerate kinetic energy. At this point it must be ensured that the battery is empty enough and in the right temperature zone to absorb as much energy as possible without overheating or losing the optimum efficiency operation. In theory, a mission from point A to B and then return to point A will have a zero gradient energy summation. Here, it is important to ensure minimum loss of energy to the efficiency losses of components supplying energy during uphill gradient and regenerating energy during downhill slope.

EMS strategies, HEV and PHEV

Even though HEV has an electric power source, its overall efficiency will never be comparable to that of a BEV. The efficiency of a HEV will always be limited to the highest efficiency of its IC engine (i.e. about 30-40%). The main idea of charge sustaining HEVs is to help its IC engine run as efficiently as possible and at times replace the very inefficient operation points with motor operation. To achieve this goal it is necessary to use optimization based real time EMS.

PHEVs aim to increase the electric component in a hybrid drive. However, in order to do so they must increase the battery weight and end up being heavier than a HEV. Hence, during a Charge Depleting- Charge Sustaining (CDCS) operation the PHEVs will be as good as BEV within its all electric range. As the distance to be traveled in one charge increases the fuel consumption of a PHEV will gradually approach that of a HEV and eventually surpass it as shown in Figure 2.12.

Regenerative braking

One of the most important advantages of electrifying the powertrain is the ability to recuperate the deceleration energy of the vehicle. Considering the overall efficiencies of the regenerative system components, approximately 60 -80% of the deceleration energy may be regained. However, the weak link in the regenerative system chain is the battery. Batteries do not exhibit charge acceptance characteristics which would be enough to absorb all incoming deceleration power. High incoming current may damage battery

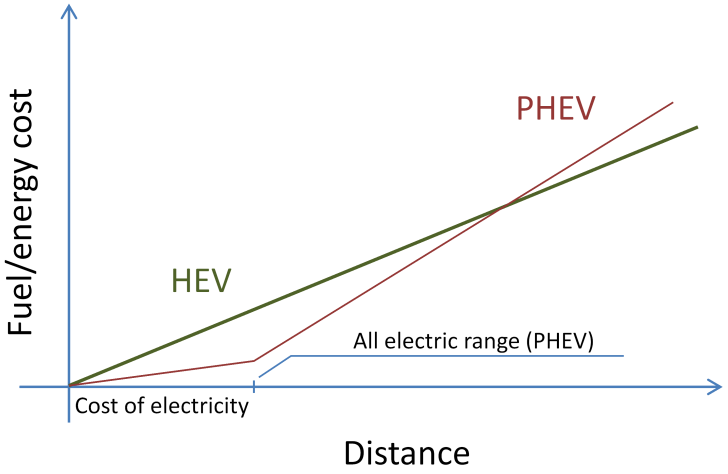


FIGURE 2.12: Comparison of HEV and PHEV as energy savers

chemistry. Therefore, OEMs have limited the BEV motor deceleration to about -1 to -1.3 m/s^2 . Normal vehicle deceleration requirements range till about -3 m/s^2 to -9 m/s^2 in emergency situations. Certain new Li-Polymer batteries [GAI09] claim to have charge acceptance characteristics which may be enough for most deceleration maneuvers in city and highways. In this case though EMS must take into consideration battery limitation in terms of battery temperature status and state of health.

ITS and ICT (Intelligent Transportation Systems and Information Communication Technology)

Recent technological advances in ICT has enabled access to real time beyond horizon information. For e.g. digital maps, e-horizon, V2V and V2I are technologies already capable of providing information to the vehicle driver which can be very useful to increase safety and economy of the vehicle. Such information may be combined with the EMS to ensure optimum use of powertrain capacity for energy regeneration or in some cases to decide the best times to charge or discharge the batteries. For e.g. it may be better to discharge the batteries before a downhill slope to ensure enough battery capacity to absorb the incoming charge. In another case it would be better to charge the battery enough before encountering a long traffic jam on a highway where it would be better to use only motor and switch the engine off. In city traffic, V2V-V2I communication data can effectively help reduce fuel consumption by providing information about traffic signal status allowing for gradual deceleration, better regeneration and smooth traffic flow.

To conclude, it must be stressed that at present, the development in autonomous vehicle control, powertrain electrification and intelligent transportation systems is too fragmented (academically and industrially). However, in the end, all these fields present

substantial potential towards efficient mobility and vehicle emission reduction. The smart and green adaptive cruise control function is a first attempt to combine various aspects of the above mentioned technologies and evaluate its potential to enhance vehicle efficiency without compromising safety.

Chapter 3

Simulation Models and Methodology

To evaluate the SAGA function on basis of energy analysis and longitudinal motion kinematics, the function is simulated using mathematical models of BEV, HEV, PHEV and conventional IC engine powertrain in Matlab Simulink environment. This chapter presents a comprehensive overview of modeling of the individual components used to generate the different powertrain models as well as the internal functioning of the overall vehicle model. The basic electric vehicle model is based on the eFuture BEV prototype. Methodology of vehicle modeling and model validation is discussed.

3.1 Component Models

The simulation models for conventional (IC engine) vehicle, BEV, HEV and PHEV are build using various component models arranged in different configuration. In the following subsection, models of the powertrain components are described in detail.

3.1.1 IC Engine

The model for an IC engine gives a relation between the mechanical energy delivered to the transmission by the engine and the chemical or fuel energy consumed in order to do so. The base for development of such a model is the fuel consumption data derived from experimental tests. This data consists of static fuel consumption recorded at constant engine speeds for increasing engine power values at predetermined intervals. There are many factors influencing fuel use, such as air properties like temperature, pressure, and

humidity, fuel properties like fuel composition (blend), octane number, and volatility, engine properties like age, wear, and maintenance state, etc., but in particular measures built into the engine controller that aim at reducing emissions. It is assumed that most of these effects are averaged out, are sufficiently small to be neglected, or can be included via model parameters [dJvKK13]. The recorded data may be used as look up tables to find the fuel consumption at a particular power and speed point or may be approximated with a piecewise affine relation referred to as Willans line approximation [Pac69]. Using such technique eliminates the need to store all the data in a look up table and saves the precious memory space in a microcontroller application. In offline simulation though, the look-up tables are used.

The IC engine model is based on a Saturn 1.9 liter, 105 ps gasoline engine with 164 Nm peak torque at around 2500 rpm. Figure 3.1 shows the engine map which indicated the fuel consumption in g/kWh.

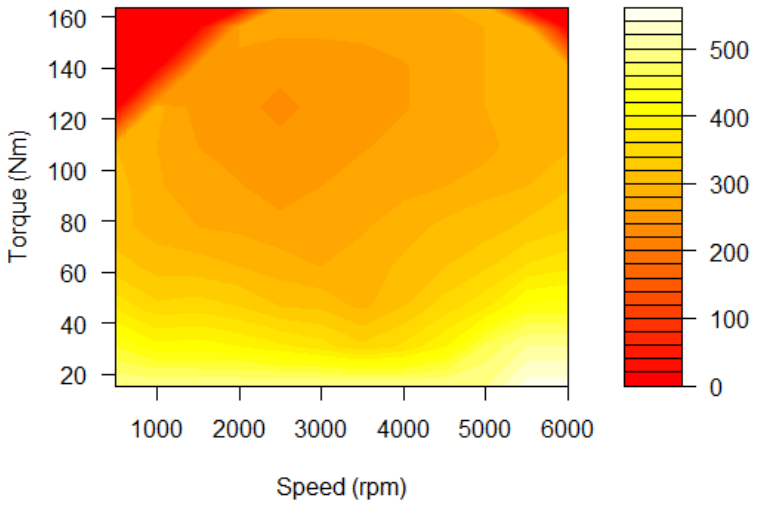


FIGURE 3.1: Base efficiency engine map for a Saturn 1.9 liter engine in g/kWh

The input for the model is engine torque and speed (operating point) values. Depending on the fuel consumption value, sample time and covered distance the overall fuel efficiency is calculated into grams and later into liters per 100 km as the simulation end result.

3.1.2 eMotor

Given its high efficiency and superior power to size ratio, permanent magnet synchronous motor (PMSM) was chosen for the powertrain in the eFuture project. A 30 kW PMSM e-Motor with 750 Nm peak torque is modeled in Simulink. The motor model is based on

look-up table data provided by motor suppliers which define the speed-torque characteristics and also the copper and mechanical power losses corresponding to the operating point of the motor. The look-up tables are generated through physical measurement of the real motor over its operating range (0 - 1070 rpm). The motor model is supplied with speed (ω), torque request and battery voltage as inputs. The motor torque is calculated by adding the driver requested torque and power losses. Power required is the product of motor torque and speed. Since the voltage is known the current requirement for this power request is calculated. The calculated current value is supplied as an input signal to the battery model.

The torque speed characteristics for the e-Motor are shown in Figure 3.2 along with the efficiency map and the maximum possible acceleration (using 2 such motors) for the eFuture project prototype vehicle. Hence, a total maximum torque of 1500 Nm is available.

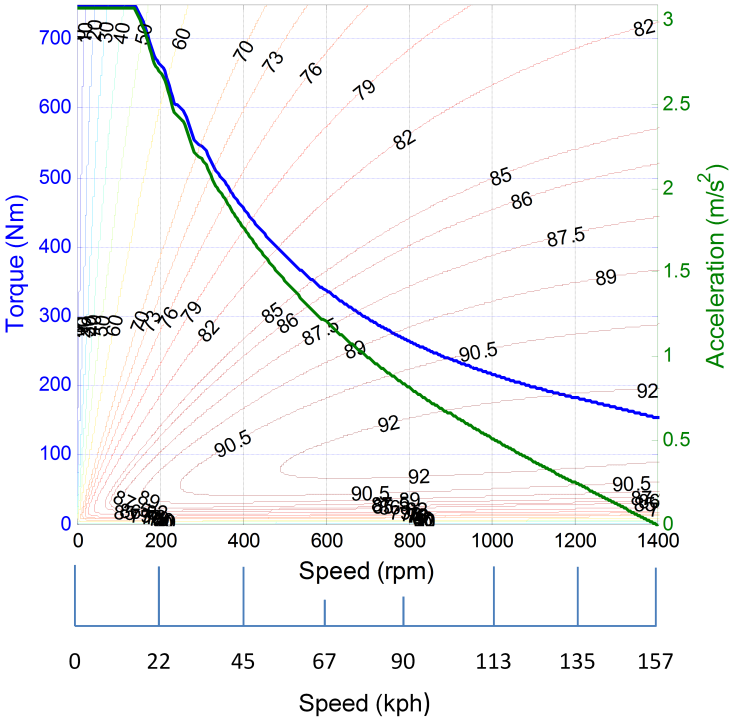


FIGURE 3.2: Motor torque-speed-efficiency characteristics

The maximum acceleration is calculated taking into consideration the vehicle data of the eFuture prototype described later. The motor has an integrated reduction gear with gear ratio of 10. The actual motor is a high speed motor with a peak torque of 150 Nm and maximum speed of over 10000 rpm. It can be observed that the gearing is chosen such that it adjusts the torque-speed characteristics so as to maintain the frequent operating points of powertrain in the high efficiency region. For example, the electric vehicle will

be driven mostly at a speed between 30 to 100 kph, here we have an efficiency range from 80 to 95 %.

3.1.3 Battery (Energy Storage System)

The energy storage system (ESS) is a lithium-ion battery developed as a part of the eFuture project by Miljøbil Greenland AS. It is a 230 V, 26 kWh battery pack based on the NMC (Lithium Nickel Manganese Cobalt Oxide) chemistry. NMC has good overall performance and excels on specific energy. This battery is the preferred candidate for the electric vehicle and has the lowest self-heating rate.

From the energy calculation point of view, the battery simply presents itself as a load with a variable resistance. Some energy is lost in overcoming this resistance and hence we speak about the battery efficiency (ohmic loss). The internal resistance of the battery depends on various factors like,

1. Battery state of energy
2. Battery temperature
3. Battery state of health

For the purpose of simulation, normally it is assumed that the battery temperature will be regulated within tolerable limits and hence, the internal resistance will not be affected adversely within these temperature ranges. However, in the eFuture prototype there is no active cooling and hence in the battery model the temperature factor is considered. An effect due to state of health is neglected in favor of reduced complexity of the battery model. In this case the battery model is partly based on the equivalent circuit or Thevenin model as described in [KDN+07] which represents the overall capacity of the battery, the internal resistance and transient behavior of the battery using a series resistance and two RC circuits. Additionally, the effect of temperature is also taken into consideration for -25 to 50 °C range based on experimental data from Miljøbil. With respect to the agreements in eFuture project it is not possible to publish the experimental data hence the battery model is to be treated as a black box. In Figure 3.3, the characteristics of battery model over a velocity cycle using the eFuture vehicle prototype is shown.

The following equations are valid for battery energy calculation in the vehicle models.

$$dE_{batt.dis} = P_{eM}dt/(\eta_{eM} \times \eta_{batt.dis}) \tag{3.1}$$

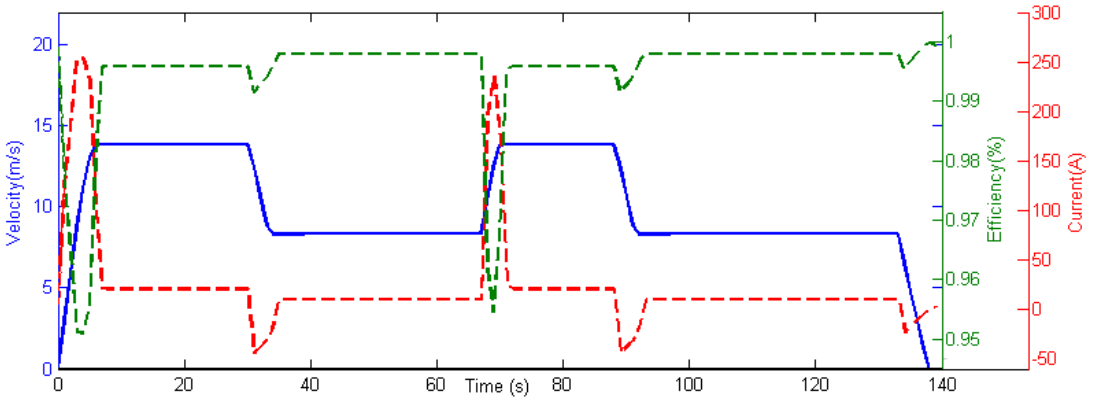


FIGURE 3.3: Battery efficiency characteristics over a cycle

$$dE_{batt.chg} = P_{eM} \times \eta_{eM} \times \eta_{batt.chg}\ dt \tag{3.2}$$

where, $dE_{batt.dis}$ or $dE_{batt.chg}$ is battery discharge or charge energy in that sample time, η_{eM} is motor efficiency, $\eta_{batt.dis/chg}$ is battery discharge or charge efficiency and P_{eM} is motor power.

3.1.4 Inverter

The inverter is an integral component of motor control. Battery power is DC whereas the vehicle is propelled with an AC PMSM motor. The inverter conditions the battery power and supplies the motor with required AC power in accordance with motor controller commands. In Figure 3.4 the efficiency for the inverter is shown. It is observed that the inverter efficiency is not only dependent on output current but also the modulation index (value which defines amplitude or frequency modulation for motor control). This makes it computationally intense to calculate the exact inverter efficiency at every sampling point. Considering that the inverter efficiency remains in the higher range (above 90%), in the simulation it is preferred to choose an average 96% flat efficiency for all operation points. This simplifies the model and allows faster computation with low complexity without heavily compromising accuracy.

3.1.5 DC/DC converter

A DC/DC converter is used to bring the battery voltage to the powertrain system voltage (like a boost converter in a Toyota Prius) or to bring the traction battery voltage down to supply energy to the 12 V powernet in the vehicle. The eFuture prototype powertrain runs on the battery voltage value. Hence, the DC/DC converter is used only to step

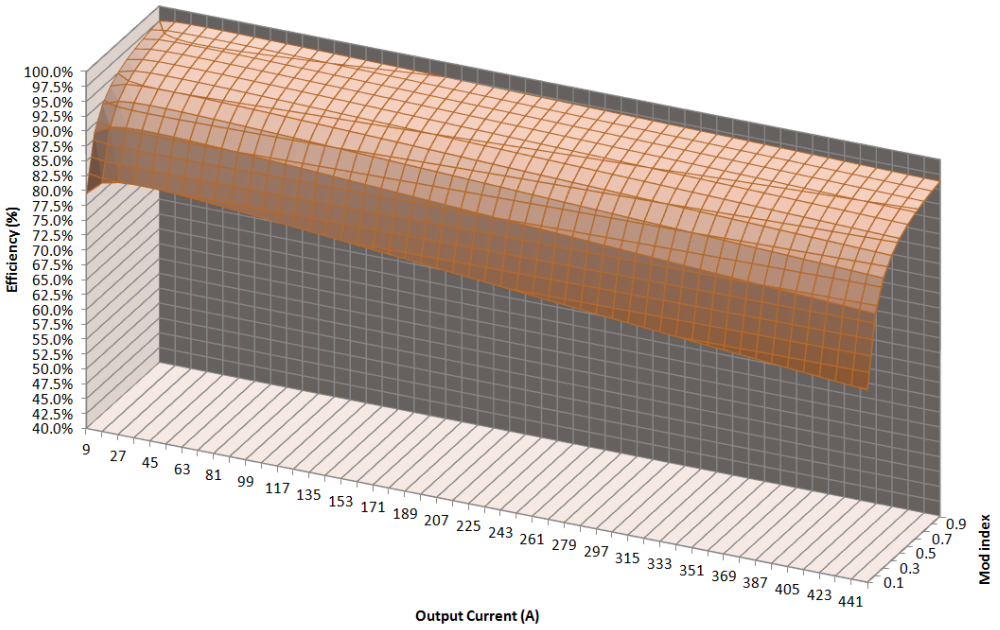


FIGURE 3.4: Data for inverter efficiency

down the battery voltage to 12 V for the electrical accessories. An efficiency of 96% is assumed for this conversion [EHZM06].

3.1.6 Power-split device

The power split device distributes the power demand between the electrical side and chemical/fuel side of the powertrain. There are different ways through which such a distribution is possible. For example, a very standard way is to use a planetary gear box as in a power split hybrid or direct addition of torques as in case of parallel hybrids. In this case though the topology used is a power-split hybrid with a through the road configuration. Since the two power sources are powering two separate axles the power exchange/addition actually occurs through the road.

Another significant part in the power-split system is the logic which decides the power-split between IC engine and e-motor. Here, the ECMS strategy is used to decide the optimum torque which is demanded from the respective power sources. A detailed description regarding this part is found in further sections.

3.1.7 Velocity cycles

Velocity cycles are a set of velocity values defined over time. Velocity cycles/drive cycles were primarily developed to validate powertrain performance with respect to vehicle

tailpipe emissions. They are also relevant to quantify the benefit of hybrid electric vehicle in terms of CO_2 emission reduction and fuel saving benefits. The cycles differ with respect to vehicle types, traffic environment (city, highway etc.), region and so on. Initial standardized cycles such as the NEDC (New European Driving Cycle) consisted of a set of constant acceleration, velocity and deceleration phases. Further development in this field led to formation of Artemis [And04] and Worldwide harmonized Light vehicles Test Procedure (WLTP) [wlt] (Figure 3.5) cycles which resemble a real world driving pattern.

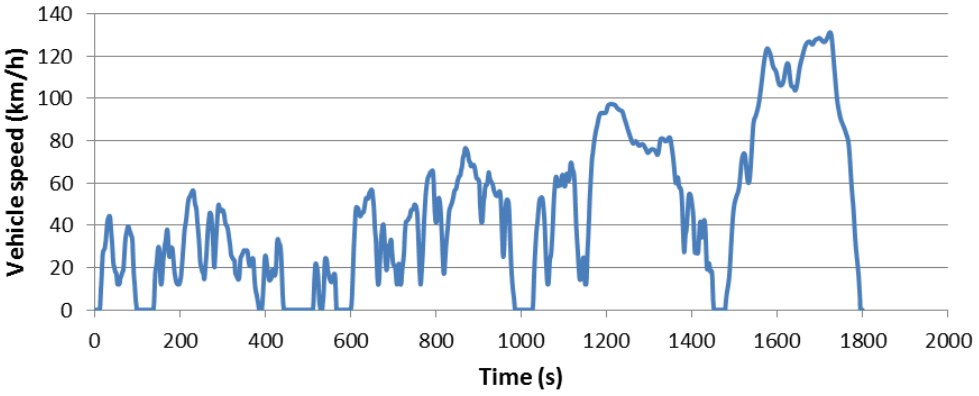


FIGURE 3.5: Worldwide harmonized Light vehicles Test Procedure

Nonetheless it is highly unlikely that in the real world situation a vehicle on the road will follow the specific velocity cycle like city or highway. Therefore, simulation results derived from velocity cycles will have considerable errors when compared to real tests. It is however important to note that the velocity cycles represent a similar average velocities and acceleration/ deceleration values as in real world and hence can be used as a base in simulations to find approximate benefits of using electric and hybrid vehicles against conventional vehicles.

In the second approach, a city cycle is defined using only speed limits and corresponding distances. Such an approach is important to find the best acceleration and deceleration behavior of an electric vehicle given a speed limit. Such a cycle is shown in Figure 3.6

3.2 Vehicle models

3.2.1 Battery electric vehicle

The BEV model is based on the eFuture prototype using the vehicle properties as listed in Table 3.1. A vehicle model may be developed with two slightly different approaches as shown in Figure 3.7. In a backward looking approach, the velocity cycles are taken

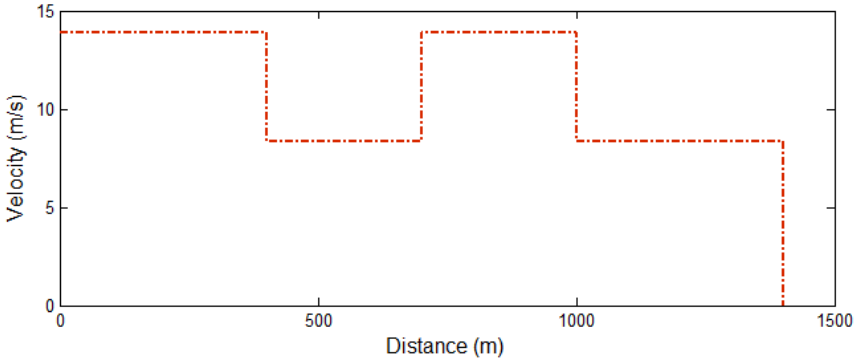


FIGURE 3.6: Cycle defined with velocity limits

into account. Here the force and the corresponding energy required to move the vehicle with respect to the given velocity cycle is calculated using the velocity and time values already specified. Since this approach considers that the vehicle has already completed the velocity cycle it is known as a backward looking approach.

On the contrary a forward looking approach uses distance based velocity limits instead of actual time based velocity points. The velocity trajectory is based on a driver model torque request. The actual velocity profile is based on the interaction between various forces acting on the vehicle like, air drag, acceleration, gradient and wheel resistance. Once the velocity profile is known, the energy required is calculated in a way similar to backward looking approach. Since the velocity profile is decided from the driver torque request, this kind of approach is known as a forward looking approach. Both kind of approaches are modeled and used in this thesis.

The BEV model is developed with an aim to calculate the energy consumption and mainly takes into account the forward longitudinal movement of the vehicle. Such a generic model for electric energy consumption is also used as a module to build the hybrid vehicle model along with the IC engine model. Details for modeling and validation for the electric energy consumption model can be found in Appendix A.

TABLE 3.1: eFuture prototype parameters

Vehicle mass	m	1550 kg
Front area	A	2.28 m^2
Drag coefficient	C_w	0.36
Wheel radius	r	0.3 m
Coefficient of rolling resistance	f_r	0.015

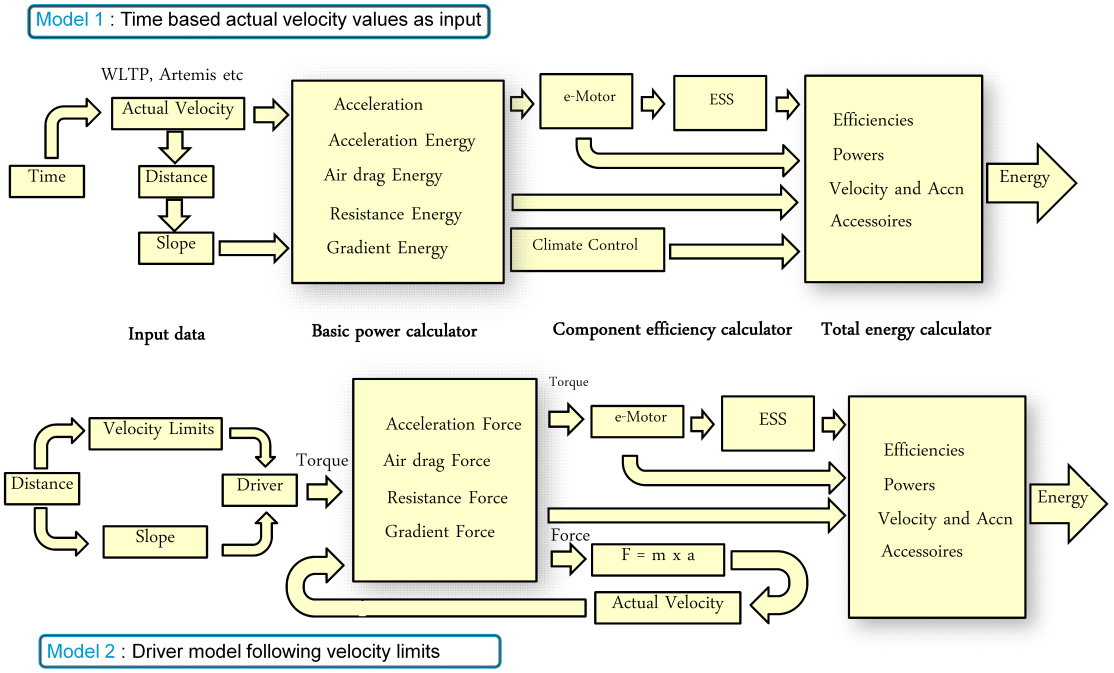


FIGURE 3.7: Forward (model 2) and backward (model 1) looking modeling approaches

3.2.2 Conventional vehicle

Figure 3.8 represents the schematic diagram of the conventional vehicle model built using Matlab and Simulink.

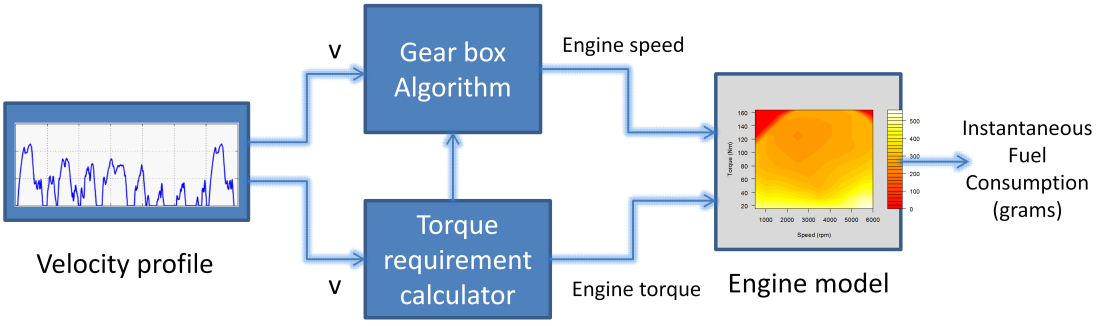


FIGURE 3.8: Schematic model of a conventional vehicle

The model is developed using the same modular building blocks of a BEV as described in previous section. For example, the torque requirement calculator block in conventional vehicle model is based on the similar basic power calculator block (inside Driver Model block) in BEV model as shown in Figure A.2. This block receives the velocity profile as input and calculates the torque required to move the vehicle in accordance with that velocity profile. This block uses the same equations as described in BEV model section (equations A.1 to A.8). The velocity profile is also supplied to the gearbox model which

calculates the actual engine speed according to the gear. The best possible gear is decided based on an efficiency based algorithm as described in Figure 3.9 using Stateflow.

This algorithm takes into consideration the best engine efficiency island contours. For example, for the first gear the engine speed is not allowed to exceed 3000 rpm. When the powertrain is shifted to next gear the engine speed drops according to the gear ratio as compared to the lower gear. This brings the engine operating point closer to the best efficiency region. Different limit speeds in decreasing order are chosen for higher gears to bring the operating point in best efficiency region as soon as possible. Simultaneously, it is also checked if the torque requirement is met, if not the lower gear is chosen. The overall fuel efficiency of a vehicle is drastically affected by the proper or improper gear selection. Hence, it is important that during the comparison of a conventional vehicle to a hybrid vehicle we consider the best possible fuel efficiencies offered by both topologies. The use of this intelligent gear selection algorithm yields the best possible efficiency from the IC engine in the given situation. In order to account for the reduction in battery weight as compared to hybrid vehicle, it is assumed that the conventional vehicle is 200 kg lighter. Apart from this all other vehicle specifications are considered to be same as the battery electric vehicle (Table 3.1).

A 5-speed manual transmission is modeled which complements the IC engine torque-speed characteristics. Since gear selection is controlled by the energy management algorithm, it may as well be classified as a semi-automatic transmission. The gear ratios in increasing respect are 3.250, 1.950, 1.423, 1.033 and 0.730. The final gear ratio is 4.063 and it yields the total powertrain gear ratio as a product with individual gear ratios.

Finally, as observed in the schematic diagram Figure 3.8, the engine model receives the engine speed and torque values and gives the instantaneous fuel consumption as output. This must be integrated and converted accordingly to get the overall fuel consumption in liters or liters/100km taking distance into consideration.

3.2.3 Hybrid electric (charge sustaining TtR)

The simulation model for hybrid electric vehicle is realized by combining the building blocks for BEV and conventional vehicle powertrain and adding a torque-split definition block with operation strategy algorithm. The model represents a charge sustaining HEV which means that the operation strategy will try to maintain the battery SOC within defined tolerance limits around the reference SOC. For a charge sustaining HEV, a 7 kWh battery is modeled as shown in Figure 3.10 which represents a schematic diagram for the Through the Road (TtR) HEV. A TtR hybrid is fundamentally a parallel hybrid which splits power between IC engine and motor both operating at same speed. As seen

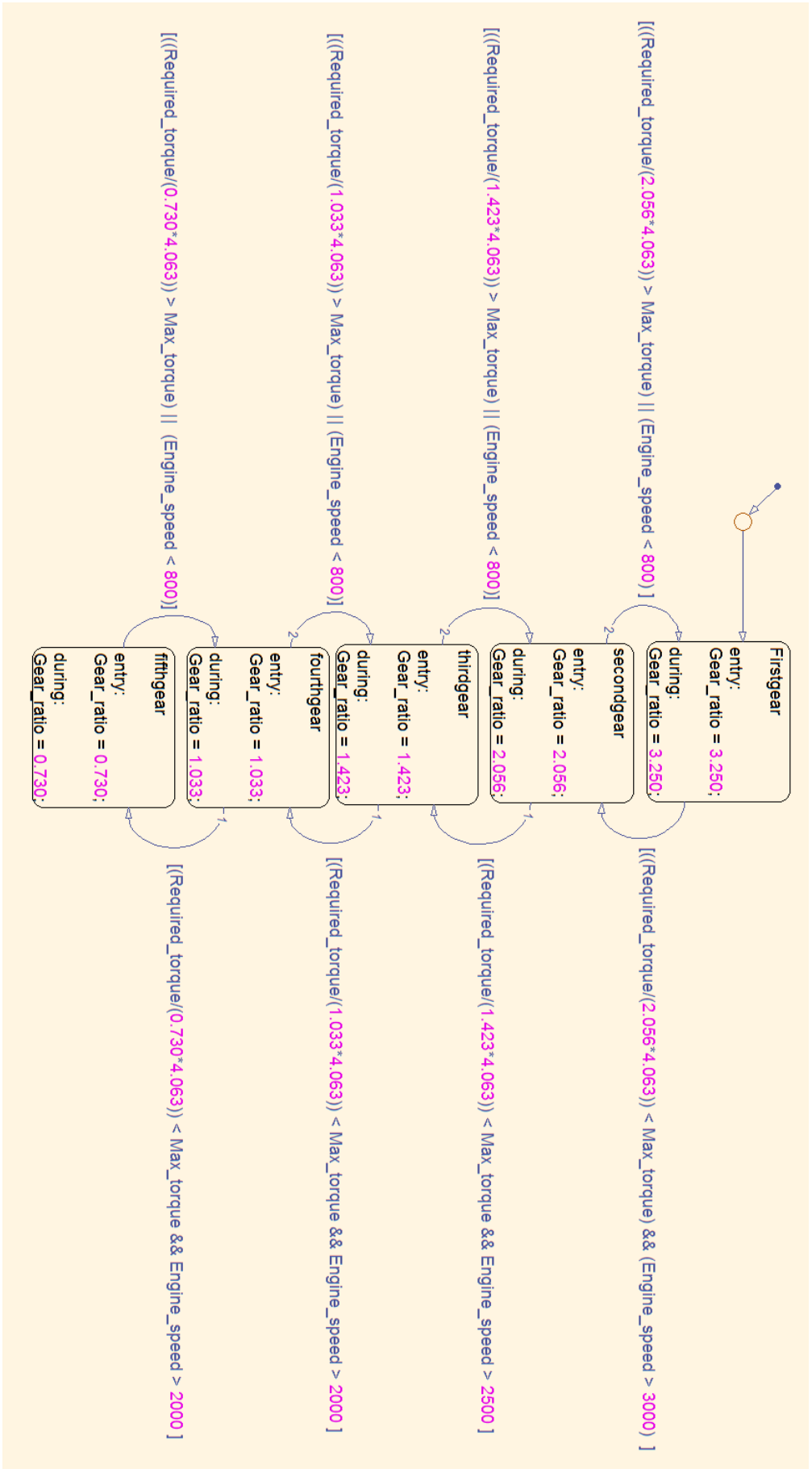


FIGURE 3.9: Intelligent gear selection algorithm

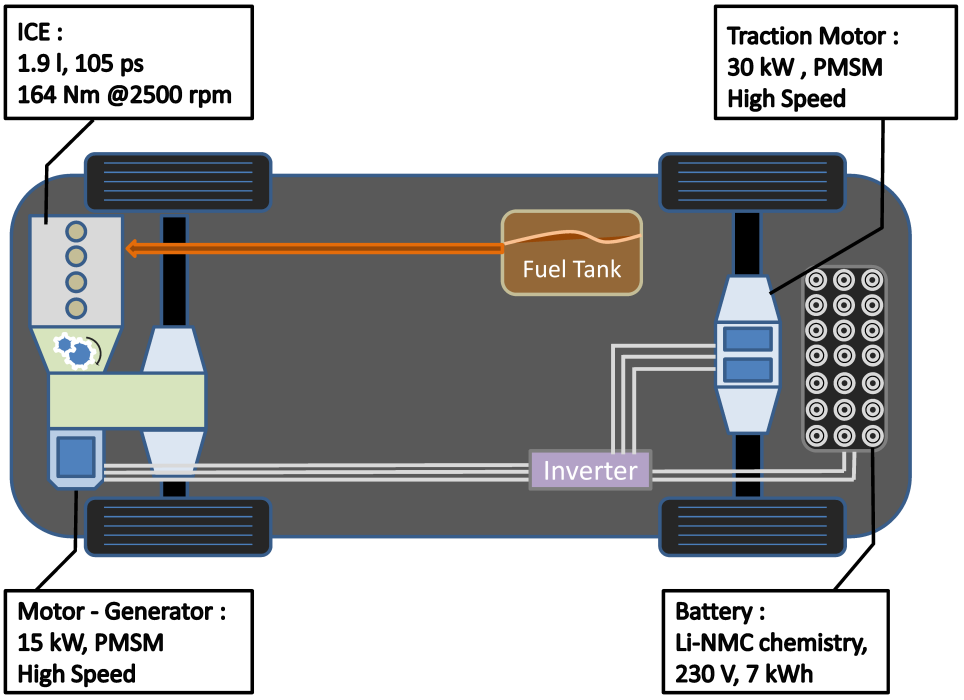


FIGURE 3.10: Through the road (TtR) hybrid electric vehicle (7 kWh battery for Charge sustaining)

in the diagram, the TtR hybrid has no mechanical connection between the front power axle and rear power axle except through the road (hence the name). This feature of the TtR hybrid allows the operation strategy logic to control the motor and engine torque with more flexibility as compared to a normal planetary gear power split hybrid. For example, in the Prius HEV which uses the planetary gear power split system, the engine has to forcibly come ON after the vehicle reaches a certain speed because if the motor runs too fast with engine at zero speed then the maximum allowable speed for generator is reached. To avoid this the engine is forced ON even if the battery has a high SOC.

The TtR hybrid uses the engine model as described in earlier sections which powers the front axle along with a 15 kW motor-generator in a parallel combination. On the rear axle, two modular motors with total power of 30 kW are used. For a charge sustaining hybrid a 7 kWh battery is used whereas for a charge depleting plug-in hybrid a 13 kWh battery is used. The HEV is defined by the following equations.

$$u_{split} = T_{eM}/T_{total} \tag{3.3}$$

$$T_{total} = F_x \times r \tag{3.4}$$

$$T_{eM} = u_{split} \times T_{total} \tag{3.5}$$

$$T_{ice} = (1 - u_{split}) \times T_{total}/g_{ice} \tag{3.6}$$

where, u_{split} is power-split ratio, T_{total} is the required torque, T_{eM} is torque demanded from electric motor, T_{ice} is torque demanded from IC engine, g_{ice} is the total drive ratio and F_x is the traction force at wheel with r as wheel radius. Apart from this the standard energy calculation equation as described in BEV and conventional vehicle model are valid for HEV. The total energy consumption is calculated according to the energy supply from respective power sources as demanded by the operation strategy.

It is assumed that because the HEV uses less kWh battery storage it saves the battery weight in comparison to a BEV. However here there is an addition of IC engine hence overall it is safe to assume that the HEV will have same weight as that of the BEV.

3.2.4 Plug-in Hybrid electric (charge depleting TtR)

The main difference between the charge sustaining HEV model and the plug-in HEV (PHEV) model is the battery capacity and the operation strategy algorithm. PHEVs are suppose to have enough all electric range (AER) to be used in the city only on electric charge. Hence, the battery for PHEV is designed to be 13 kWh as compared to 7kWh of HEV. Also, the main aim for the PHEV operating system is to use the battery energy as much as possible to compensate for the low efficiency of IC engine. Hence, unlike the charge sustaining HEV, the PHEV uses a blended or charge depleting charge sustaining (CDCS) strategy.

Chapter 4

The Smart and Green ACC function

This chapter introduces the entire concept of a Smart and Green Adaptive Cruise Control in detail. It discusses the necessity, feasibility and limitations of the proposed concept for an intelligent vehicle longitudinal motion controller. The fundamental ideas which enable an ACC to be smart and green are presented along with the problem definition and possible solutions for the SAGA function.

4.1 Introduction

The adaptive cruise control (ACC) is certainly not a new concept. With an Adaptive Cruise Control system, the driver delegates the longitudinal vehicle-control task. When the system is active, the vehicle speed is controlled automatically either to maintain a given clearance to a forward vehicle, or to maintain the driver desired speed, whichever is lower. Since as early as the 90s, car manufacturers offer this system on their high-end cars. However, research is still active. Researchers aim at evaluating the impact of the ACC on traffic, under congested situation [MMB01] or with improved strategies [KTSH07]. They also extend the range of possible speeds, driver comfort, safety or road capacity [VE03], [MMY09]. In 2006, the introduction of a vehicle to vehicle communication (cooperative ACC, C-ACC) allows to decrease drastically the clearance to a forward vehicle [NVP+09] and also to create stable vehicle platoon. The evaluation of the C-ACC [VAvDV06], [NSC+10] shows promising results on road capacity and safety. An ISO standard now defines the intended performance of the ACC [ACC10].

SAGA is an acronym for the Smart and Green Adaptive cruise control. Throughout the history of the ACC, right from its inception till the recent development of co-operative ACC, it has been implemented and researched with respect to conventional IC engine based vehicles. The normal modus-operandi for ACC has largely remained same wherein the system generates a command based on the driver/front sensor input and the powertrain has to fulfill the demanded torque request irrespective of other operation parameters like efficiency or future (beyond horizon) traffic conditions which the front sensors are oblivious about.

However, recent development in fields like robotics, environment sensing, processors speeds and information and communication systems have provided an array of advanced applications which are being actively explored and researched for a direct implementation in the automotive field. This has enabled the development of autonomously driven vehicles, vehicle to vehicle communications and vehicle to infrastructure communications. With implementation of these technologies, the actual definition of ACC as an ADAS becomes obsolete. ACC itself becomes a part of the main control system which can longitudinally and laterally control the vehicle on its own without any direct driver commands. This system is aware of traffic situation and events beyond horizon and is capable of initiating appropriate control actions in order to enhance safety and efficiency based on overall information provided to the system. Thus, these capabilities make such a system smart and green.

Furthermore, the next generation of vehicle powertrains are no more based on only IC engines. Considering the need for environmentally friendly modes of transportation, the trend in vehicle propulsion systems is towards electrification and hybridization. To reduce the adverse effects of conventional IC engine vehicles, it is sought to substitute the oil energy by clean electric energy. Nevertheless, the limited range and expensive components of a battery electric vehicle means that it will never completely replace the conventional powertrain, whereas a hybrid electric vehicle is only as efficient as its IC engine. Each modern powertrain topology presents its own efficiency characteristics and hence it must be carefully evaluated in order to operate as efficiently as possible. Hence, the ACC for the new generation of vehicles is not just about converting driver commands into vehicle motion safely, but also to achieve highest level of possible energy efficiency thereby reducing air pollution by utilizing the accessible information and propulsion component's capabilities in a smart way preferably applicable in an autonomous vehicle. In this context a Smart and Green ACC is proposed.

From previous literature research, simulations and energy analysis we develop certain approach towards energy saving potential of strategies. The SAGA function is built on these strategies.

1. Reduction in acceleration energy by supplying energy at best component efficiencies
2. Regenerating as much energy as possible with respect to component limitations
3. Reduction in air drag energy by limiting the velocity to an optimum level
4. Adapting speed according to speed limits before hand to allow smooth energy regeneration
5. Tailoring SAGA for specific powertrains like BEV, HEV and PHEV
6. Tailoring SAGA for specific traffic situations like city and highway
7. Optimizing safety and efficiency in the system by computing a unique blend for every situation

4.1.1 Basic concept

Since the SAGA function is based on the standard ACC concept, like the normal ACC, the SAGA also operates in two modes. When there is no obstructing vehicle in the motion path then it must follow the driver desired speed with respect to legal speed limits. This is the "speed control mode". In case of an obstructing vehicle being present, the SAGA must follow the front vehicle at safe distance headway in the "distance control mode". Here two possibilities emerge. If the SAGA is applied to a partially automated vehicle then a driver activation is required to engage the SAGA function, else in a completely automated vehicle the function may be permanently activated as a full speed range ACC (FSRA). Figure 4.1 gives a schematic representation of the modes of operation for the SAGA function whereas Figure 4.2 and Table 4.1 presents the terminology for a generic case of SAGA. The modes are described in detail in the following.

Speed Control Mode

This mode is active in the phase where there is no front vehicle detected. As there is no interaction with other road users in this mode, it is not mainly safety critical. In this mode, SAGA behaves like a normal ACC. In some cases, acceleration is directly proportional to the velocity difference between actual and function desired speeds. In others, the acceleration may be optimized. Similarly, deceleration is optimized for maximizing recuperation. For both, acceleration and deceleration, SAGA must follow the standard performance guidelines as defined in ACC guidelines [ACC10].

To simplify the initial version of a SAGA function, it is assumed that the vehicle will move with respect to the driver desired velocity or the speed limit whichever is lower. It

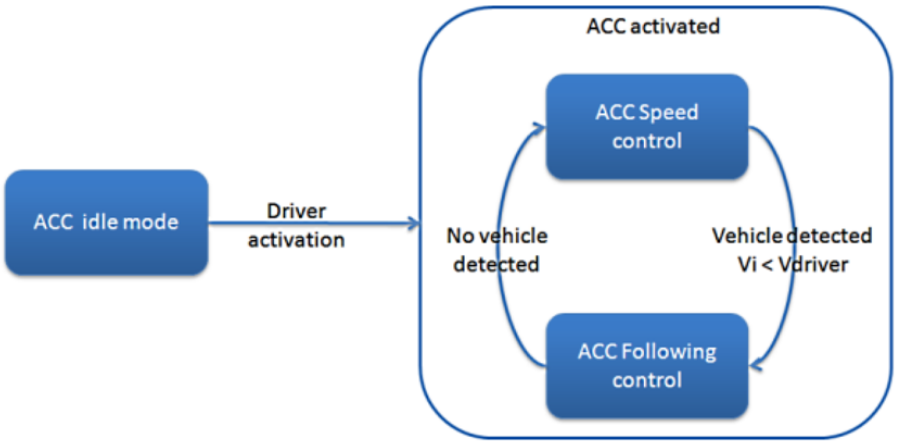


FIGURE 4.1: SAGA: Modes of operation

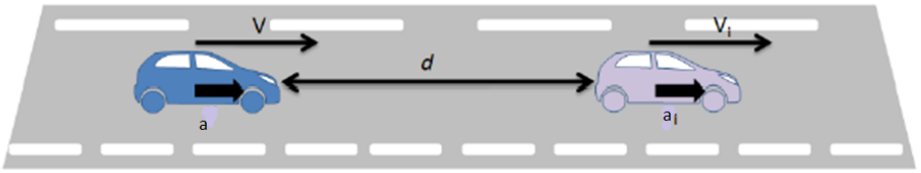


FIGURE 4.2: SAGA: Generic use case

TABLE 4.1: Terminology SAGA generic case

Clearance to the lead vehicle	d	m
Speed of the ego vehicle	V	m/s
Driver desired speed	V_d	m/s
Time headway	T	s
Desired time headway	T_d	s
Speed of lead Vehicle	V_i	m/s
Relative speed	ΔV	m/s
Acceleration of lead vehicle	a_i	m/s^2
Acceleration of ego vehicle	a	m/s^2

must be however taken into account that such a strategy would not be optimum for every vehicle topology. For example, in highway scenario, driving with a very high velocity will require higher power due to the higher velocity drag losses. While such a phenomenon will have less effect on the range of an IC engine vehicle (high energy density of fuel), or a HEV and PHEV or range extender vehicle, it will drastically reduce the range of a BEV. It will also result in considerable increase in fuel consumption and CO_2 emissions of conventional and hybrid vehicles. On the other hand driving with higher velocity will result in lower time to destination which is again another important factor. Hence, the question which arises here is that whether an individual would be ready to spend some extra time driving with lower velocity and saving energy and generating lower CO_2 or time is of more importance. Perhaps in future with the arrival of autonomous driving, there may be a possibility to govern the speed of vehicles according to optimization of energy and time where the passenger in the vehicle may be able to use the extra travel time for personal activity.

For now however, it is assumed that the vehicle accelerates according to proportional rule and maintains a driver desired or speed limit velocity. If ΔV is the difference between present velocity and desired velocity and K_s is a tuning constant then, the resultant acceleration a is given by the following formula.

$$a = K_s \cdot \Delta V \tag{4.1}$$

In specific cases it is sought to optimize the acceleration. Such instances are discussed in details in further sections where applicable.

Distance Control Mode

This mode is activated upon detection of front vehicle. Normally, the sensor range is 150 m. This headway can be further divided in two sub-phases. Figure 4.3 depicts a generic case for the SAGA distance control mode. The "speed equalization phase" where the ego vehicle (with higher velocity V) approaches the front vehicle (with lower velocity V_i) and decelerates in order to equalize speeds. After this, the ego vehicle follows the front vehicle with constant headway spacing (2 seconds considered safe) in the second phase. In the distance control mode, the objective is to regulate the error on the headway clearance e_d ($e_d = d - T_d \cdot V$) around 0 except during a special case where vehicle deceleration to a stop is considered where V becomes 0 and hence a certain constant headway to front vehicle must be specified. The terminology used to describe the equations is stated in Table 4.1. The algorithm behavior can be made more smoother and robust (for

safety response) by including the relative speed ΔV into control equation. The resulting acceleration is the control output defined by these two errors.

$$a = K_{cv} \cdot \Delta V + K_{cd} \cdot (d - T_d \cdot V) \tag{4.2}$$

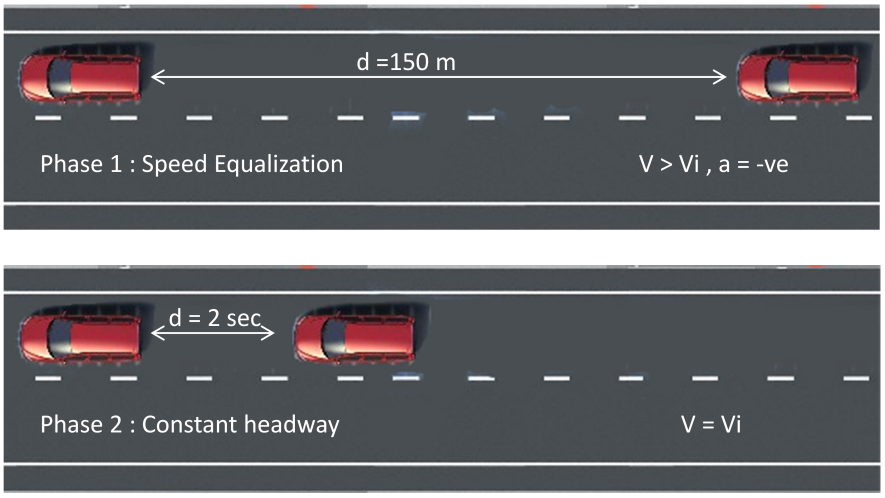


FIGURE 4.3: Phases in distance control mode

Here, the constants K_{cv} and K_{cd} are tuning parameters which adjust the control feedback intensity of velocity and distance error respectively on the resultant acceleration or deceleration. If during distance control phase the front vehicle accelerates and increases the distance headway then an appropriate positive acceleration is generated by the SAGA function to close the resulting error. Such a value is made to saturate at 2 m/s^2 with respect to the ACC guidelines.

4.1.2 Constraints of the regeneration system

The SAGA function is developed as a safe and efficient longitudinal vehicle controller. The aim is to achieve same level of safety as any other standard ACC while ensuring a higher level of operating efficiency through various measures. Regeneration of energy using the regenerative motor braking system is one of the most effective ways to increase operation efficiency. Hence it becomes imperative that during braking maneuvers, as much energy should be regained as possible. For this purpose the complete braking maneuver must be organized in such a way that it is possible to decelerate the vehicle using only motor brake but without compromising the safety of passengers.

There are two limitation which define the total deceleration performance of a regenerative system namely,

1. Negative torque limitation of the motor.
2. Energy absorbing or charge acceptance capacity of the regeneration system (mainly battery system)

To design a system which must operate within these constraints it is important to analyze them beforehand. In this regard, the maximum deceleration performance of the motor is analyzed in Figure 4.4. This analysis results are obtained assuming that the motor model described in Section 3.1.2 is used in the eFuture prototype. The data for such a vehicle model is defined in Table 3.1. This vehicle model is simulated over its operating velocity range to find the balance of forces acting on the vehicle at various velocities and then compute the maximum deceleration offered by the system under the influence of only motor braking (exclusive motor braking).

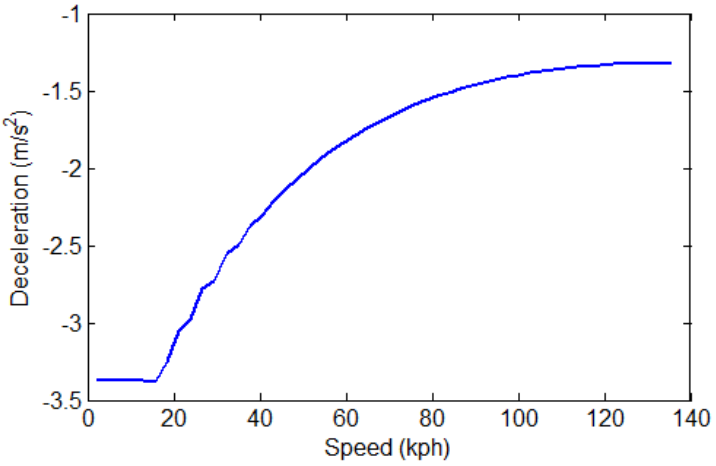


FIGURE 4.4: Maximum deceleration offered by motor (eFuture)

From Figure 4.4, it is clear that for low speeds of about 10 - 45 kph (city driving) motor braking is quite sufficient for normal braking situations requiring -2 to - 2.5 m/s^2 deceleration values. Emergency braking in city averaging below -3 m/s^2 may not be achievable through only motor braking. Again, looking at speeds above 60 kph (country roads) and above 100 kph (highway domains) it is clear that motor braking would be clearly insufficient for average deceleration maneuvers averaging less than -2 m/s^2.

In this context, as observed in Figure 4.3, in the distance control mode there are two phases where the vehicle undergoes deceleration. First is the speed equalization phase where normally a headway spacing of 150 m is available. Such scenarios will be mainly encountered on highways. From various SAGA simulations on eFuture prototype model it is observed that, given the motor torque limitations, if the velocity difference between the lead and the ego vehicle is above 20 m/s then exclusive motor braking is dangerous. Situations with velocity difference below 20 m/s are good application areas for SAGA

function as applied to eFuture prototype which has a limited motor performance. Furthermore, in the vehicle following phase, it is expected that a constant headway spacing of 2 s is maintained as stated in the ISO ACC guidelines [ACC10]. In such situation if the front vehicle undergoes emergency braking then unless the ego vehicle applies conventional brakes, a collision is inevitable.

Therefore, while designing the SAGA function it is necessary to take into account the constraints from the motor torque limitations and adjust the algorithm accordingly so as to achieve the required safety standard while, in parallel, also aiming for a higher operating efficiency.

Apart from motor, there are constraints on the battery side. During the regeneration phase battery must absorb the incoming charge. Any battery will have an internal impedance which must be overcome to absorb the incoming power. This results into heat losses which increases the battery temperature. Within tolerable limits an increase in battery temperature will not have a considerable effect on its internal resistance. However large amount of incoming power may increase battery temperature above permissible limits depending on the cooling system at work. High temperature increases the internal resistance in turn producing more heat again increasing the temperature (a pronounced effect is observed above 50 °C internal cell temperature). This type of cycle may lead to a thermal runaway in battery (battery melts). Hence, limitations on the amount of incoming current have been defined for every battery type. These limitations define the restriction on the performance of the regenerative braking system.

Considering the trend in automotive battery applications, it is clear that in future too the most preferred battery would be a lithium based one. In the eFuture vehicle prototype a NMC chemistry based lithium battery is used. NMC chemistries are very suitable as traction batteries owing to their good power and energy density characteristics. These characteristics can be tuned to obtain a desirable battery behavior. Figure 4.5 gives an idea about the charge acceptance characteristics of the eFuture traction battery. These are obtained after taking an appropriate safety factor into account. In accordance with non disclosure agreement in the eFuture project, it is restricted to publish details about calculation process of battery current acceptance limits.

For a 26 kWh battery pack, it is seen that within normal temperature operating range and for most of the SOC region, a 10 sec pulse of 100 amperes is allowable. This battery contains 2 parallel modules with each module having a 3 Parallel- xx Series (3PxxS) configuration ("xx"refers to number of cells). Another configuration with more cells in parallel may help increase the permissible incoming power.

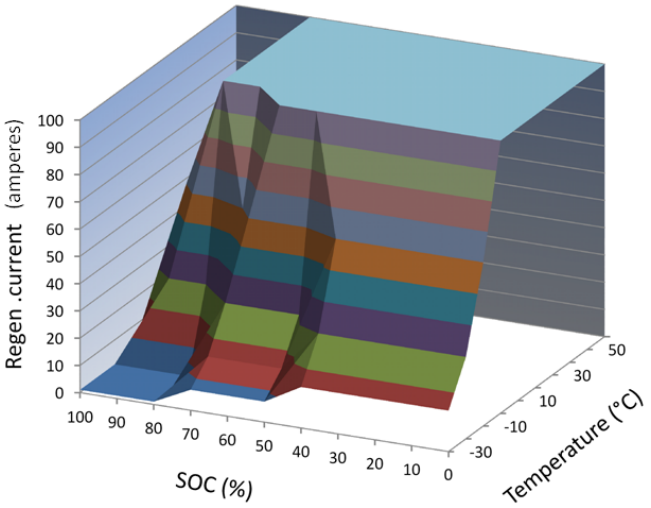


FIGURE 4.5: Regenerative charge acceptance characteristics of a NMC battery

In some other chemistries like the Lithium iron phosphates [A12] it is seen that a even single 18650 cell packs enough charge acceptance (power absorbing) capacity as compared to a complete battery pack of NMC chemistry. Figure 4.6 shows the details of one the Li-iron phosphate cells.

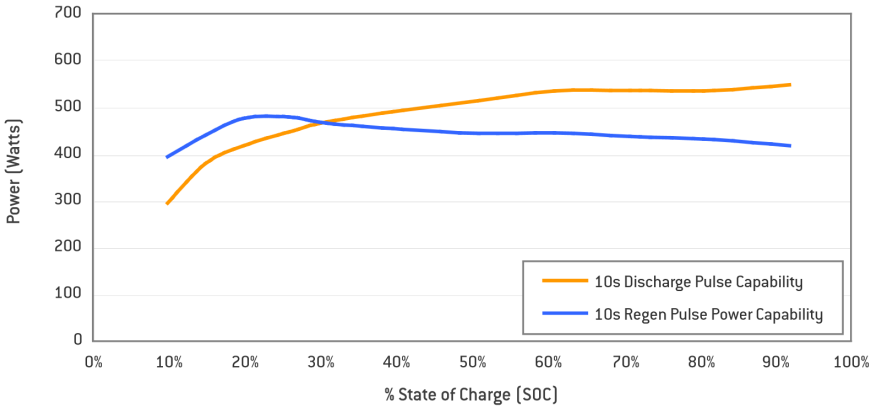


FIGURE 4.6: A123 cell characteristics for pulse charge acceptance (V_{cell} = 3.8 - 1.6)

It is claimed that the cell can absorb on an average 450 Watts power with voltage range 3.8 to 1.6 V. It may be inferred that the current acceptance in this case would be in range from 118 - 281 amperes. Theoretically, a configuration of 3P xxS using these cells must suffice most of the regenerative braking requirements. With the eFuture prototype, if the highway scenario is considered where the speed equalization phase is being performed, then a maximum incoming power of 30 kW can be expected (motor peak power capacity). Therefore, the design for battery pack configuration (xxP-xxS) for cells and modules must be decided taking the regenerative charge acceptance requirements into account. This will define the final battery pack voltage which would in turn decide the amount of current flowing in each parallel cell line. This current must be within permissible

limits for the 10 s regeneration pulse and must suffice the incoming regenerative braking power requirements. A regenerative pulse need not be only for 10 s, however for longer regenerative braking maneuvers it must be ensured that the amount of average energy absorbed in the time (maximum 60 sec) must be the same as that in maximum allowable energy in a 10 s pulse.

Finally, it can be concluded that if a battery is designed to required specifications of regenerative braking, it will not be a constraint for smooth operation of the SAGA function. The required current characteristics during the regenerative braking for the eFuture powertrain model are discussed in Section 5.4.5.

4.1.3 Concept of Safety envelope

From earlier discussion, it is clear that regenerative braking has a limited performance as compared to conventional braking systems. While regenerative motor assisted braking can achieve minimum -3 m/s^2 deceleration depending on motor speed, a conventional barking system is capable of decelerating with -4.5 m/s^2 in emergency situations. On paper it can even achieve a minimum of -9 m/s^2. This is however limited by the tire material (the softer the better) and Anti-lock braking system performance.

Therefore, to take into account the limited braking capacity of regenerative braking system and its effect on safety the concept of safety envelope is introduced. Figure 4.7 shows the safety domains for the conventional braking and regenerative braking systems.

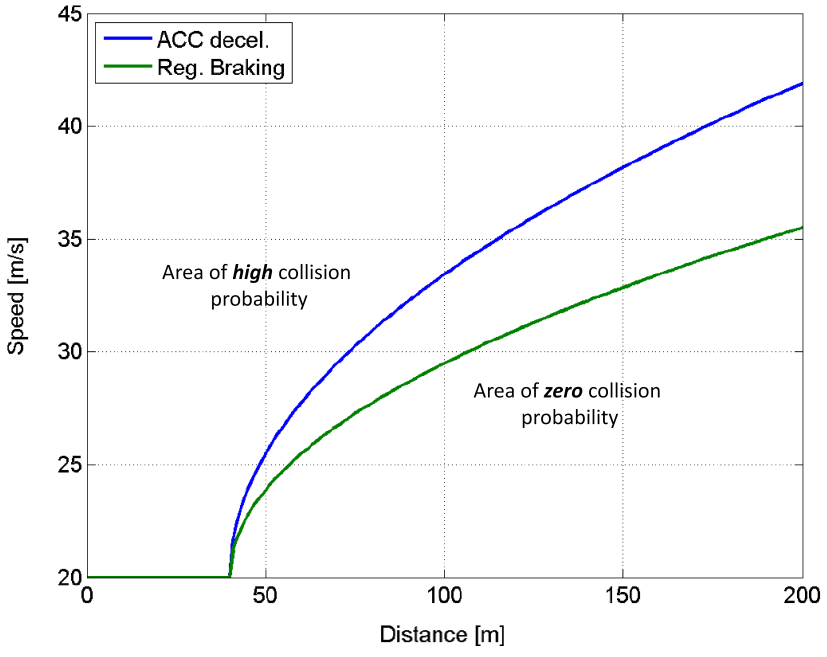


FIGURE 4.7: Comparison of conventional ACC and regenerative braking safety domains

The y-axis represents the ego vehicle speed whereas the x-axis gives the headway distance spacing between the vehicles. In this figure, we suppose that a front vehicle has a constant speed of 20 m/s and that the driver sets the time headway at 2 s. The objective is then to regulate the acceleration of our vehicle to reach the point (40 m, 20 m/s). We can define a limit curve as being the points (d, v) which allow to reach this point with a given braking capacity. Points above this curve represent the condition where a collision with front vehicle is highly probable (unless front vehicle accelerates or a lane change maneuver happens). The points below this curve are in a safe area. As the regenerative braking has limited performance compared to conventional ACC, the safe area is smaller. If we want to keep the performance in terms of speed, the sensing range must be greater, on the other hand, if we want to keep the same performance on the sensors, then the maximal speed must be smaller.

On the basis of the concept of safety envelope it is possible to define the phase 1 (speed equalization, Figure 4.3) of the distance control problem in the SAGA function. Figure 4.8 represents the safety envelope for SAGA function using regenerative braking.

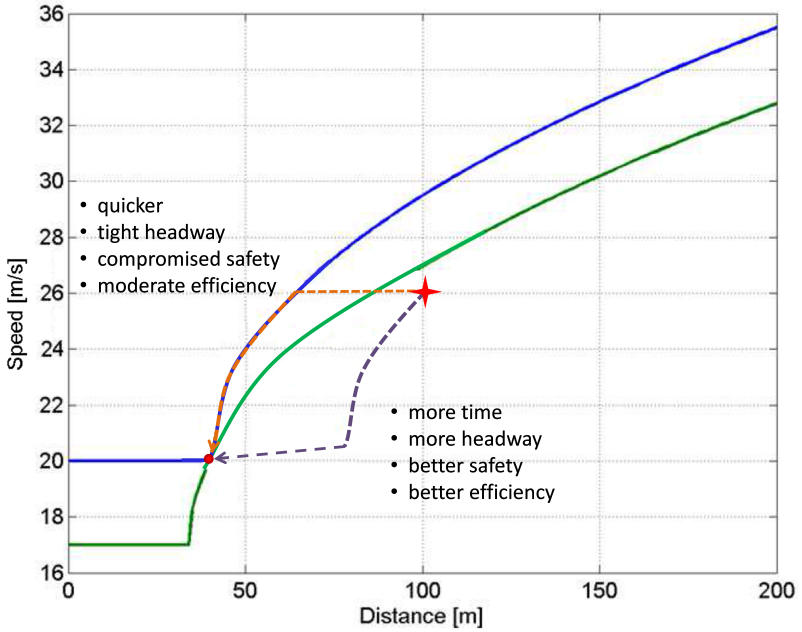


FIGURE 4.8: Variation of the safe domain with a deceleration of the lead vehicle

Here, we consider a hypothetical case where the lead vehicle is traveling at a constant velocity of 20 m/s and the ego vehicle approaches with 26 m/s velocity and is at a distance of 100 m from the lead vehicle. With respect to the gradual reduction of headway spacing, there are several ways with which the ego vehicle can approach the lead vehicle to equalize their speeds. In Figure 4.8, two extreme ways are shown where in the first one (orange path) the ego vehicle maintains its the velocity until it reaches the safety envelope limit. From here on, it undergoes maximum possible regenerative

deceleration thereby following the safety envelope till the equalization of speeds at the specified headway spacing distance of 40 m (corresponding to 2 s headway). On the contrary, the second path (indigo) follows an immediate deceleration maneuver in order to remain well within the safety envelope. The speed is reduced till it is slightly higher than the lead vehicle, thereafter a smooth and gradual deceleration is applied to equalize the speeds and attain the specified distance headway.

Comparing the two approaches, it is clear that the first approach (orange) is the quicker maneuver which will close the headway between the two vehicles early to avoid any chance of third vehicle cut-in. On the other hand, it must be noted that in case the front vehicle undergoes deceleration during the speed equalization phase and say, reduces its velocity to 17 m/s (green curve) then it is observed that the ego vehicle goes out of safety envelope into the high collision probability area where it must resort to conventional emergency braking and lose on the efficiency side. Due to its tendency to remain well within safety envelope from start, the second path (indigo) will remain within the safety envelope even when the front vehicle reduces its speed. However, the second path is much slower compared to the first path which means that it will take more time to close the gap between the two vehicles. This presents an opportunity for a third vehicle to cut-in which will make the situation even worse. Hence, it is necessary to find a trade-off between the two approaches where it is possible to maintain safety in all situations without losing the regenerative capability.

4.1.4 ISO guidelines

The International Standards Organization (ISO) has set certain guidelines regarding the definition, performance requirements, operational limits and test procedures for conventional adaptive cruise control systems in the document "Intelligent transport systems - Adaptive Cruise Control systems - Performance requirements and test procedures" [ACC10]. SAGA function is an extension of the normal ACC systems. Since, the SAGA function is aimed at partial automation (similar to normal ACC) and fully automated (or autonomous) application, there are certain operational limits which need to be re-considered. A document for guidelines for an autonomous longitudinal controller for an autonomous hybrid electric is as of now not yet available from ISO, hence for SAGA function a new set of guidelines must be developed which would be based on ISO 15622:2010 and adapted accordingly.

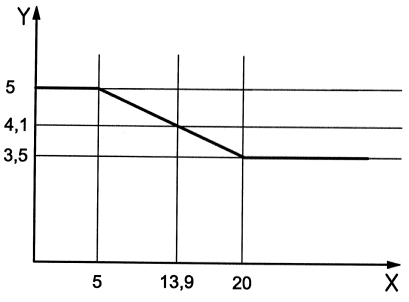
Operational Guidelines for ACC systems

1. The minimum set speed shall be $v_{low} \geq 7$ m/s

2. The average automatic deceleration of ACC systems shall not exceed 3.5 m/s^2 (avg. over 2 s)
3. The average rate of change of automatic deceleration (negative jerk) shall not exceed 2.5 m/s^3 (average over 1 s)
4. Automatic acceleration of ACC systems shall not exceed $a_{max} \leq 2$ m/s^2

Operational Guidelines for Low Speed Following (LSF) systems

1. v_{max} shall not exceed 13.9 m/s
2. v_{min} shall not exceed 1.39 m/s
3. There shall not be a sudden brake force release in case of an automatic deactivation of LSF system
4. The average automatic deceleration of LSF system shall not exceed 3.5 m/s^2 (average over 2 s) when the vehicle is above 20 m/s (13.9 for LSF) and 5 m/s^2 (average over 2 s) when the vehicle is travelling below 5 m/s.
5. The average rate of change of automatic deceleration (negative jerk) shall not exceed 2.5 m/s^3 (average over 1s) when the vehicle is travelling above 20 m/s and 5 m/s^3 (average over 1 s) when the vehicle is travelling below 5 m/s
6. No limits on maximum acceleration are mentioned in guidelines for LSF



Key
X subject vehicle speed, expressed in m/s
Y maximum deceleration, expressed in m/s^2

FIGURE 4.9: Deceleration limits for LSF system

Operational Guidelines for Full Speed Range ACC (FSRA) Systems

1. The average rate of change of automatic deceleration (negative jerk) shall not exceed 2.5 m/s^3 (average over 1 s) when the vehicle is travelling above 20 m/s and 5 m/s^3 (average over 1 s) when the vehicle is traveling below 5 m/s (similar to LSF)

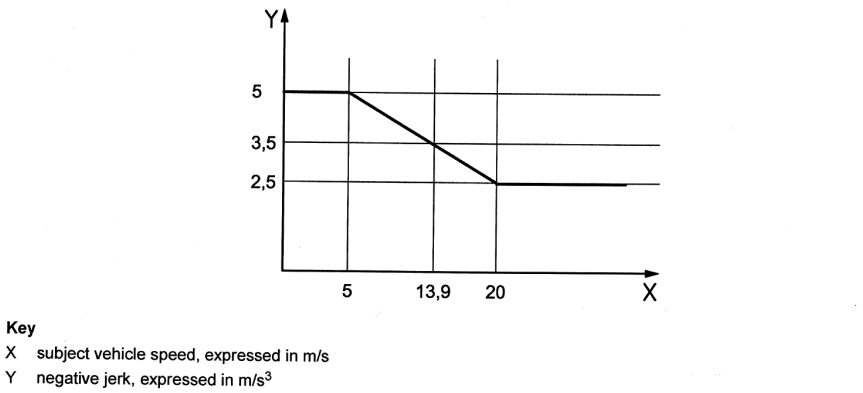


FIGURE 4.10: Jerk limits for LSF system

2. The average automatic acceleration shall not exceed 2 m/s^2 (average over 2 s) when the vehicle is traveling above 20 m/s and 4 m/s^2 (average over 2 s) when the vehicle is traveling below 5 m/s

Operational Guidelines for SAGA Function

The SAGA function was initially developed as an ACC (activation above 7 m/s). Later with addition of further steps it is finally developed as a FSRA function which resembles as a autonomous longitudinal vehicle motion controller. Hence the operational limits for SAGA are a combination of operational limits for the above three functions namely ACC, LSF and FSRA.

1. The average rate of change of automatic deceleration (negative jerk) shall not exceed 2.5 m/s^3 (average over 1 s) when the vehicle is traveling above 20 m/s and 5 m/s^3 (average over 1 s) when the vehicle is traveling below 5 m/s (same as in Figure 4.10)

2. The average automatic deceleration of SAGA function shall not exceed 3.5 m/s^2 (average over 2s) when the vehicle is above 20 m/s and 5 m/s^2 (average over 2 s) when the vehicle is travelling below 5 m/s like shown in Figure 4.9 (except in case of emergency where no limits on deceleration is proposed)

3. Till 55 kph the vehicle acceleration has not been capped according to guidelines in LSF, except the ACC guidelines cap it at 2 m/s^2 above 7 m/s. In SAGA the acceleration is optimized till 55 kph and mostly remains within ACC guidelines. Above 55 kph there is no optimization for acceleration and ACC guidelines are strictly followed

4.2 Problem definition

Following the introduction of the SAGA concept in the earlier sub-sections above, it is necessary to summarize the highlights of the broader concept and set up a problem definition. In the following, the main idea and constraints are concisely presented.

4.2.1 Safe headway spacing

This parameter is most relevant to the vehicle following phase (Figure 4.3) i.e. the constant headway phase and mainly in highway driving situations. Normal ACC guidelines suggest a headway spacing of at least 2 s between front and following vehicle. In Germany, by law the minimum allowable headway on freeways is 0.9 s [BS98]. However, these values are decided taking into consideration the conventional braking performance of the vehicle. Regenerative braking performance is relatively lower than conventional braking as seen in Figure 4.4. Therefore, to decide a safe headway spacing for SAGA function it is necessary to consider the following points.

1. Headway spacing d may not be so small that it will compromise safety or activate emergency or conventional braking every time the front vehicle decelerates
2. It must support a realistic possibility for regenerative braking so as to regain the large energy packets of depleting kinetic energy
3. It may not be so large so as to allow a third vehicle to cut in. This will lead to cycle of events where more vehicles will likely cut into the large gap while the ego vehicle gets pushed back to adjust the headway spacing according to the new front vehicle

Therefore, the headway spacing d will have to be tuned according to the above mentioned constraints and the regenerative braking performance of the vehicle.

4.2.2 Minimization of energy consumption

The main reason behind integrating a smart and green concept with a normal ACC is to improve the vehicle operating efficiency and reduce the CO_2 emissions. In this task, it is assumed that the powertrain components are constants i.e. any increase in efficiency is to be solely achieved by smartly utilizing the capabilities of present powertrain components to the fullest by conditioning the vehicle motion characteristics to reflect best overall vehicle efficiency. In this context, two approaches are considered, namely, from energy

supply side and from energy regeneration side. These approaches are constrained with the following points.

1. Energy supply at best overall powertrain efficiency operating points
2. Achieving an acceptable Energy/Distance ratio by optimizing energy required and time required for the travel distance
3. Maximum energy recuperation: This requires maximum use of regenerative braking system without compromising safety. The limitation posed from limited motor braking torque and limited battery charge acceptance characteristics must be considered

4.2.3 Passenger comfort

In order to achieve the ideal safety and efficiency characteristics, the SAGA function must modify the motion characteristics of vehicle taking into consideration the regenerative braking system constraints. This can be better explained by referring to Figure 4.8 with two possible approaches of ego vehicle to front vehicle in phase 1 of speed equalization. While the first approach (orange) is quicker, it closely resembles the braking method of most human drivers who prefer to equalize speeds as late as possible. The other approach (indigo) tries to equalize speeds early and then closes gap with mild but long deceleration phase. This deceleration phase will try to push the passenger in forward direction which might be a seating position of compromised comfort. Frequent repetition of such long events may cause fatigue and irritation to some individual who may dislike the experience.

On the other hand, in the phase 2 of constant headway (Figure 4.3), it must be ensured that the ego vehicle must not frequently apply emergency brakes and strictly abide with the ACC guidelines.

4.3 Possible solutions for the deceleration phases

It is clear that the most attractive situation for energy regeneration is at highway speeds where large amount of kinetic energy depletion takes place during the speed equalization phase. To absorb this energy it would be necessary to employ regenerative braking during the entire deceleration phase. In the constant headway phase, it might be at times necessary to decelerate to maintain the headway distance to front vehicle. If possible such decelerations may also be obtained from regenerative braking system. In

the following, certain possible solutions are presented and discussed. In next sections, feasibility of these solutions will be demonstrated on the basis of simulation results. It must be noted that the eFuture prototype does not have the ability to control the hydraulic brakes electronically, in other words brake-by-wire is not possible. This limits the feasible braking strategies that can be applied on the prototype. However, for simulation purposes, this fact is ignored and a system capable of brake-by-wire ability for hydraulic brakes and eMotor braking is investigated.

4.3.1 Exclusive motor braking

One solution is to simply use motor braking in all situations. This would ensure maximum regeneration of braking energy. Of course such a strategy must be tuned beforehand with respect to maximum allowable velocity difference between the front and following vehicle at the point of detection (headway of 150 m). In case of eFuture prototype, the twin motors can provide an average deceleration of -1.7 m/s^2 in the highway speed domain. For most deceleration maneuvers on highway, such braking performance might be acceptable as long as it does not compromise safety by breaching the safe headway space buffer. There are several other traction motors which offer better deceleration performance (higher negative torque capacity) than the eFuture prototype motor. In such cases, this strategy of exclusive motor braking may prove useful. Here, the constraints from battery charge acceptance must be respected. For example, the next generation product of the motor which was used in eFuture performs far better with continuous power of 67 kW as compared to 30 kW for eFuture prototype [YAS]. The Yasa-250 motor achieves a peak power of 180 kW at 700 V. This is enough power to compare with conventional braking. For 65 kW continuous power rating, the incoming regeneration current at 700 V battery voltage would be 92 amperes and at 350 V, 184 amperes. From earlier discussion (Section 4.1.2), it can be stated that it is possible to design a battery compatible for the required charge acceptance performance.

In this context it is helpful to take a glance at the highway deceleration characteristics for different types of vehicles compiled by [MB12] presented in Figure 4.11 and Figure 4.12.

From the comprehensive data on various deceleration rates from [MB12] and Figure 4.13 [Kam] and comparing it with the eFuture prototype regenerative braking deceleration performance (Figure 4.4) it can be concluded that on highway speeds of about 100 kph, the regenerative braking does provide just enough performance to fulfill the deceleration requirements. Therefore, a strategy with only/exclusive motor braking can indeed be

Various Parameters of Deceleration Manoeuvre

Vehicle Category	Max. Speed Range (km/h)	Max. Speed (m/s)	Mean Speed (m/s)	Decel. Time (sec)	Decel. Distance (m)	Speed at Max. Decel. (m/s)	Max. Decel. Rate (m/s^2)	Mean Decel. Rate (m/s^2)
Truck	20-30	7.54	4.33	16	70.88	3.748	0.719	0.474
	30-40	10.46	5.84	21.3	124.39	3.82	0.753	0.457
	40-50	13.26	7.32	20.33	148.81	3.85	0.876	0.518
	50-60	14.55	7.92	30.75	243.54	3.93	0.88	0.512
Car	92-94	25.83	10.32	8.08	83.38	10.28	1.532	1.151
	94-96	26.38	12.77	8.32	108.8	16.17	1.56	1.124
	96-98	27.12	13.14	8.60	113.04	23.28	1.608	1.208
	98-100	27.67	14.61	8.78	129.59	24.24	1.625	1.335
Motorized Three-Wheeler	27-31	8.2	5.49	19.85	107.52	3.154	0.845	0.353
	31-35	9.19	5.82	27.33	159.33	3.21	1.12	0.306
	35-39	10.24	6.54	26.45	172.31	3.63	1.14	0.357
	39-43	11.37	7.07	28.42	201.05	3.21	1.059	0.364
Motorized Two-Wheeler	40-50	12.75	8.22	18.30	152.01	7.52	1.603	0.581
	50-60	14.90	10.28	21.21	214.82	7.27	1.327	0.473
	60-65	16.95	12.73	23.00	292.79	9.65	0.59	0.411

Max. – Maximum, Decel.– Deceleration

FIGURE 4.11: Reference for deceleration rates

Deceleration Rates Observed by Various Researchers

Author	*Year*	*Speed range (km/h)*	*Deceleration Rate (m/s^2)*
Gazis et al.	1960	72	4.9
St. John and Kobbet	1978		1.07
Parsonson and Santiagio	1980		3
Bester	1981		0.6-1.9
Lee et al.	1984		0.28-0.96
Wortman and Fox	1994	48.3-80.5	2.1-4.2
Wortman and Matthias	1983	57.6-76.4	2.5-4
Brodin and Carlsson	1986		0.5
Watanatada et al.	1987		0.4-0.6
McLean	1991		0.5-1.47
Bennett and Dunn	1995	60-70	1.39
		70-80	1.78
		80-90	2.22
		90-100	2.34
Akçelik and Besley	2001	60	3.09
		40-50	2.4
Wang et al.	2005	50-60	2.39
		60-70	2.67
		70-80	2.52
		80-90	2.55

FIGURE 4.12: Reference for deceleration rates

Reference	When	Deceleration	Comments
ITE (Traffic Engineering Handbook)	2009	3.0 m/s²	Constant value of deceleration at an intersection
Gazis et al.	1960	4.9 m/s²	Deceleration rate of a vehicle traveling at 45 mph to stop.
Williams	1977	2.95 m/s²	Average maximum deceleration rate of vehicles traveling at or below 25 mph
Parsonson and Santiago	1980	3 m/s²	
Wortman and Matthias	1983	2.1~4.2 m/s² Mean = 3.5 m/s²	Test speeds ranged from 30 to 50 mph
Chang et al	1985	Mean = 2.9 m/s²	For speeds higher than 20 mph
Haas et al	2004	0.1g at 25 mph 0.18g > 45mph	Haas model suggests lot of variability in deceleration, but the mean increases from speeds 25 mph to 45 mph and remains constant after that.
Ihab et al	2007	3.27 m/s²	Found that deceleration rate depended on time to intersection.

FIGURE 4.13: Reference for vehicle decelerations at intersections

considered for further simulation and investigations regarding its pros and cons. However, this can be only considered for speed equalization phase. For constant headway following phase, strict exclusive motor braking cannot be recommended for 2 s time headway. In [GAO+13], simulations show that to implement an exclusive motor braking strategy (with eFuture prototype) for constant headway following phase, the safe headway must be increased to 5 s. This means that at 100 kph the distance between lead and following vehicle must be about 138 m. Such a setup hardly makes sense with respect to vehicle cut in and highway capacity performance and hence must be discarded.

On the other hand, as seen in Figure 4.13, the deceleration requirements for intersections (e.g. signals in city traffic) is more than 3 m/s^2. Hence, implementation of exclusive motor braking strategy in city traffic (especially intersections) cannot be recommended from safety point of view at present. However, these data values are from traffic measurements without any V2V or V2I influence. It is highly probable that with implementation of ITS, which would transmit relevant traffic events data regarding intersection traffic like time to green/red to autonomously driven vehicles, the deceleration requirements at intersections can be brought down considerably. Furthermore, if the regenerative braking system is actually designed to generate about -5 m/s^2 deceleration, this strategy may be implementable in city traffic at present conditions.

Considering that Δt is time headway in seconds and $a_{vehicle}$ being ego vehicle acceleration, the strategy is defined as,

for all Δt,

$$a_{vehicle} = a_{regen} \tag{4.3}$$

4.3.2 Threshold braking strategy

Since the exclusive motor braking strategy does not hold good for constant headway phase as described earlier, a modified strategy has to be developed to improve on the safety factor of the exclusive motor braking strategy. This can be done by compromising on the efficiency side and allowing partial conventional braking only if required.

In this regard, it is proposed to reduce the required time headway spacing of 5 s to 3.7 s or less to minimize the risk of vehicle cut in. The deceleration is still demanded through motor braking in speed equalization and constant headway phase. However, if the time headway drops below the threshold of 1.5 s then conventional braking is engaged with its maximum braking force to bring the ego vehicle back into safety envelope. Once the vehicle is outside the safe headway space buffer (2 s headway), the regenerative braking is again engaged.

Emergency conventional braking performance can generate braking of 0.9 g depending on road surface conditions and tire material. However, it would be a problem if frequent emergency braking procedures are engaged every time the front vehicle undergoes deceleration. In this case, system acceptance from drivers will be low. From simulations, it must be determined if the increase in energy efficiency is worth the passenger discomfort.

Considering that Δt is time headway in seconds, Δt_{safe} is the safe time headway for following the front vehicle and $a_{vehicle}$ being ego vehicle acceleration, the strategy is defined as,

$$\Delta t_{safe} = 3.7s \tag{4.4}$$

for all $\Delta t \geq \Delta t_{emergency}$ (set at 1.5 s),

$$a_{vehicle} = a_{regen} \tag{4.5}$$

for all $\Delta t < \Delta t_{emergency}$ (set at 1.5 s),

$$a_{vehicle} = a_{emergency} \tag{4.6}$$

4.3.3 Optimized blended braking

The effectiveness of SAGA function will directly depend on driver/passenger acceptance of the concept. The person travelling in the vehicle is assumed to be a layman in terms of automobile energy consumption or regenerative braking system behavior and hence will have difficulty in trusting a system which

1. Frequently employs emergency braking
2. Employs risky control like getting too close to the front vehicle
3. Deviates from normal ACC behavior

The driver/passenger will have little tolerance towards systems which enhance efficiency by compromising safety. Therefore, for vehicles like eFuture prototype which are "under-powered"in terms of motor braking capacities must resort to sacrificing regenerative energy for road safety. In this case, it is proposed to have blended braking by simultaneously combining conventional braking with motor braking and achieve a deceleration performance which respects a headway spacing of 2 s. However, ratio of the blend between conventional and regenerative braking must be optimized such that the main aim of SAGA i.e. energy efficiency must be fulfilled.

For this purpose it is necessary to know the system state at every instant. With the given system variables which define the system state, namely, velocity difference ΔV, remaining headway d and motor capacity, it must be clear at any given instant whether it is possible to safely complete the given deceleration maneuver using pure motor brakes without compromising the safety. If such a possibility confirmation is not present then the system must be forcibly manipulated into safe region. This action of steering the system into safe region is achieved by blending the motor brakes with additional conventional braking.

To determine the system safety status, a safety indicator (SI) is calculated and the system is tuned to a threshold value of this indicator. If this threshold value is breached then the blended braking is activated. If not, a pure motor braking maneuver is allowed to proceed.

$$SI = \frac{\Delta V}{d} \tag{4.7}$$

$$a_{blended} = a_{regen} + a_{correction} \tag{4.8}$$

$$a_{correction} = -SI \cdot K_b \tag{4.9}$$

for $SI < SI_{threshold}$,

$$a_{vehicle} = a_{regen} \tag{4.10}$$

for $SI \geq SI_{threshold}$,

$$a_{vehicle} = a_{blended} \tag{4.11}$$

4.4 SAGA as an FSRA

As a culmination point of the SAGA function concept, it is proposed to develop a function which can act as an autonomous vehicle longitudinal motion controller. Such concepts are already in development and are known as full speed range ACC (FSRA) [MMY09], [ACC10]. FSRA, as the name suggests, is an ACC which will operate over entire speed range of the vehicle. Figure 4.14 shows the domain characteristics with respect to acceleration and velocity for typical traffic in respective domain segments which form the complete operating range for a vehicle.

City traffic is typically characterized with low average velocity and high acceleration values. Moreover, it is worth noting that the city traffic will have frequent start-stop traffic behavior. This means that it is a domain with "low air-drag energy"and "high acceleration energy". Normally such a domain is controlled with LSF systems. In this domain, it makes sense to save on the energy supply side as well as regenerative braking.

The highway traffic domain is characterized with high average velocity and low acceleration values. Here, due to high vehicle velocity, the kinetic energy stored inside vehicle mass is very high as compared to the city traffic scenario. Hence, this domain can be

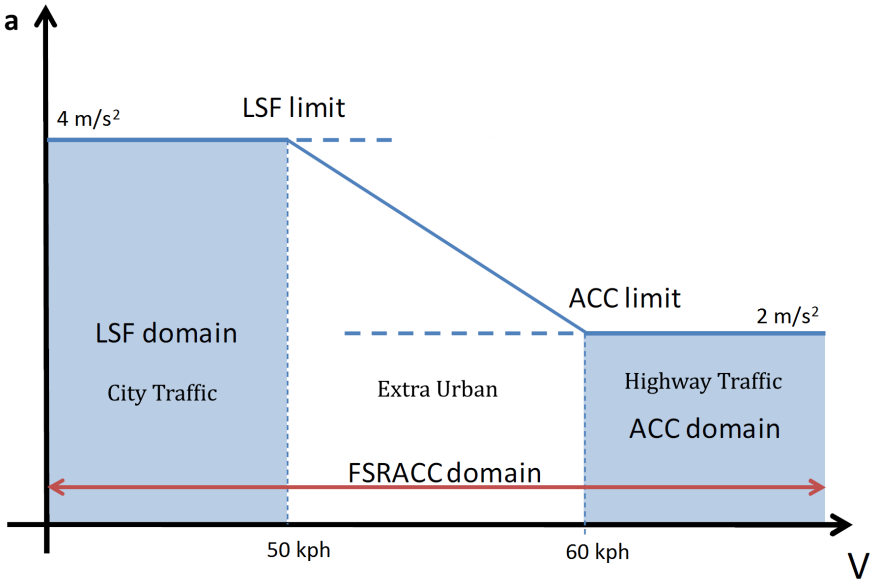


FIGURE 4.14: SAGA as an FSRA

categorized as a "high air drag energy"and "low acceleration energy"domain. In this domain it makes sense to employ the regenerative braking strategy considering the high potential of available energy packets to be regained. In terms of thermodynamics, the kinetic energy stored in the vehicle at high speeds can be perceived as high quality energy since it can be easily tapped into and stored using available equipments. Furthermore, the domain between city and highway can be categorized as an extra urban domain with mixed characteristics. This domain can be assumed to typically exist from about 55 kph to 80 kph. The SAGA function treats this domain as an area where it must carefully switch from LSF control to ACC control and vice-versa. To simplify the problem, it is proposed to have the transition between 55 - 60 kph as upper and lower limits.

Conclusion

It is clear that energy characteristics of different traffic domains exhibit variance. In addition to this, there are different vehicle topologies with their own power source behavior. Furthermore, the regenerative braking system offers variable levels of performance over complete operating range. Hence to develop a vehicle motion controller which optimizes safety and efficiency, the concept of "one system fits all situation "cannot be applied here. In this context, it is necessary to classify and state the various ideas which are adapted to specific situation under one roof.

Figure 4.15 shows a hierarchical representation of the various ideas that are developed under the SAGA function.

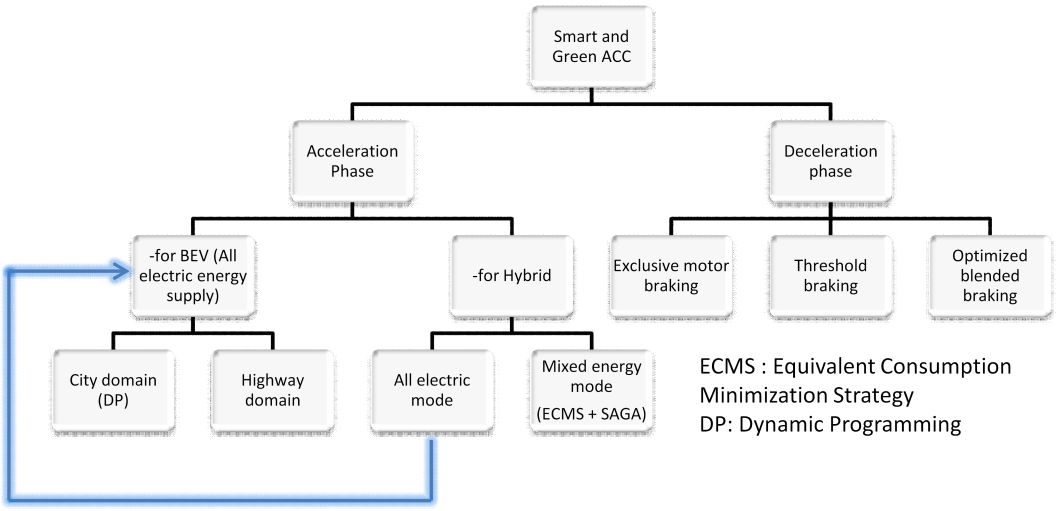


FIGURE 4.15: Overall concept application for SAGA function

These can be classified mainly under the acceleration (energy supply) phase and the deceleration (energy regeneration) phase. A constant velocity phase is not considered for optimization as it is assumed that the vehicle would follow the road speed limit or front vehicle speed. The acceleration phase is further classified as concept for BEV and hybrid vehicles. For all electric mode, the optimization is further discriminated with respect to highway or city scenario (optimization using dynamic programming). For mixed energy supply mode in hybrid vehicles, the optimization is based on a bi-layered control system consisting of SAGA and ECMS for powertrain control.

In deceleration phase, the three regenerative braking control strategies are investigated for their advantages and disadvantages through simulations and analysis.

Chapter 5

SAGA as an autonomous controller for BEV

The following chapter is dedicated to evaluation of the potential of SAGA function to efficiently and safely control the longitudinal motion of a BEV. The function is evaluated separately for city and highway driving scenarios. A dynamic programming (DP) based acceleration controller is proposed and simulated for city domain whereas the previously proposed braking strategies for highway domain are evaluated for safety and efficiency.

5.1 BEV component behaviour and energy optimization

A battery electric vehicle can be viewed as a simple electrical load circuit where the battery is loaded electrically by motor to supply mechanical energy to the wheels in order to move the vehicle. From energy point of view, electrical energy (voltage $\times$ current) is supplied by the battery, conditioned by inverter and supplied to motor to be further transformed into mechanical energy used to move the vehicle against the forces as described in Section 3.2. In this process, there are power losses in battery, inverter, motor and mechanical transmission inside reduction gearbox and wheel joints. The inverter and transmission losses form a small part of total losses (2-3%). As described in Section 3.1.2, it is observed that the motor performs in the efficiency range of approximately 70-92% depending on the operating point. The battery on the other hand performs at almost above 90% for most of the operating range. Even after considering the worst performance scenario, the BEV will deliver an overall efficiency range of approximately 65-90%.

Traditionally, with conventional vehicles or hybrid electric vehicles, the energy management strategies aim at increasing the overall efficiency of powertrain by helping the IC engine to run at the best possible efficiency. However, in a BEV, the operating efficiency of the powertrain is already at such levels that there is very little potential to further improve it. Hence, traditional energy management systems do not hold good with respect to BEV efficiency optimization. Reduction in energy consumption of a BEV cannot be achieved only by powertrain optimization. Here, it is necessary to take into account optimum vehicle motion control to reduce the energy required to move the vehicle itself. In this context, the following concepts are investigated.

1. Optimization of vehicle velocity trajectory by controlling acceleration or motor torque values till the vehicle reaches the specified velocity speed limit
2. Energy saving by reducing the average vehicle velocity in vehicle acceleration phase
3. Limiting acceleration values to optimum levels thereby avoiding large energy packets to be stored in vehicle mass as kinetic energy, which would go waste as brake friction heat or regeneration losses, in case sudden deceleration maneuver is required to be performed during acceleration phase
4. Optimizing energy and travel time for an acceptable solution
5. Maximizing energy regeneration using the SAGA deceleration concept

5.2 Motor operation domains and energy analysis

In order to analyze the potential concepts for energy saving in a BEV or any electric motor propelled vehicle, it would be helpful to understand the motor operation map characteristics in various applicable traffic situations. Figure 5.1 represents the motor operation map for eFuture prototype for the single motor module. The acceleration performance at various velocity points is calculated using the eFuture prototype values and simulating the various forces acting on the vehicle at the specific velocity point using BEV model in Simulink. Here, we consider that 2 motor modules are used and hence an effective torque of 1500 Nm is available. The motor gear reduction ratio is 10, using this information the y-axis is represented in rpm as well as kph values.

In Figure 5.1, the motor map can be divided into two domains depending on vehicle velocity. Below 55 kph, is considered to be the city traffic scenario and above that is classified as highway traffic scenario. Normally city speed limit is 50 kph whereas usual highway speed limits start at 60 kph. Hence, a median value of 55 kph is chosen to divide the operating area into respective domains.

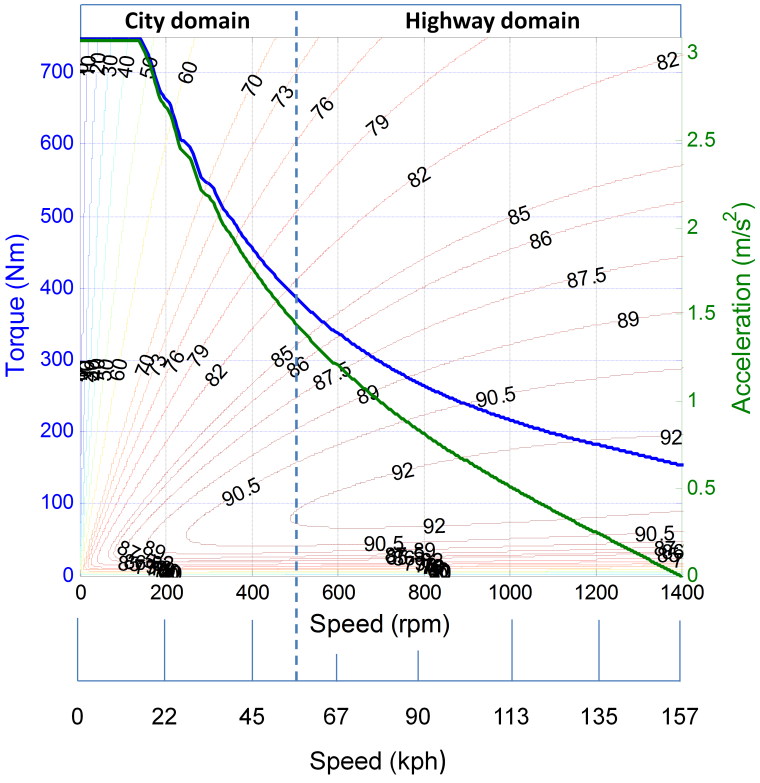


FIGURE 5.1: City and highway domains on a motor map

City Domain

The city traffic scenario is characterized with frequent start-stops which are often performed from standstill till velocity limits and vice versa. It is a high acceleration and low average velocity scenario. In the city domain operation, the motor is mostly in its peak torque region. This means that it is capable of high acceleration maneuvers in tune of 3 m/s^2. It is however observed that in the city domain, there is vast difference in the efficiency values of the motor. Interpolated values suggest that, if a BEV accelerates with value above 1.5 m/s^2 below the velocity of 22 kph its motor efficiency drops below 70%. This implies that very high acceleration maneuver from standstill (e.g. start from a signal) results in extremely inefficient powertrain operation.

Acceleration energy is stored into vehicle as momentum. It should be ideally dissipated through road resistance, air drag and gradient energy requirements. Furthermore, in a city driving scenario, high acceleration leads to a high average velocity which means more air drag. Also, a vehicle which undergoes high acceleration stores a large quantum of its battery energy into the vehicle as momentum. If in such a situation the vehicle must brake then the stored momentum will be wasted as heat or regeneration component losses.

According to this philosophy, a very low acceleration value will lead to maximum energy savings. However, it will also lead to long time duration to cover the same distance. Hence, taking into consideration the powertrain efficiency behavior in the city traffic, there must be certain optimum velocity trajectory defined by specific acceleration values which optimizes the energy and time requirements. Thereby, a dynamic programming based acceleration controller is developed in [ANP+12] and [AGNH13]. Such a controller is elaborated in the later sub-sections.

Highway Domain

The highway scenario is characterized with high average speeds and low acceleration values. From Figure 5.1, it is observed that the eFuture vehicle can only achieve on an average an acceleration of 0.6 - 0.7 m/s^2 in the highway domain. Therefore, optimization or limitation of acceleration values has no potential to save energy in the highway scenario. It is also observed that in the highway domain, the efficiency values are in their higher range of about 85 - 92% where a good overall operational efficiency from the powertrain can be expected. Hence, the idea to enhance efficiency from the energy supply side does not hold true here. Since highway scenario is a high speed high air drag energy domain, there is a possibility to reduce the required energy for a highway trip by reducing the average velocity of the trip. Though this is surely effective method of energy saving, it is controversial as application of such a method on highway may increase trip time by hours, something which would be absolutely unacceptable.

Another method of reducing the required energy in a highway scenario is by regaining it during the braking maneuver. Since vehicle velocity on highways is mostly on the higher side, there is a lot of kinetic energy stored in the vehicle. Typical barking maneuvers in highway scenario can be listed as follows.

1. Approaching a slow moving car or truck
2. Approaching a lower speed limit
3. A traffic jam
4. A highway construction zone
5. Elastic traffic moving at moderate highway speeds characterized with mild deceleration-acceleration phases

During these maneuvers there are large packets of kinetic energy being depleted. Normally these would go waste as brake friction and heat. The state of art BEV however,

has the ability to regain part of this energy by rerouting it through its regenerative system back to its energy storage system. Most OEMs allow deceleration not lower than -1 m/s^2 from their regenerative system as observed with the Mitsubishi MIEV and Nissan Leaf vehicles running at 80 kph on highway. This is owing to the limitation from the battery charge acceptance and temperature characteristics. In order to absorb all the kinetic energy depleted during the above stated maneuvers, it is necessary to control the maneuver in a way such that the energy inflow is within the limitation of the regenerative system. In this context, the deceleration related part of the SAGA function is investigated with the help of simulations.

5.3 Dynamic Programming based Acceleration controller for city domain

This section is dedicated towards developing that part of SAGA function which deals with BEV acceleration phase optimization in the city domain. It is aimed to reduce the energy requirement of the vehicle from the energy supply side by combining the powertrain efficiency improvement and vehicle motion dynamics.

As discussed earlier, the concept is based on limiting maximum allowable acceleration for the BEV in city domain in order to reduce the required energy by effect of three phenomena,

1. Reduction in average velocity of the BEV resulting in reduced average air drag during the trip
2. Lower acceleration from standstill helps keep the motor operating point within high efficiency region and also avoids high power discharge from the battery thereby increasing its life and ensuring high efficiency
3. Gradual increase in velocity ensures smooth built up of momentum till the traffic is streamlined. If one must brake suddenly due to erratic front traffic behavior, it is best not to have accelerated to a high velocity where all the braking energy cannot be absorbed by regenerative system

From energy saving point of view, lower the acceleration lesser would be the energy required for the trip. However, low acceleration implies low average velocity which means high time to destination. Hence, there can be only so much limitation in the acceleration value so as not to increase the time to destination to unacceptable levels. This means that there must be some kind of optimization between energy and time.

The BEV model is comprised of various sub-systems like velocity limit input, driver model, motor model, battery model etc. It is a classic case of time varying, non-linear, nondeterministic system. Hence, optimization systems which try to find a minima by using a mathematical equation of the model cannot be used. If the aim for optimization is to be defined with a slightly broader approach, it would be to find the best acceleration values at any particular velocity point such that the vehicle is in its optimum powertrain operation points, optimum vehicle motion dynamics and clocking an acceptable time to destination. In this regard, we focus on the acceleration phase in the complete velocity cycle.

Figure 5.2 shows some of the various different velocity trajectories that are possible in the acceleration phase.

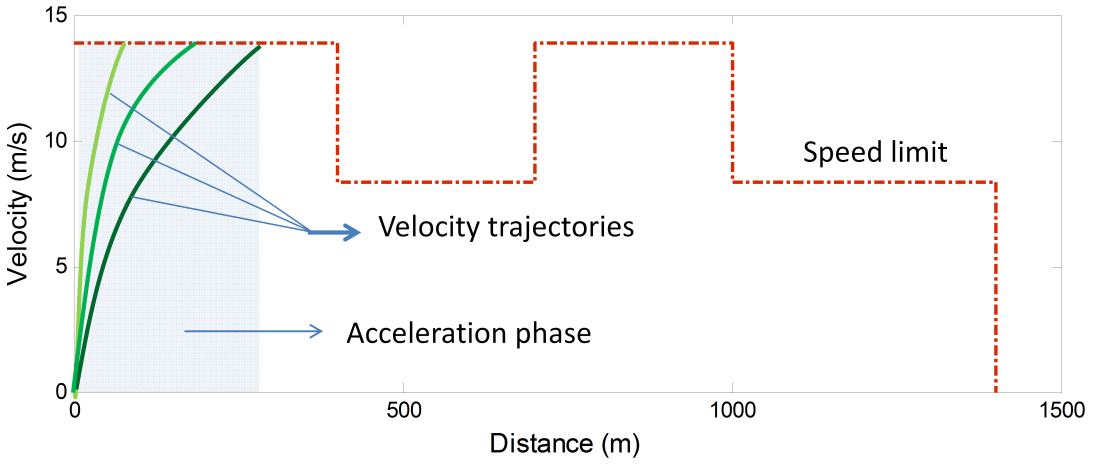


FIGURE 5.2: Some of the possible different velocity trajectories in acceleration phase

Here, a non-standard city cycle is defined which is based on combination of frequently occurring events in a city traffic scenario for e.g. acceleration from standstill (perhaps from a signal stop), constant velocity driving at speed limit, entering a low speed limit area, exiting a low speed limit area, speed reduction due to slow moving traffic and stopping at a signal. Such a cycle is defined in terms of speed limits. Since we are limiting this part of SAGA function to city traffic, a speed limit of maximum 50 kph and a lower speed limit of 30 kph is considered. In the acceleration phase, three possible velocity trajectories are shown with decreasing intensity of acceleration values. The light green trajectory (extreme left) exhibits quicker vehicle behavior and higher energy consumption on the contrary the dark green trajectory (extreme right) represents slower vehicle motion dynamics but saving on the air drag energy and smooth built up of momentum which is good for the powertrain. Let us assume that the middle (green) trajectory is the most optimal with respect to time and energy. To determine the properties of such a trajectory in terms of velocity and acceleration values, we attempt to find a global optimum over the acceleration phase.

For such a time varying non linear system, the best optimization technique to find the global optimum over the acceleration phase is dynamic programming (DP) [Bel54]. The term dynamic programming was originally used in the 1940s by Richard Bellman to describe the process of solving problems where one needs to find the best decisions, one after another. This process fits perfectly to the problem at hand where one must find the best acceleration value at different time steps, one after another. By 1953, he refined this to the modern meaning, referring specifically to nesting smaller decision problems inside larger decisions. It forms a central result of dynamic programming which restates an optimization problem in recursive form. In line with this, we attempt to discretize/break the whole global acceleration phase into small steps. Here we hope to achieve global optimization by reaching a local minima and adding the parts together to find a global minima. To simplify the problem further and reduce the computation time we employ a greedy algorithm, which picks the locally optimal choice at each branch in the road. Therefore, instead of backward recursive process, a forward recursive process is used. Since this set-up is very similar to the shortest path method, it very much resembles the process of Dijkstra's algorithm [Dij59].

In the eFuture project, a parallel research on similar problem of global optimization was carried out using Dijkstra's and A-star algorithms. The results for these are compiled in [GAO+13].

5.3.1 DP problem formulation

The acceleration phase is discretized in $N+1$ steps of equal distance from 0–N. If J is the objective function which depends on energy and time then J can be defined as,

$$J = Q_1 \cdot Energy + Q_2 \cdot Time \tag{5.1}$$

Where Q_1 and Q_2 are the weightage coefficients. Since J is a function of acceleration a of the vehicle where $a \in A$. The control problem can be formulated as follows and is partly based on [LNM10].

$$\begin{aligned} min \sum_{k=0}^{N-1} J_k(A_{k-1}) \\ A_{k-1} \ \in [a_{low},\ a_{high}] \end{aligned} \tag{5.2}$$

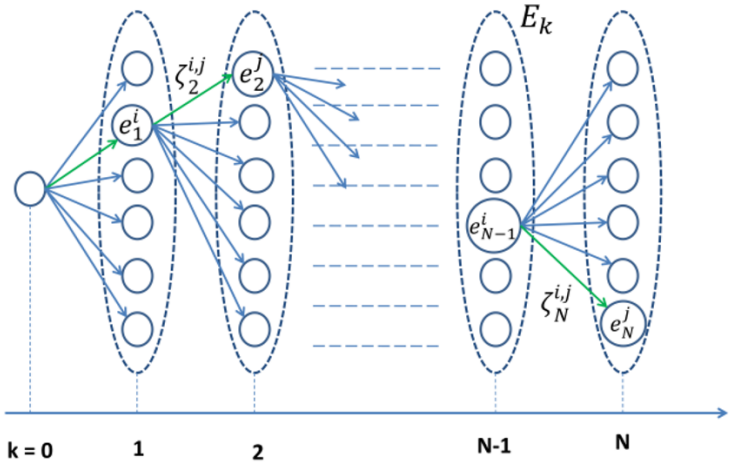


FIGURE 5.3: Formulation of a DP algorithm

In Figure 5.3, e_k^i denotes the state i at the step k. E_k is the set of the states e_k^i at the step k and is defined by the discretized control set A_{k-1} which is a set of acceleration values from 0.5 m/s^2 to 2.5 m/s^2 with an interval of 0.1 m/s^2. $\zeta_k^{i,j}$ is the cost associated to each transition from the state $i \in E_{k-1}$ to the state $j \in E_k$. Thus it can be stated that for a transition from step $k = 1$ to $k = 2$ where the initial state e_1^i at step 1 is already defined, the goal is to find a state $e_2^i \in E_2$ at step 2 where the cost of transition $\zeta_2^{i,j}$ is minimum. This minimum cost is nothing but $J_2(A_1)$ as defined in expression 5.2. Therefore the dynamic programming technique can be defined as follows.

Let $\pi^* = a_0^*,\ a_1^*, \ldots\ldots, a_{N-1}^*$ be an optimal control strategy for this problem where "a"is the acceleration value. Suppose that, when a_{k-1}^* is used, the state e_k^i was reached at time τ_i during the acceleration phase. Considering the sub-problem for which, from the state at time τ_i, we seek to minimize the cost to go from k to N: $J = \sum_k^{N-1} \zeta_k(A_{k-1})$, then the optimal control strategy $\pi^* = a_0^*,\ a_1^*, \ldots\ldots, a_{N-1}^*$ is optimal for that sub-problem.

The algorithm for the code in Matlab is as follows.

Input:

1. $a \in A$, $A = \{0.5, 0.6, ..., 2.5\}$
2. Velocity limits (V_{limits})
3. Corresponding distance points (d_{limits})

Simulate:

For the next sample distance of 10 m, for each acceleration value from 0.5 to 2.5 at present velocity, find the required torque T_{req} as an input for the simulation model.

Using the T_{req}, simulate the eFuture prototype BEV model for the next 10 m distance and record the energy and time values corresponding to each acceleration value "a" which is responsible for formation of that state. The total number of possible states formed will be equal to the number of control variable values (acceleration) that are evaluated.

Processing:

After the simulation for each control variable in the state space A_{k-1}, each state e_k^j in the newly formed set E_k will have different properties namely the new velocity, energy and time. To calculate the cost function, the values for energy and time are further modified so that the cost function value is normalized to 1 using following formula

$$\text{Value share of property (energy or time)}$$

$$= \frac{\text{Actual value of the property} - \text{Minimum property value in } E_k}{\text{Maximum property value in } E_k - \text{Minimum property value in } E_k}$$

Finally, one can expect the results of normalization for this step as presented in Figure 5.4 along with the cost function.

Acceleration (m/s^2)	Energy	Time	Cost Function (J)
0.5	0	1	1
0.6	0.0571	0.4661	0.5232
0.7	0.1417	0.2937	0.4355
0.8	0.2390	0.2010	0.4400
.....	..	..	....
2.5	1	0	1

FIGURE 5.4: Calculation of normalized values for E_k as the set of the states e_k^j at the step k, along with its corresponding cost functions $\zeta_k^{i,j}$ starting from the step *k-1*

Based on expression 5.2 for J the cost function is calculated using both coefficient Q_1 and Q_2 as 1. That state which has the minimum cost function value is considered as the minima for the local area. The vehicle motion properties are updated for the vehicle motion state at step k as,

$$d = d + 10 \tag{5.3}$$

For state of cost function minima

$$a_{optimum} = a_{e_k^j} \tag{5.4}$$

$$t_{optimum} = t_{e_k^j} \tag{5.5}$$

$$v_{k+1} = v_k + a_{optimum} \cdot t_{optimum} \tag{5.6}$$

The whole process is repeated starting from step k for formation of step $k+1$ and so on till the velocity reaches the specified velocity limit.

For the algorithm run at every step transition we get the following cost function results.

From Figure 5.5 it is clear that each optimization step gives a local minima for the cost function value. For example, for the first 10 m an optimum acceleration of 1.2 m/s^2 is suggested for the next 10 m it is 1.4 m/s^2 and so on. The optimization process suggests that for this vehicle an average acceleration value not more than 1.5 m/s^2 must be followed during the acceleration phase.

5.3.2 Deceleration strategy for City domain

In scope of the eFuture project, in addition to a deceleration strategy for highway domain, another deceleration strategy for city domain was investigated using the motor braking limitations of eFuture vehicle prototype where a negative torque of only -260 Nm was available. This translates into a regenerative braking deceleration of not less than -1 m/s^2. In the city traffic scenario, there are certain typical braking maneuvers which have a good potential to yield sizable kinetic energy back to the energy storage system like,

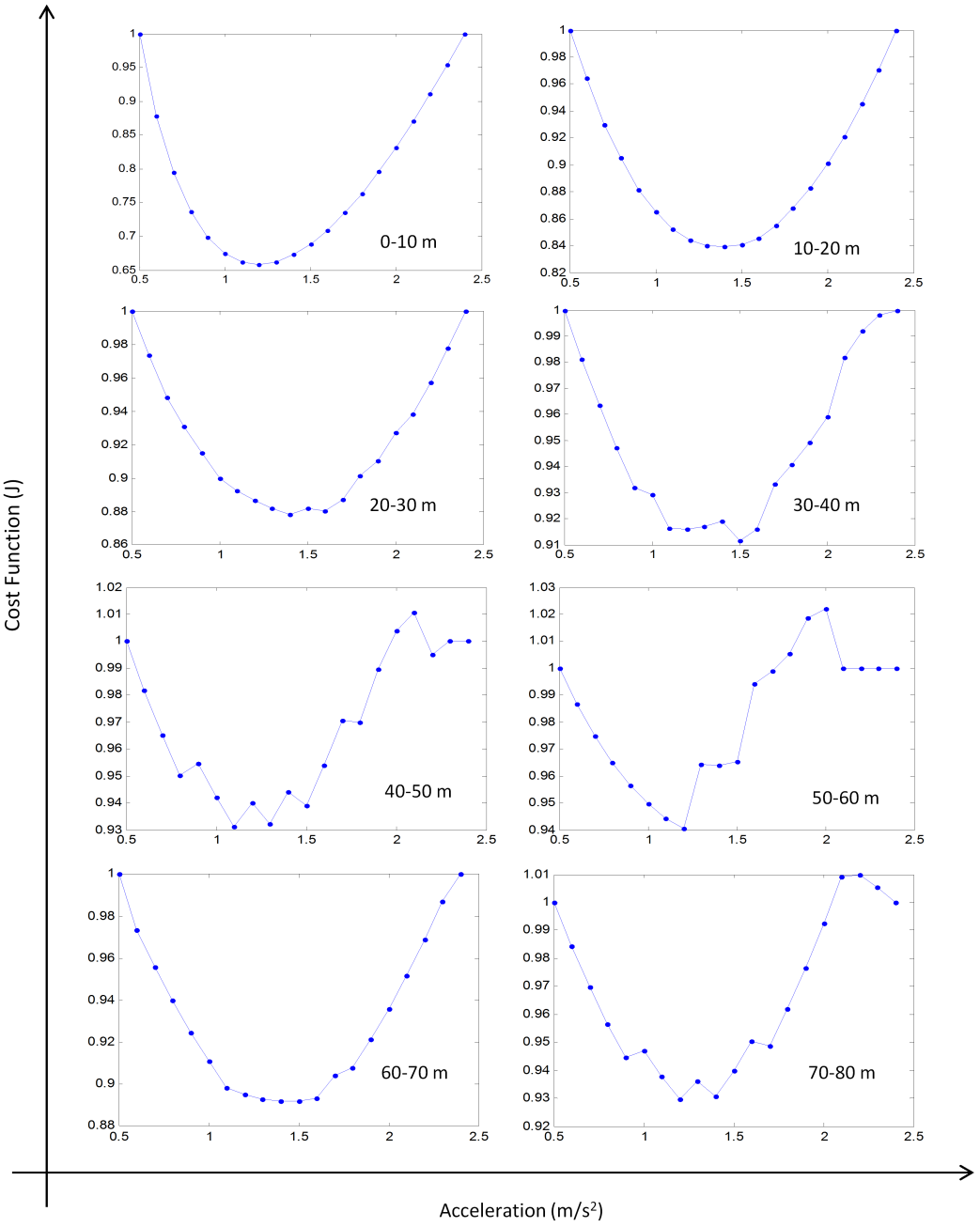


FIGURE 5.5: Optimization results for the acceleration phase using $Q_1 = 1$ and $Q_2 = 1$

1. Deceleration maneuver for approaching a red signal from speed limit (50 kph)
2. Deceleration to enter into a low speed zone (30 kph) from high speed limit zone (50 kph)

The limited deceleration performance offered by -260 Nm motor torque does not suffice for a timely speed reduction after the red signal or low speed traffic sign is in the sight of the driver. This means that any further requirement of deceleration torque has to be supplied by the conventional braking system where the depleted kinetic energy goes waste. This phenomenon is better explained in Figure 5.6.

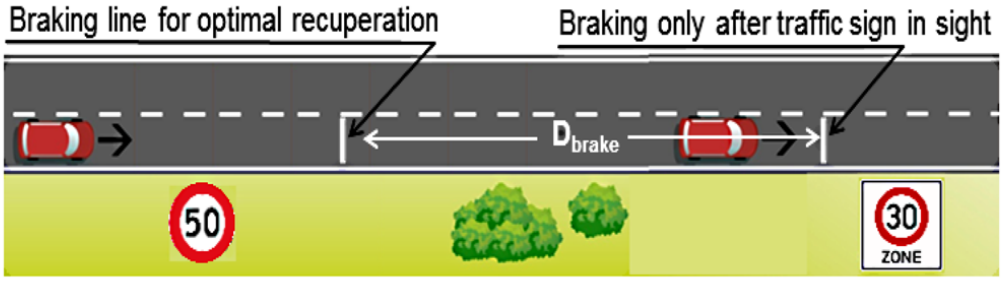


FIGURE 5.6: Deceleration maneuver (Entering a low speed zone)

Here, the example of a vehicle entering a low speed zone is considered. For a normal driver, the deceleration phase will only start after the traffic sign is in sight. In order that maximum depleted kinetic energy is regenerated using the motor braking for the eFuture prototype, the deceleration phase has to be started much earlier so that the vehicle safely reduces the speed by time the low speed zone starts. For such a set-up to work it is necessary to know,

1. How early the braking must start (the distance D_{brake} as shown in Figure 5.6)
2. The position of oncoming stop or speed reduction events

To know the position of speed limits or traffic signal events, we can rely on the modern ITS like e-Horizon systems and Intelligent traffic signal information systems which use DSRC to communicate the signal status to the vehicle or high definition on-board digital maps with GPS. In order to determine an approximate distance D_{brake} where the vehicle must start braking for an optimum regenerative effect, the BEV model was simulated to brake using only the motor braking over a suitable velocity range. The recorded data is as shown in Figure 5.7.

The simulation results are stored in a look-up table. To find the distance D_{brake} , the corresponding distances for the present speed and final speeds must be processed. Thus

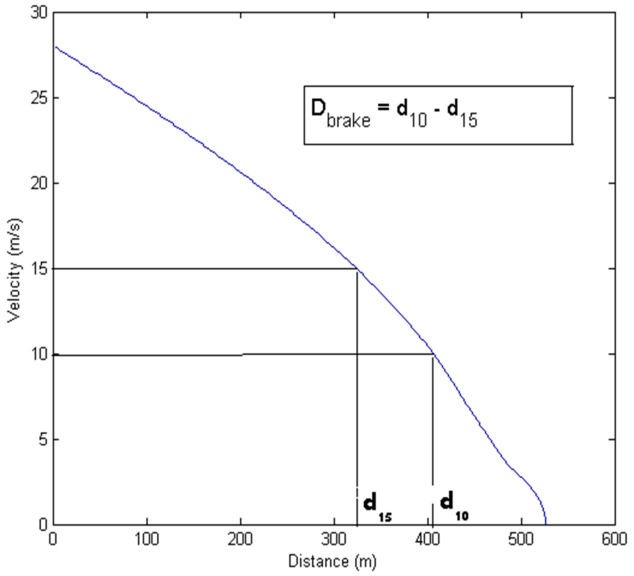


FIGURE 5.7: Optimum braking distance estimation

to enter a speed limit zone of 10 m/s from 15 m/s an early braking distance of almost 70 meters must be observed for optimum regeneration of energy.

5.3.3 Results: City domain

The algorithms for DP based acceleration phase optimization and early deceleration in city domains are combined in one Matlab code and simulated with the eFuture BEV model. To compare the results of such an optimization over the city cycle previously described, a separate simulation is run over the same cycle using a driver model tuned for aggressive driving style. Such a driver model is explained in Figure 5.8.

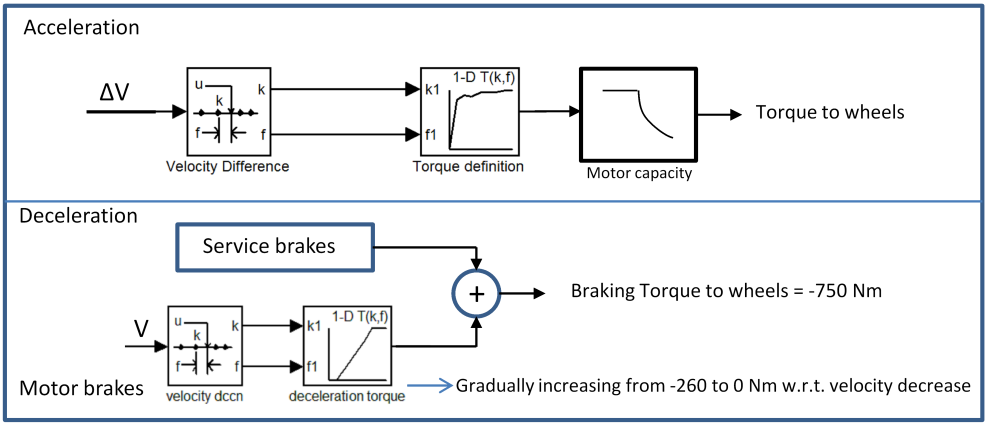


FIGURE 5.8: Aggressive driver model

For the acceleration or constant velocity phase, the driver model generates a torque request depending on the difference between present and desired velocity. Since the model is tuned to be aggressive, it will demand the torque on the higher side than most drivers. If this torque is more than motor can supply at that velocity then the motor model will saturate the torque request at the possible supply value. In the deceleration phase, it is assumed that the vehicle always brakes with -750 Nm torque. Depending on the velocity at that point, the motor may supply as much deceleration torque as defined by the motor limitations. Here the torque gradually increases from a constant -260 Nm till 8 m/s to 0 Nm at 3 m/s as the velocity falls.

Using the optimization algorithm code and driver model, the vehicle performance is compared. The results comparing the city domain optimization algorithm and an aggressive/Sport driver model are presented with respect to time (Figure 5.10) and distance (Figure 5.9) to have a comprehensive view. It is seen that the DP based acceleration optimization results in considerably low acceleration values as observed through the gradual rise in the green velocity curve as compared to the blue curve of the driver model. Furthermore, the early braking of the green curve is clearly visible in Figure 5.9 to ensure enough time for maximum regeneration of deceleration energy. Owing to this, the optimized velocity profile is seen to be lagging behind the aggressive driver model as seen in Figure 5.10.

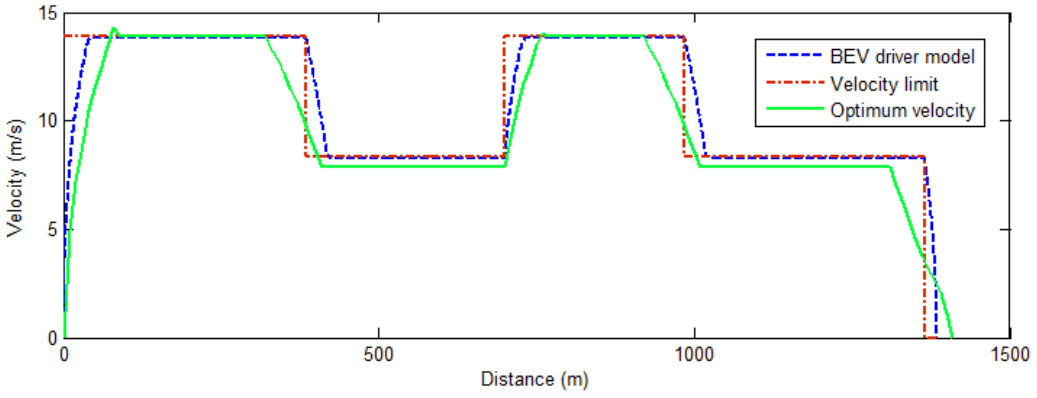


FIGURE 5.9: Comparison of optimum velocity trajectory against aggressive driver model with respect to distance

Additionally, it is worth mentioning the abnormal peak at the end of acceleration phase of the green curve and the fact that the green curve decelerates to a velocity value slightly less than the specified velocity limit. This is not an intentional effect and can be attributed to the way the algorithm functions. The algorithm uses a sample distance of 10 m which means that the algorithm will detect that the actual vehicle velocity has become greater than the target velocity (velocity limit value) only after the 10 m sample

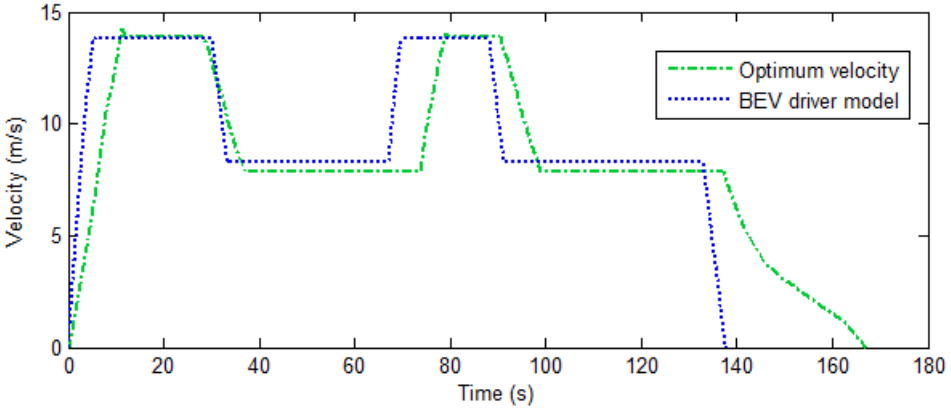


FIGURE 5.10: Comparison of optimum velocity trajectory against aggressive driver model with respect to time

distance calculations are over and vice versa for deceleration phase. This effect will disappear when the results are recorded in a look-up table for on-board implementation.

While the initial results are as expected, there are certain points of concern which are considered to further improve the algorithm.

1. In Figure 5.5 (optimization results for cost function) it is seen that for optimization steps higher than 40 m distance, the cost function points corresponding to acceleration values greater than 2 m/s^2 appear to be distorted. This creates a false value property normalization for the cost function calculation. The reason for the distortion is that the algorithm considers a fixed control variable range from 0.5 to 2.5 m/s^2 irrespective of the velocity value and the fact that motor may not be able to provide the required acceleration value for sample control variable at every velocity. For example, as seen in Figure 5.1, at a velocity of 45 kph (12.5 m/s), the motor cannot provide acceleration higher than 1.7 m/s^2. Therefore at this velocity point, all evaluation of cost function value for control points above 1.7 m/s^2 become invalid and hence the result appears distorted.

2. As observed in Figure 5.10, due to the limitation motor deceleration in the eFuture prototype, a lot of time is being invested in the deceleration phase which in turn increases the total trip time. In the end it is seen that the optimized cycle requires 167 s as compared to 138 s for driver model. Such delay defeats the purpose of optimization for time during the acceleration phase.

5.3.4 Modified strategies for City domain

To improve upon the city domain optimization strategies certain changes are made to the original algorithm, namely,

1. To obtain a valid cost function spread for the control variable, it is necessary to consider the motor torque limitation with respect to velocity. For this reason, the previous control variable (acceleration) is replaced by motor torque for simplicity. This is actually only a nominal change (since torque translates into acceleration) for the ease of choosing the range for control variable within the limits of the motor capacity so that a cost function spread of only valid control points is evaluated.

2. Instead of sample distance of 10 m, a sample look-ahead of distance which corresponds to approximately 2 s headway is implemented in the new algorithm. This facilitates to calculate better sample distance values which are directly proportional to the present vehicle velocity. In line with this idea, corresponding sample distance segments are assigned to velocity ranges (e.g. for 0-5 m/s the sample distance is 10 m, for 5-7 m/s it is increased to 15 m and so on...). These distance samples correspond to a headway of approximately 2 s. In the previous algorithm, at higher velocities a 10 m sample distance was too small with respect to time.

3. If a city domain deceleration optimization concept is to work according to driver expectations, then a better regenerative system deceleration performance than, as demonstrated in eFuture prototype, has to be assumed. In the new algorithm, the limitations on motor braking as defined in eFuture prototype are discarded. With proper energy storage design, enough power acceptance characteristics can be assumed for a total motor braking power absorption.

The original algorithm for DP acceleration domain is modified with the following problem definition while DP problem structure is maintained.

The acceleration phase is discretized in $N+1$ steps of equal distance from $0-N$. If J is the objective function which depends on energy and time then J can be defined as,

$$J = Q_1 \cdot Energy + Q_2 \cdot Time \tag{5.7}$$

where Q_1 and Q_2 are the weightage coefficients. Since J is a function of torque t_α of the vehicle where, $t_\alpha \in T$. The control problem can be formulated as follows and is partly based on [LNM10].

$$\begin{aligned} &min \sum_{k=0}^{N-1} J_k(T_{k-1}) \\ T_{k-1} \ &\in [t_{\alpha.low},\ t_{\alpha.high}] \end{aligned} \tag{5.8}$$

$$t_\alpha \in T, \;\; T = \{0.1 \cdot T_{max}, 0.2 \cdot T_{max} \ldots, T_{max}\}$$

In Figure 5.3 e_k^i denotes the state i at the step k. E_k is the set of the states e_k^i at the step k and is defined by the discretized control set T_{k-1} which is a set of motor torque from $0.1 \cdot T_{max}$ to T_{max} with an interval of $0.1 \cdot T_{max}$. $\zeta_k^{i,j}$ is the cost associated to each transition from the state $i \in E_{k-1}$ to the state $j \in E_k$. Thus it can be stated that for a transition from step $k = 1$ to $k = 2$ where the initial state e_1^i at step 1 is already defined, the goal is to find a state $e_2^i \in E_2$ at step 2 where the cost of transition $\zeta_2^{i,j}$ is minimum. This minimum cost is nothing but $J_2(A_1)$ as defined in expression 5.8. Therefore the dynamic programming technique can be defined as follows.

Let $\pi^* = t_{\alpha 0}^*, t_{\alpha 1}^*, \ldots \ldots, t_{\alpha N-1}^*$ be an optimal control strategy for this problem where t_α is the motor torque value. Suppose that, when $t_{\alpha k-1}^*$ is used, the state e_k^i is reached at time τ_i during the acceleration phase. Considering the sub-problem for which, from the state at time τ_i, we seek to minimize the cost to go from k to N: $J = \sum_k^{N-1} \zeta_k(T_{k-1})$, then the optimal control strategy $\pi^* = t_{\alpha 0}^*, t_{\alpha 1}^*, \ldots \ldots, t_{\alpha N-1}^*$ is optimal for that sub-problem.

For the transition step from every optimum state e_{k-1}^i to the next probable state e_k^j with a constant applied torque t_α, the initial and final velocities are recorded along with the time and energy requirement. Using the normalization concept as discussed earlier, the final value of cost function for each valid transition corresponding to the specific control variable t_α ($t_\alpha \in T$) is evaluated. Using velocity and time values, the acceleration for the state transition is calculated. Results for optimum values of acceleration depending on cost function J of energy and time for equal distance steps are shown in Figure 5.11.

The cost function is normalized to return a value in range of 0 - 1. Each box represents an optimization process. It can be observed that for a specific sample distance, an optimum acceleration value is obtained. The velocity v in the boxes is the velocity attained by the vehicle when it has covered the given sample distance with the constant optimum acceleration. As the velocity increases the sample distance is also increased so as to optimize approximately 2 s of the drive ahead. It can be observed that as the velocity increases the maximum acceleration which corresponds to the control points decreases (as shown in Figure 5.11). For example, in the transition from 0 - 10 m, an acceleration of 3 m/s^2 is possible owing to higher motor torque capacity at low velocity. In transition from 40 - 60 m the maximum acceleration taken into consideration for cost function comparison is 2 m/s^2 since the velocity reached at this point is almost 11 m/s. Hence a valid spread of the control parameters for calculating the cost function is achieved which was not the case for the previous algorithm.

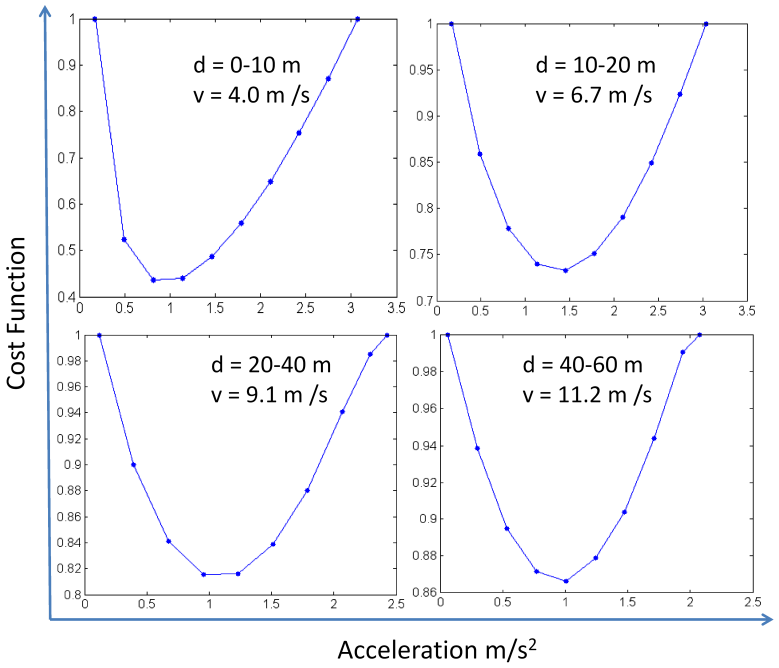


FIGURE 5.11: Cost function results ($Q_1 = 1, Q_2 = 1$)

In case of the deceleration algorithm for early braking (Figure 5.6), it is essential to have enough regenerative braking performance to achieve the deceleration maneuver within acceptable time frame. Hence, complete capacity of motor negative torque is made available for deceleration in the new algorithm. In line with the previous concept, the vehicle model is simulated within certain velocity range for a braking maneuver using only motor braking. Figure 5.12 yields similar results to Figure 5.7.

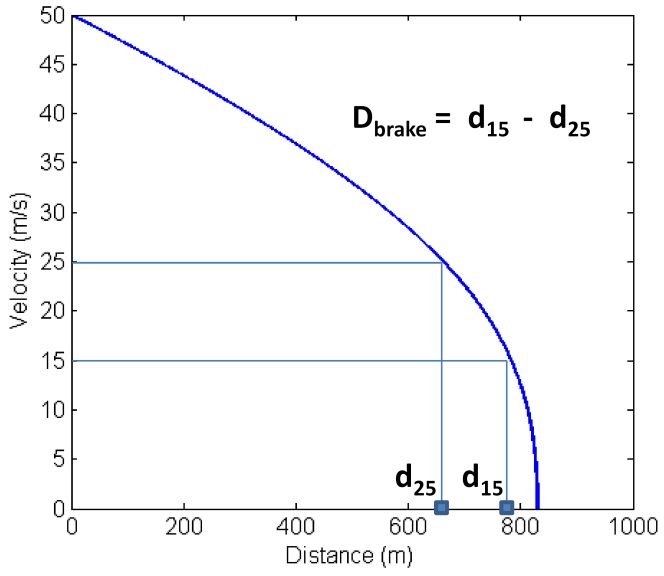


FIGURE 5.12: Optimum braking distance

In the new algorithm, the optimum distance D_{brake} is calculated using the new results as shown in Figure 5.12. In comparison with earlier algorithm, it can be observed that within the city traffic velocity range, the regenerative braking intensity is quite strong as compared to previously modeled regenerative system. This is due to the fact that instead of using -260 Nm motor torque limitation, the new model uses full motor capacity.

The final city domain algorithm combines the strategies for acceleration and deceleration phases as described earlier. In an actual operating mode the vehicle is supposed to follow the optimum acceleration values till it reaches the specified velocity limit, where then the speed is maintained till the optimum braking distance is reached. At this point the motor braking is applied. The system behavior is presented by means of a use case where the algorithm is applied to a city cycle. This cycle is non-standard and consists of defined speed limits at specific distances as discussed earlier. Velocity cycles such as NEDC or Artemis [And04] are not used since they are more applicable to emission calculation and not to the real electric vehicle behavior.

Figure 5.13 compares the dynamic programming based algorithm to a sport/aggressive driver model (Figure 5.8). This driver model is tuned to maximize the performance offered by the vehicle by setting higher torque demand values in the driver model look-up table. Therefore it tends to apply strong acceleration and braking values. It is assumed that the driver model applies brakes when it notices the traffic signs i.e. when a negative change in velocity limit is supplied as an input. In the Figure 5.13 velocity profiles over traveled distance are plotted for two driving styles namely DP optimized and sport/aggressive.

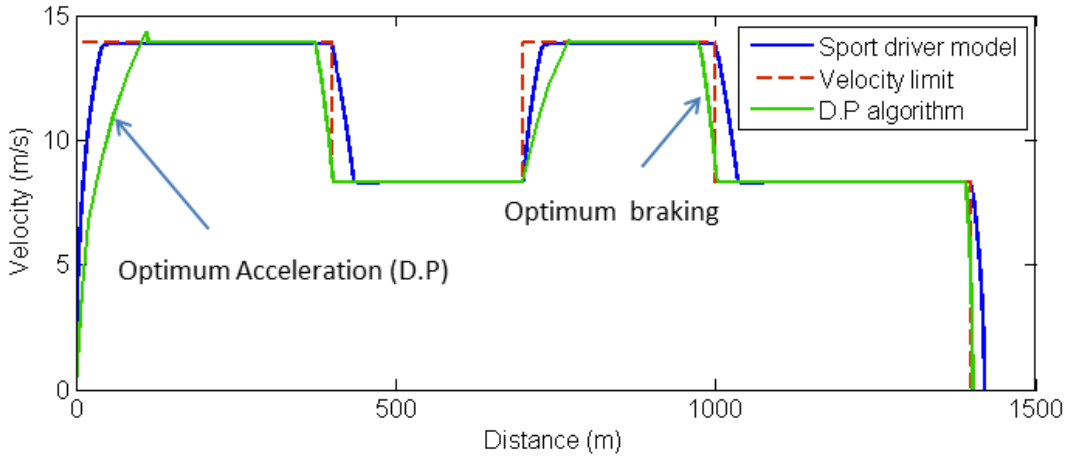


FIGURE 5.13: Comparison of new city domain optimization algorithm with the BEV driver model

It can be observed that the velocity profile for D.P. based algorithm has a gradual increase in velocity compared to a strong acceleration profile of the driver model. The

optimum velocity profile balances the energy consumption and time to travel. Also, since the D.P. algorithm strategy already knows about the speed limits beforehand, it can start the optimum exclusive braking maneuver earlier. Thereby it absorbs all the available braking energy which would normally go waste. As compared to the previous algorithm (Figure 5.9), the use of maximum motor capacity for braking has resulted into comparable braking performance to driver model which is designed to brake with a -750 Nm torque. The total cycle distance is 1400 m which is covered by the driver model in 138 s and the D.P. algorithm in 145 s. As compared to the previous algorithm (167 s), the modified algorithm requires much less time to cover the same cycle because of the increased braking capacity. It is assumed that the driver model can recuperate with -260 Nm (out of total -750 Nm) while D.P. algorithm uses full motor capacity for braking.

The velocity values with respect to time are recorded for city domain algorithm and BEV driver model. These values are supplied as an input for the backward looking BEV energy model. While the driver model requires 0.259 kWh, the D.P. based controller requires 0.241 kWh for same distance, **saving approximately 9% energy**. This figure will change depending on frequencies of acceleration and braking events over the cycle.

After complete optimization for the velocity range from 0 - 50 kph is done, these results can be stored as a look-up table and used in an on-board controller. Therefore, for every velocity point, an optimum value for acceleration can be computed. This look-up table can be used for real-time implementation of the city domain controller. It is however possible that not every customer for an electric car prefers an optimally tuned energy and time system. Some individuals may be efficiency oriented while other may be interested in sporty vehicle dynamics. For such a situation, a concept is proposed where the energy-time optimization system may be further tuned according to owner preference as shown in Figure 5.14 where the blue curve represents the optimal system, red curve allows for more sporty acceleration values where more energy will be required, whereas the green curve further reduces the acceleration intensity and saves more energy. Such a system could be realized by tuning the weight coefficients (Q_1 and Q_2) according to priority for time or energy. However, further investigations in this area have not been attempted in this work and could be a topic for future research.

5.3.5 Slope and Climate control

Although gradient energy and climate control system represent a recognizable part of total energy consumption, they are not considered as one of the system variables while designing the optimization for city domain.

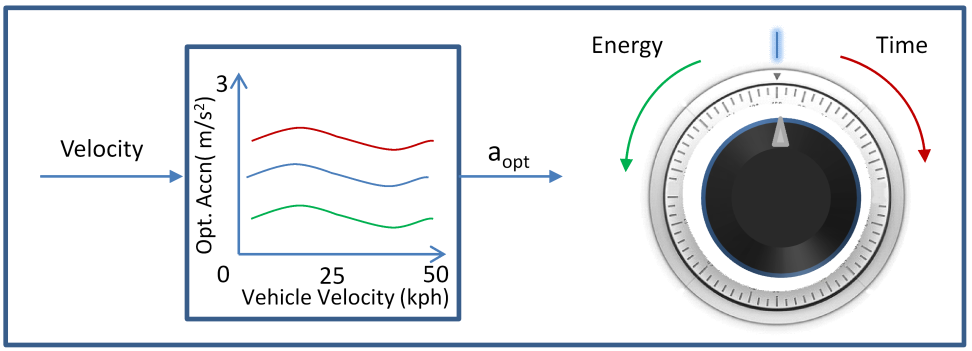


FIGURE 5.14: Tuning the city domain controller for individual preferences

Slope and Gradient Energy

The expression for gradient energy (Equation A.8) is derived from expression of gradient force,

$$F_d = \ M \cdot g \cdot \sin\beta \tag{5.9}$$

Here, $\sin\beta$ represents the height (as a product with distance covered) which is climbed or descended by the vehicle. Form the expression, it is clear that certain fixed amount of energy must be spent in order to make the vehicle climb to a specific height. On the other hand, a fixed amount of energy is regained as momentum for the vehicle descending a slope. For a vehicle, which starts its trip from point A and returns to point A at the end of its trip, the total sum of gradient energy for this vehicle is zero. Therefore, from energy spending point of view, for an electric vehicle, there is no possibility of optimization for gradient energy expenditure.

However, it must be ensured that the amount of energy spent on climbing a grade must be regained during the downhill descend or spent to overcome the negative forces of inertia, wheel resistance and air drag on the vehicle. For this reason it must be checked in advance whether the battery has enough empty space to store the deceleration energy during a descent. Such a strategy is however not in the scope of this thesis.

Climate Control System

Depending on the deviation of temperature from human comfort range, there are various levels of power which the climate control system may consume. To simplify calculation, the climate control system in the BEV model is based on [ACI94]. Since the climate control system can consume at the maximum about 3 - 4 kW, it was necessary to examine the effect of climate control on the optimization strategy. Limiting the acceleration

will increase the time to destination, so the climate control system will be working for that increased amount of time. Taking this into consideration, it may be expected that the optimization algorithm might suggest faster velocity profile with higher acceleration values to save the climate control energy drain during that increased time period. To find whether it actually affects the optimum acceleration values, the optimization was performed in both modes, namely, with and without climate control system. The results are presented in Figure 5.15. On the first glance, it may seem that at the end of acceleration phase the profile with climate control has a slightly higher velocity as compared to the one without climate control. This is however the effect of the abnormal peak. On closer observation it is found that there is no major change in the velocity trajectories with or without climate control system. Since there is no major effect on optimization values, the normal optimization is certified to be valid for both modes.

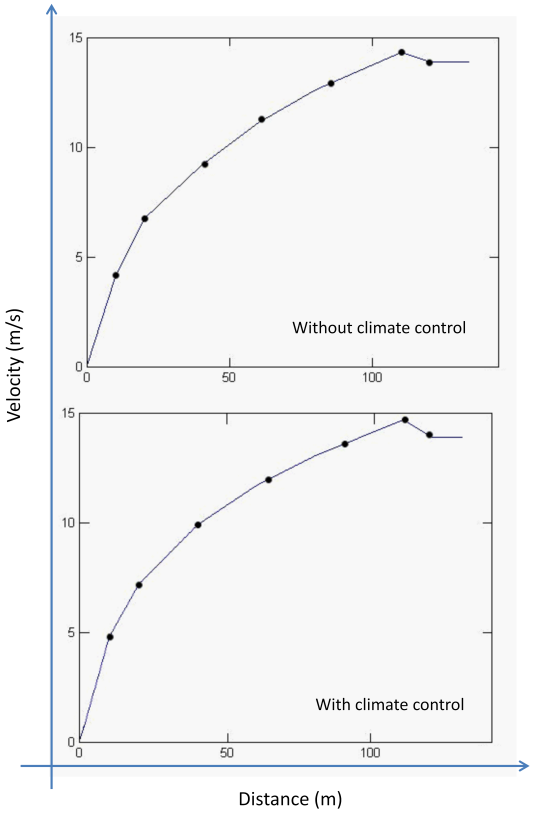


FIGURE 5.15: Effect of Climate control on optimization results

5.4 SAGA function for BEV: Highway domain

The characteristics of traffic dynamics in the highway domain are starkly different from those in the city domain. Hence, a separate concept for safety and efficiency optimization is developed as discussed in Chapter 4. In continuation of the SAGA highway domain

concept definition earlier, in that section, the results for the three braking methods are discussed, namely,

1. Exclusive motor braking
2. Threshold braking
3. Optimized blended braking

5.4.1 SAGA function simulation model

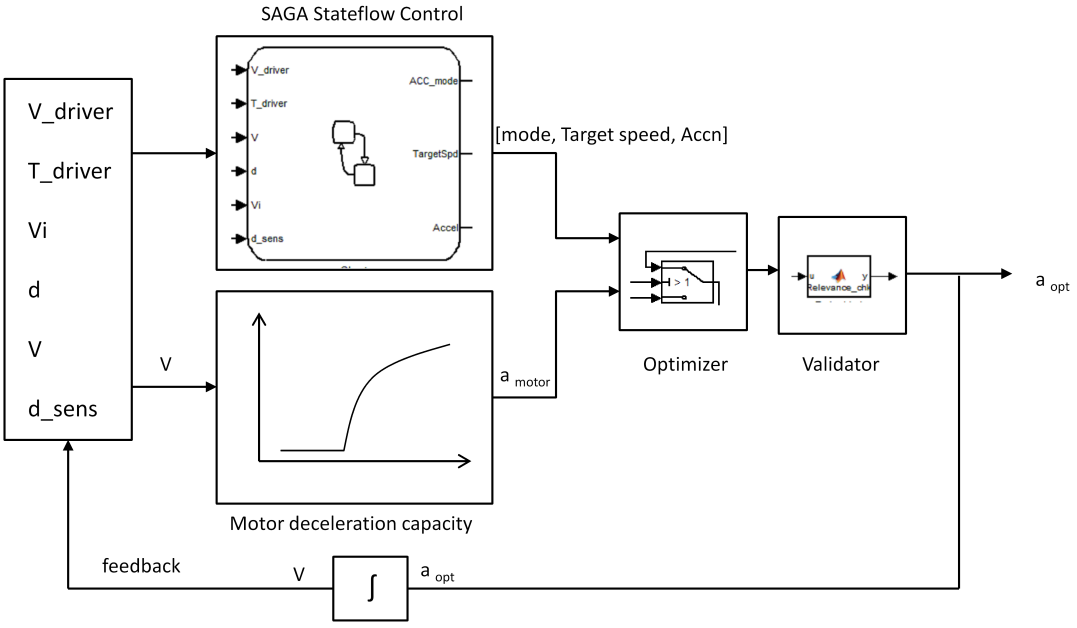


FIGURE 5.16: SAGA simulation model

Figure 5.16 represents a schematic diagram of the SAGA simulation model developed in Simulink platform. Various braking maneuvers using the earlier proposed SAGA deceleration concepts are simulated using the model. On the input side the model receives the driver set desired velocity V_{driver}, set desired time headway, T_{driver}, front vehicle speed V_i which can be set as constant or variable using a signal builder, distance between the vehicles d, ego vehicle speed V and sensing distance d_{sens}. The SAGA stateflow control box uses the equations defined in section 4.2 to determine a nominal acceleration value, ACC mode and target speed. The optimizer processes the nominal acceleration value and tries to adjust the vehicle dynamics so as to use maximum regenerative deceleration provided by the motor till the safety threshold allows such a deviation. The acceleration value suggested by optimizer must be checked to comply with the ACC guidelines, this is done in "Validator" system where both positive and negative acceleration values are

filtered. The optimum acceleration value is sent as a feedback to the input system which updates the dynamic input variables like V, d, V_i.

5.4.2 SAGA highway domain: Simulation results

To evaluate the various SAGA deceleration strategies for highway domain, certain scenarios are considered where typical braking maneuvers in highway traffic are simulated namely,

1. Speed limits, slow moving cars, road construction (130 kph - 80/60 kph)
2. Traffic jams (130 kph - 0 kph)
3. Sudden deceleration of front vehicle
4. Traffic signals (50 kph - 0 kph)

Initial results and comparison to conventional ACC

The green ACC (GACC) function was a preliminary step towards designing an optimized SAGA function. The GACC is a part of overall SAGA function which deals with optimized deceleration maneuvers on highways. In Figure 5.17 a standard result template is created where time based values for headway spacing (distance between two vehicles), ego vehicle velocity and ego vehicle acceleration are shown together to have a better understanding of the deceleration maneuver.

In this scenario set-up, the lead vehicle velocity is 10 m/s, ego vehicle is traveling at 20 m/s and the desired velocity set point is at 30 m/s. The headway spacing is set at 2 s. Sensor sensing distance is 150 m. This is considered as an extreme case scenario where the resulting velocity difference will be of 20 m/s (from 30 to 10 m/s). A velocity difference above 20 m/s is not suitable for exclusive motor braking. Also vehicle which drives at 10 m/s on highways is an exaggeration to demonstrate that even in extreme cases the safety is not compromised.

It is observed that as far as driver comfort is concerned the Green ACC does not offer degraded performance as compared to the conventional ACC. The deceleration phases for both the ACCs start at the same time, while Green ACC manages speed equalization earlier. The only difference is that the major part of deceleration is performed by GACC in the later phase as compared to ACC. It must be stated that behavior of ACC or GACC would change depending on the gain factors (equation 4.2) corresponding to the error (ΔV and e_d) input to the controller. Here, the gain factors, K_{cv} as 0.75, K_{cd} as 0.25,

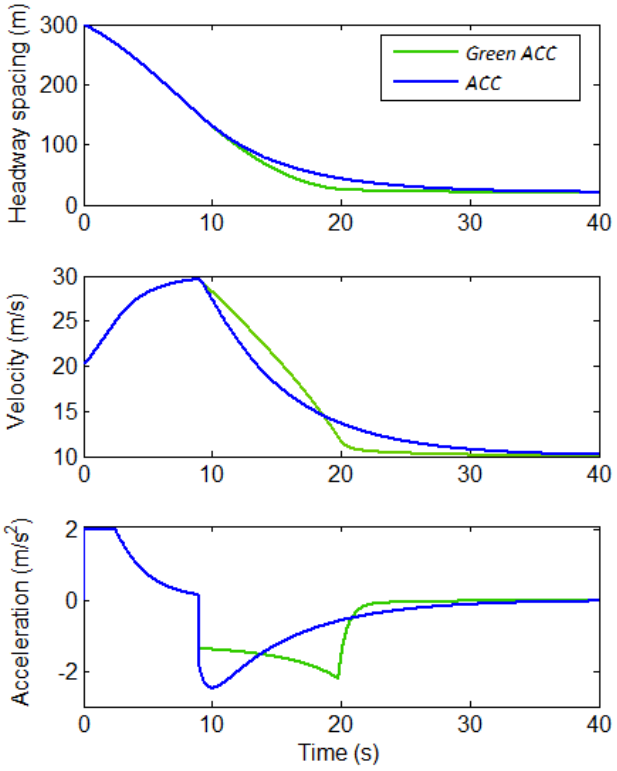


FIGURE 5.17: Comparison of Green ACC function to conventional ACC

are chosen to maximize safety in GACC and same factors are then applied to ACC for a fair comparison. The Green ACC uses the motor braking over the complete range of braking maneuver and hence manages to recover most of the energy.

Exclusive motor braking

The SAGA strategy using only motor braking is evaluated as shown in Figure 5.18.

Here, two typical highway traffic based deceleration maneuvers are simulated using the simulation model in Figure 5.16. In this case the optimizer is biased towards using only motor braking irrespective of the vehicle safety state whereas the SAGA Stateflow control uses the standard tuning factors of K_{cv} as 0.75, K_{cd} as 0.25. The purpose of such an evaluation is to find the boundaries of using such a system with the specifications of eFuture vehicle and propulsion system. It is observed that for a deceleration maneuver from 130 - 80 kph, the system behaves as expected, without compromising the safety and smoothly absorbing all the kinetic energy depletion in the maneuver. From their own experience, most drivers who frequently drive on the highway will know that most deceleration maneuvers on the highway fall within the 130 - 80 kph range. Furthermore, the evaluation for a deceleration maneuver from 130 - 60 kph clearly shows that only motor braking strategy using the eFuture prototype will not work. For such a set-up

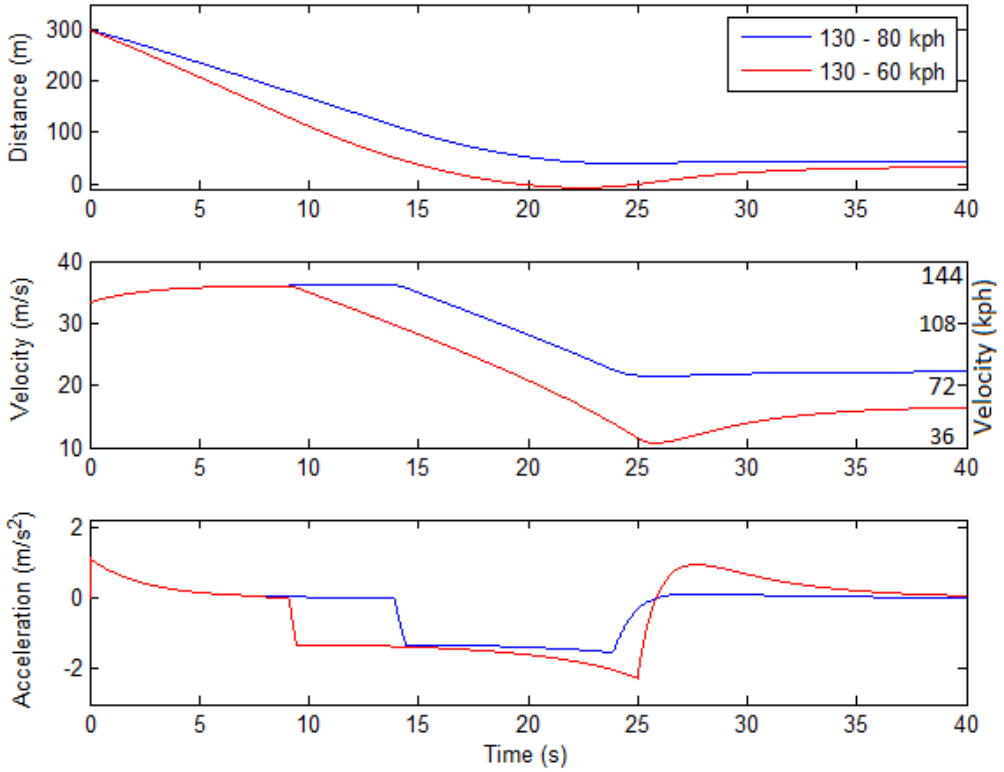


FIGURE 5.18: Deceleration maneuver with only motor braking application

with a propulsion motor offering moderate power absorption capacity as compared to other vehicles (For e.g. Tesla Model S), the validity of using a SAGA function based on exclusive motor braking strategy is limited to a maximum velocity difference of 20 m/s between the front and ego vehicles.

Threshold Braking

To address the shortcomings of the exclusive motor braking concept, the threshold braking concept is investigated. As discussed earlier in Section 4.3.2, this system allows motor braking till a specified threshold of 1.5 s headway is breached after which it engages emergency braking. A deceleration maneuver from 130 kph – 50 kph using Threshold braking concept is shown in Figure 5.19.

It is observed that the motor brakes are not sufficient for this deceleration phase and the threshold of 1.5 s is breached. At this instant the emergency brakes are activated. With a friction coefficient of 0.9, it is assumed that a total deceleration of -9 m/s^2 can be achieved. This could be uncomfortable, physically and emotionally for the passenger.

In threshold braking systems, the advantage is that by proper system tuning it can successfully apply exclusive motor braking in most deceleration maneuvers. From my own extensive experience as an avid highway driver, I observed that on highways, most deceleration maneuvers involve decelerating for a slow moving vehicle or speed limits

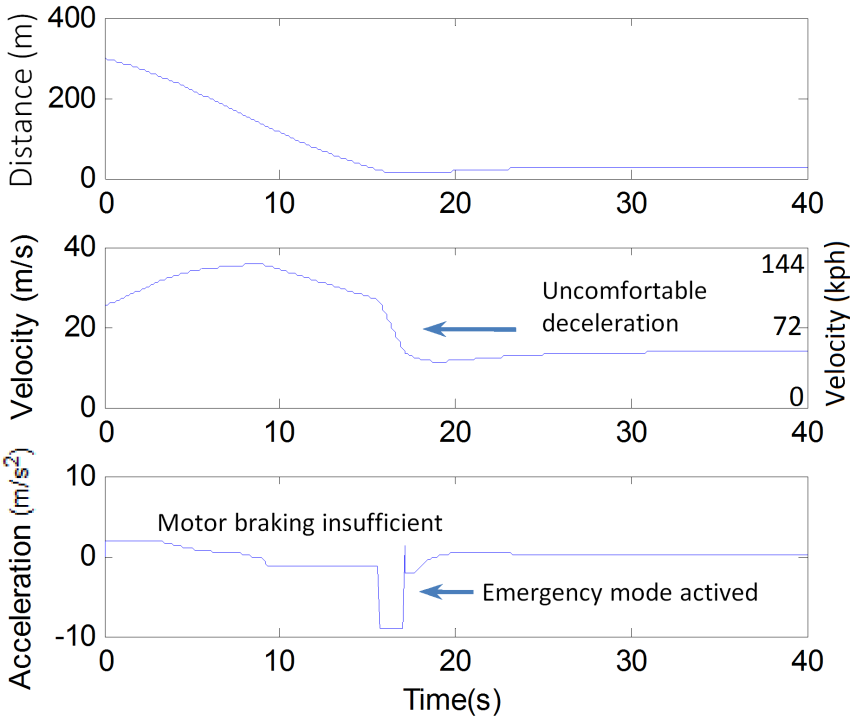


FIGURE 5.19: SAGA deceleration 130- 50 kph, threshold braking, emergency mode below 1.5 s (Set-up: V_{driver}: 130 kph, T_{driver}: 2s, V_{init}: 100 kph, V_i: 50 kph)

where total velocity difference is not more than 50 kph. These maneuvers contain very high potential for recoverable energy. While some other less frequent maneuvers like traffic jams or sudden deceleration of front vehicle carry safety risks. Although most braking situation can be safely handled with threshold braking, there are certain situations where such a system has high probability of failure. For example, if the front vehicle suddenly decelerates or there is a traffic jam. To be on the safe side, even with threshold braking, a regenerative braking maneuver would not be recommended if the difference between speeds of front and ego vehicle at the time of sensing (normal headway 150 m) is more than 20 m/s.

Optimized blended braking

With the implementation of certain rules, the threshold braking strategy can be efficient and safe, although frequent employment of emergency brake and close proximity maneuvers (1.5 s headway) will be an uncomfortable feeling for the passengers which will always be in two minds whether to trust the system or not which will affect the driver acceptability of the system. Hence, it is important to take ergonomics into consideration and develop a system which has a smooth behavior along the operating range.

For this purpose it is necessary to know the system state at every instant. With the given system variables which define the system state, namely, velocity difference ΔV,

remaining distance between the vehicles d and motor capacity, it must be clear at any given instant whether it is possible to safely complete the given deceleration maneuver without compromising the safety. If such a possibility confirmation is not present then the system must be forcibly manipulated into safe region. This action of steering the system into safe region is achieved by blending the motor brakes with additional conventional braking.

To determine the system safety status, a safety indicator is calculated and the system is tuned to a threshold value of this indicator (SI) as discussed in Section 4.3.3 and defined in equations 4.7 - 4.10. If this threshold value is breached then the blended braking is activated. If not, a pure motor braking maneuver is allowed to proceed. With activation of blended braking, the additional braking is computed from the safety indicator and a proportional control is executed using a gain of $K_b = 10$.

In order to ensure enough time for motor brake to absorb the regeneration energy, it is necessary to activate the motor brakes as soon as the front obstacle is detected. Hence, in blended brake SAGA system, the gains K_{cv} as 0.75, K_{cd} as 0.1 are tuned accordingly. Figure 5.20 demonstrates the behavior of the blended braking system.

The deceleration phase for 130 kph – 80 kph (blue) is managed by the motor as expected. Here the SI does not breach the 0.22 mark and the blended braking is not activated. In case of deceleration phase for 130 kph – 60 kph, the activation barrier is breached. If no action is taken then the SI indicator quickly rises (red) to indicate safety risk. It is seen that without any intervention, although the maneuver is completed without collision, the headway spacing has dropped dangerously close. At front vehicle speeds lower than 40 kph a collision is inevitable.

At the activation limit breach, the blended braking is activated (green) additional braking power is applied with conventional brakes and the SI indicator is suppressed to the safe position. More importantly, due to continuous evaluation of safety state, the risk to safety is known much earlier as compared to threshold braking strategy (at 1.5 s headway), hence the corrective action is less intense and more comfortable for the passengers.

Traffic Jam

Furthermore, the behavior of blended braking strategy in the situation of a traffic jam is evaluated. Most scenarios for a traffic jam unfold in a manner that there is enough warning from the front vehicles and a gradual deceleration in speed takes place. In such scenarios it is highly unlikely that the threshold limit of SI indicator (0.22) would be breached. However, in some traffic jam scenarios, there is less/no warning especially in the starting phase of the jam where first set of vehicles arrive at the scene (perhaps

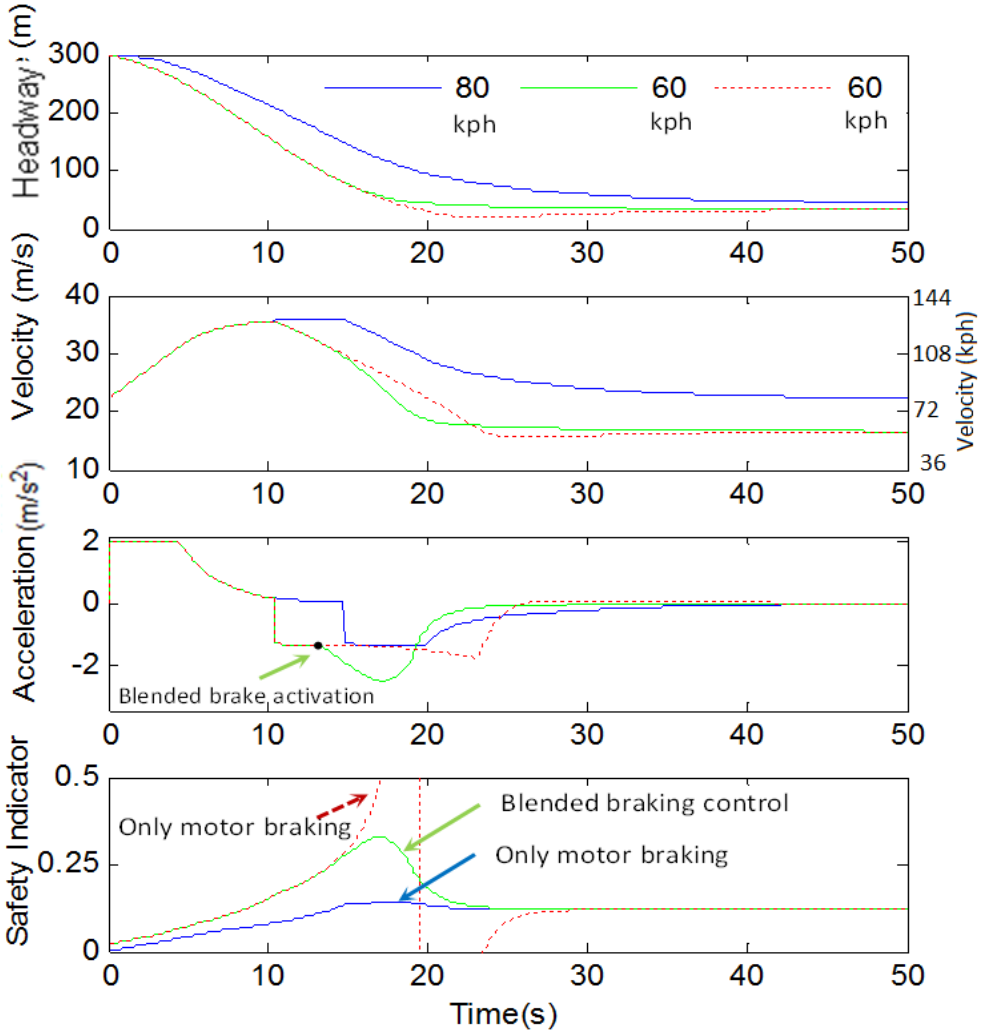


FIGURE 5.20: SAGA deceleration 130-80/60 kph, Blended braking control with safety indicator activation at 0.22

accident/lane closure). In such situations the vehicle speed must drop suddenly and since there is no warning, the vehicle is likely to be traveling at speed limit. To be on the safe side, we evaluate such a situation where a sudden traffic jam presents itself when the vehicle is traveling at 130 kph.

In Figure 5.21, a traffic jam situation is maneuvered with blended braking strategy where the ego vehicle must suddenly decelerate when it detects a front vehicle at a standstill in a traffic jam. Three situations are considered with respect to the sensor performance (multiple sensor fusion including RADAR, LIDAR, cameras and V2V and V2I). In normal situation, the sensor will detect the front vehicle at 150 m headway. It is however possible in case of a bad weather or road curve that the sensor performance might degrade, for this case a 100 m sensing is evaluated. On the other hand using V2V and V2I communications or highway DSRC it might be possible to inform the vehicle

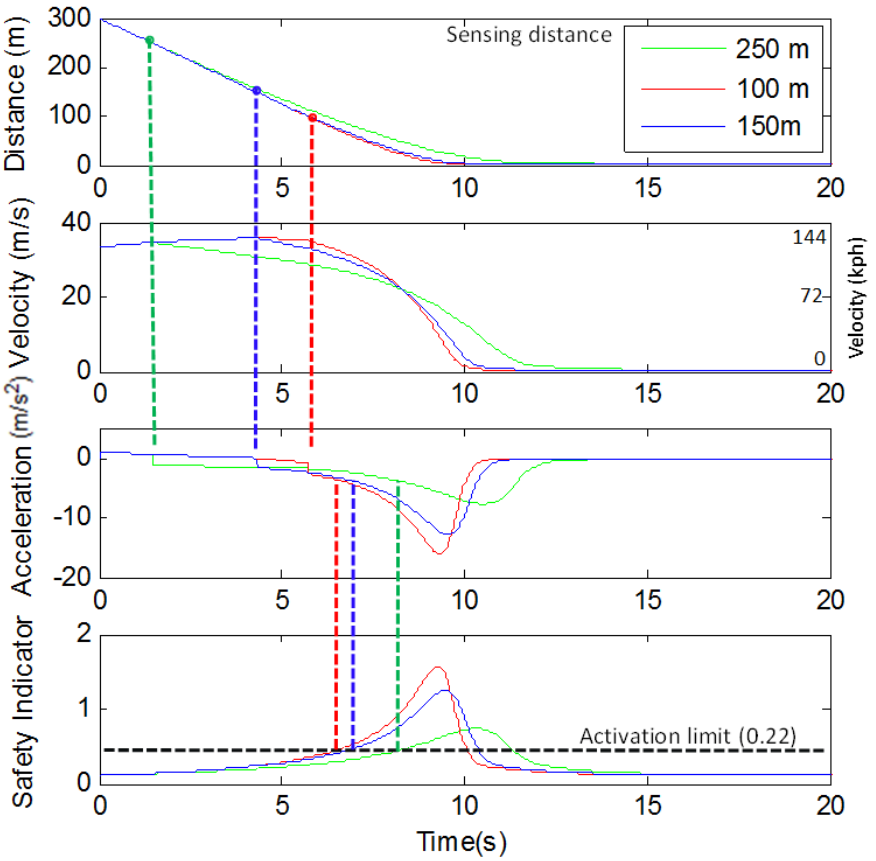


FIGURE 5.21: SAGA deceleration 130-0 kph, Blended braking control, for various sensing distance in case of a traffic jam

controller about the traffic jam even before the sensor senses the front vehicle. In this case a headway distance of 250 m is assumed.

The results show that the system is activated depending on the sensing distance. Furthermore, the system recognizes the need for blended braking activation earlier for the 100 m sensing case and immediately shifts the priority from efficiency to safety. As for the 250 m sensing, the motor brakes are allowed to absorb the energy for an extended period of time till the threshold is finally broken. In the simulation all the cases show a complete ego vehicle halt without any front vehicle contact. However it must be noted that for the 100 m sensing case, the required deceleration goes till about - 15 m/s^2 is required. This kind of performance is not possible even for the conventional braking system. In fact, reducing velocity from 130 kph to 0 kph in emergency mode would require a constant deceleration of -6.5 m/s^2 right from the moment of sensor detection signal. Clearly a blended braking strategy would fail in 100 m headway case and hence for such scenarios a emergency mode activation is recommended.

In normal headway sensing of 150 m, the vehicle is again pushed to the limits of its deceleration capacity. This suggests that perhaps the activation limit must be reduced

to a lower level, however it must be taken into account that 130 kph to 0 kph is an extreme case situation and for most of the other highway scenarios the blended braking works satisfactorily. As seen for the case where a 250 m headway is available the blended braking strategy handles the situation in a smooth manner. One modification to the strategy could be to mark the traffic jam scenario as a special situation, lower the activation threshold and retune the K_{cv} and K_{cd} for a safety oriented setting rather than efficiency biased setting.

Decelerating front vehicle

One of the most risky situations with the SAGA function is the vehicle following phase where the ego vehicle must follow the front vehicle with a constant headway spacing. For safety, the ACC guidelines recommend this headway spacing to be a minimum 2 s. This is however taking into consideration the conventional braking capacity of the vehicle which may be about 8-9 times better than the regenerative braking of the eFuture prototype at highway speeds. Therefore, the evaluation of such a set-up where the front vehicle suddenly decelerates in SAGA vehicle following phase, is an important one.

As observed in Figure 5.22, the front vehicle velocity is simulated using a signal builder in Simulink, where it is made to drop from 100 kph to 20 kph in 5 s at a constant rate of - 4.4 m/s^2 and then gradually to 0 kph simulating an approach to a traffic jam.

It can be seen that the optimized blended braking strategy flawlessly handles the maneuver by shifting its bias towards safety as soon as the threshold for safety indicator is breached.

5.4.3 Energy analysis for typical braking maneuvers

In order to analyze how exactly the SAGA function will affect the energy consumption, the SAGA function model (Figure 5.16) was integrated into the BEV energy consumption model. Here, the time based velocity and acceleration data from the SAGA function model was passed as an input to the BEV energy model. In this way, various deceleration maneuvers were simulated using the SAGA function and simultaneously all the energy components associated with these maneuvers were calculated in the BEV energy consumption model.

Figure 5.23 presents the velocity and energy recuperation analysis for a braking maneuver from 140 - 80 kph using SAGA function.

It is observed that, to achieve the target velocity, the ego vehicle reduces speed below 80 kph and then re-accelerates to 80 kph. This happens because at the end of deceleration

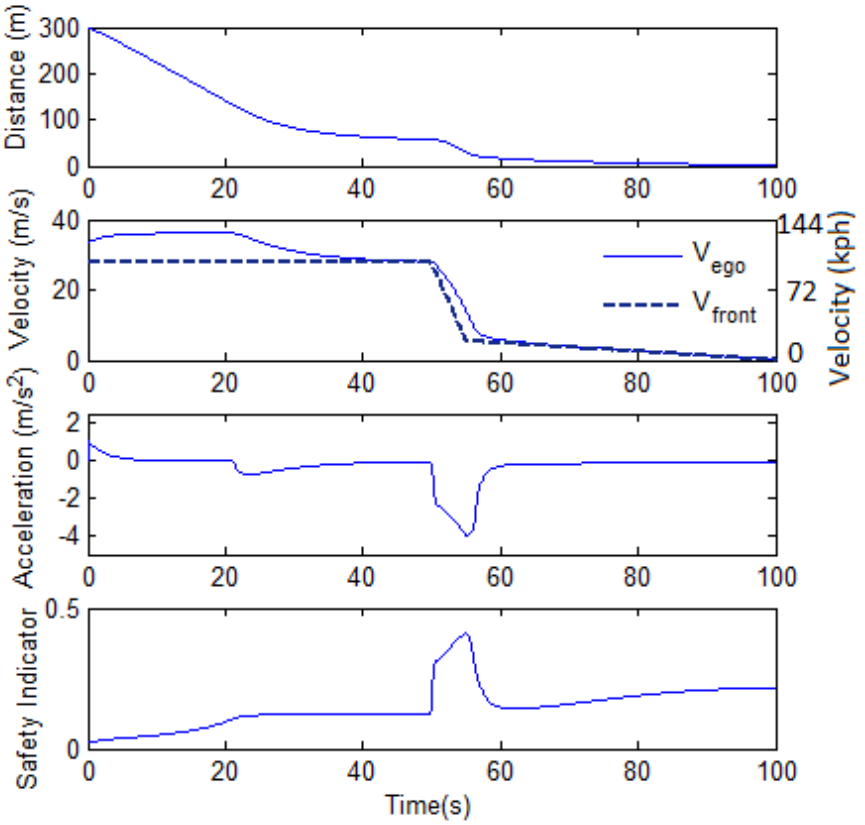


FIGURE 5.22: Suddenly decelerating front vehicle maneuver

phase (at 25 s, point B), the ego vehicle achieves 80 kph but is too close to the front vehicle (headway less than 2 s). So, it must decelerate till the safe headway is achieved. However, such an effect creates confusion regarding energy recuperation analysis. The kinetic energy depletion in the vehicle undergoing 140 - 80 kph maneuver (point A-B) is calculated as 219 Wh from which, as per simulation results, 50.5 Wh is spent to overcome air drag and 23.3 Wh is spent to overcome wheel resistance. Out of the remaining 145.2 Wh, the regenerative braking system absorbs 117 Wh at an efficiency of 80.5%. But as observed in Figure 5.23 the vehicle actually undergoes more deceleration till about 70 kph (point A-C) where it recuperates a total of 134 Wh. Later it must re-accelerate and spend some energy to achieve target velocity of 80 kph (at point D). Therefore, at the end of complete maneuver (A-D), effectively only 62 Wh were recharged in the battery. A similar effect is repeated during the simulation for the deceleration maneuver from 130 - 80 kph but with a less intensity. Here, 95 Wh were recuperated till target velocity (point B), whereas 98 Wh were actually recuperated due to extended deceleration (point C). In the end, after re-acceleration phase, 56 Wh were recharged in battery during this maneuver (point D). While the energy recuperation values at the end of maneuver (A-D) might seem to be the measure of performance for energy recuperation potential of

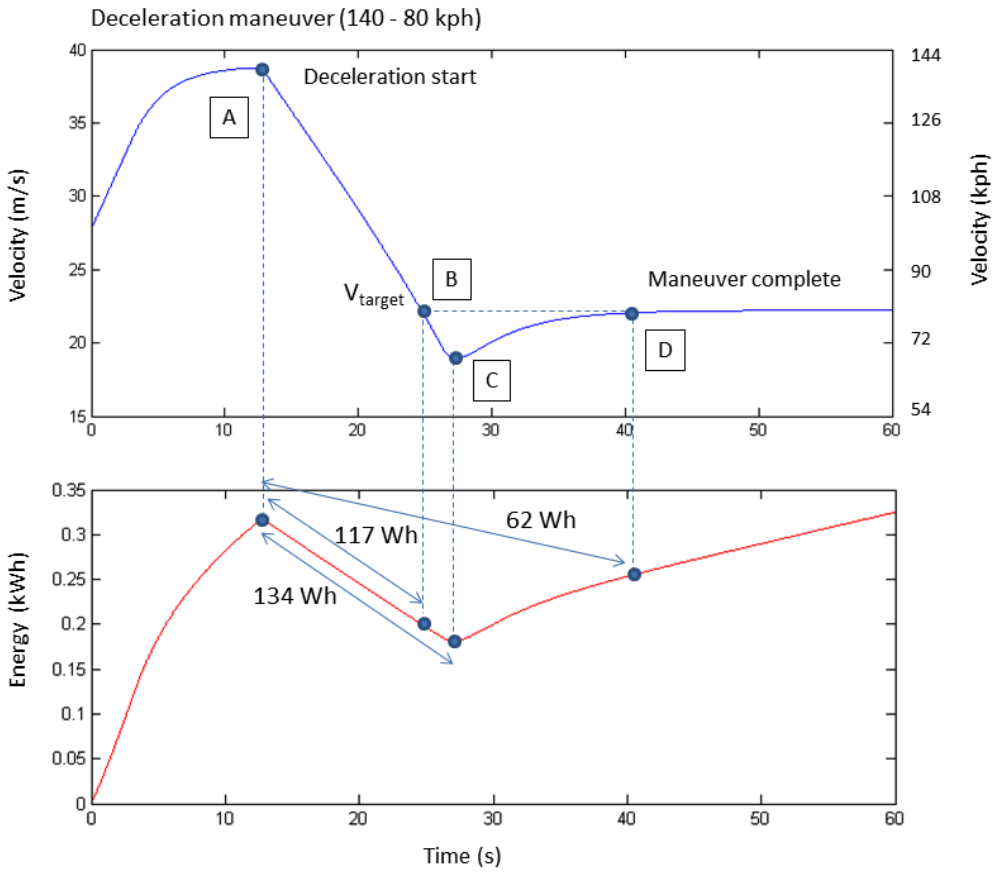


FIGURE 5.23: Energy analysis for braking maneuver 140 - 80 kph

SAGA function, they are actually not. It is argued that for energy analysis purposes only the part A-B must be considered because the re-acceleration phase (C-D) translates into traveled distance and hence is not wasted energy and extended deceleration phase (B-C) extends beyond target velocity.

For a deceleration maneuver from 140 - 100 kph in Figure 5.24, the demand for deceleration is less intense as compared to 140 - 80 kph maneuver. It is observed that the effect of extended deceleration and re-acceleration completely disappears and a smooth deceleration to the target velocity 80 kph is achieved. Here, a direct inference to the recuperated energy can be made as opposed to the earlier discussed case (140 - 80 kph). It is observed that at a certain point along the velocity curve the vehicle continues to decelerate but no more energy is being recovered. The recovered energy till this point is taken into consideration for energy analysis.

A brief analysis of the results for various SAGA deceleration maneuvers performed using motor braking are presented in Table 5.1.

A Pareto 80:20 analysis shows that 80% of braking which contains a high potential of recoverable energy is during the slow front vehicle approach, highway construction,

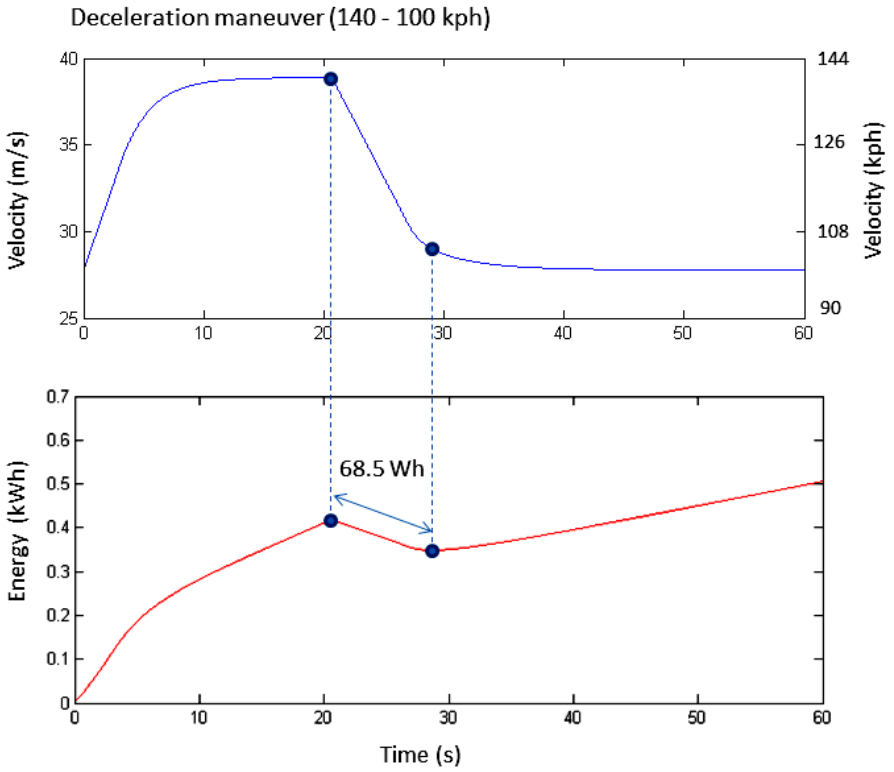


FIGURE 5.24: Energy analysis for braking maneuver 140 - 100 kph

TABLE 5.1: Energy recovery potential for various maneuvers

Braking Maneuver	Recovered Energy (Wh)	K.E. depletion (Wh)	Time (sec)
140 – 80 kph	117	219	27
130 – 80 kph	95	174	22
140 – 100 kph	68.5	159	20
100 – 60 kph	57.5	106	20
50 – 0 kph	24	41	6

speed limits and traffic signals. Table 5.1 gives an idea of the recoverable kinetic energy (KE) during these maneuvers. For example, in the deceleration maneuver from 140 – 80 kph, about 219 Wh of kinetic energy is depleted. Out of this, 117 Wh is recovered by the regenerative braking system at an efficiency of about 80% as explained earlier. Here, the energy recovery from point A to point B is taken into consideration. The time values indicate time required for complete braking maneuver from point A to point D. Since the vehicle comes to a complete halt in the 50 - 0 kph maneuver, there is no speed equalization phase and hence this maneuver requires noticeably less time in comparison to other maneuvers.

The battery for the most of the fully electric vehicles available as of today is around 16

- 26 kWh. This means that if 117 Wh is recovered each time a speed limit is hit, about 0.5 % of the battery is recharged.

5.4.4 Field trial in the eFuture prototype

In scope of the European Union funded project "eFuture" a preliminary version of SAGA function was tested at the Gaydon test track in UK. For this purpose, the eFuture prototype BEV (Figure 5.25) with real time measurement equipment, front cameras, radar sensors and a data fusion box is used.



FIGURE 5.25: eFuture prototype for SAGA function test

A part of test sequence is discussed in the following. The main aim of testing was to demonstrate system ability to sense front vehicle and control ego vehicle with respect to the SAGA function. It must be noted that the eFuture vehicle prototype has a software regulated inherent regenerative torque limitation due to battery charge acceptance limits. This limits the regeneration torque to a maximum of about -260 Nm and hence at this stage of development, the actual strategy of SAGA function to employ strong exclusive motor brakes cannot be evaluated in this testing. Nonetheless, the control part consisting of sensing and actuation is successfully evaluated and validated.

As seen in Figure 5.26, at about 34s, the data fusion box is activated and the system acknowledges the front vehicle presence. At this stage the SAGA function senses the small headway of about 25 m and the front vehicle deceleration. It requests a deceleration of about -2 m/s^2. It is seen that the vehicle has responded with a deceleration of about -1 m/s^2.

At about 55 s when the headway is sufficiently increased, SAGA tries to equalize the speeds. From 70 - 80 s the controller chattering is evident while it tries to regulate the speed. As the front vehicle increases its speed, SAGA tries to follow.

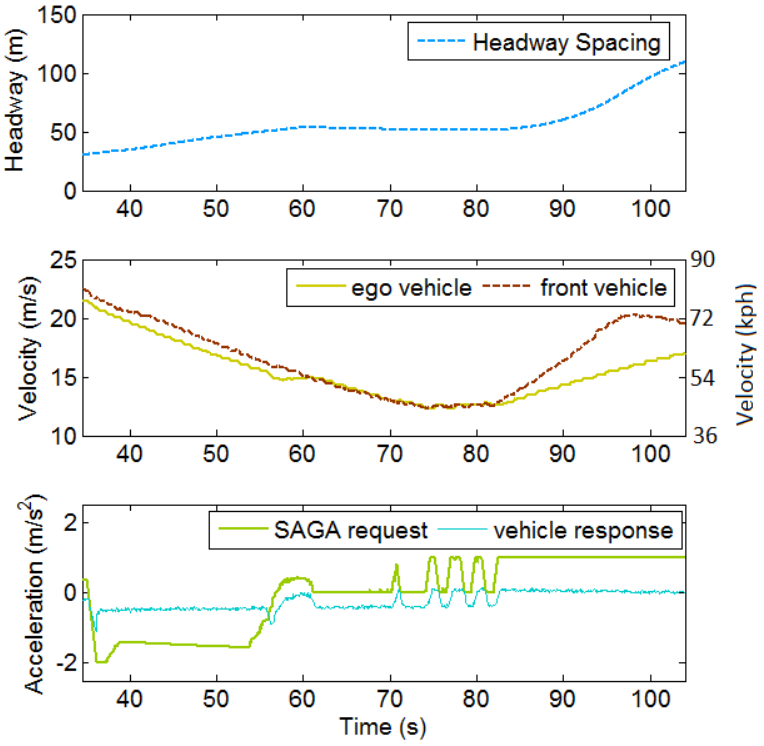


FIGURE 5.26: eFuture prototype field tests for SAGA function

Unfortunately, in the eFuture project, no such opportunity was planned where a version of SAGA function employing full motor deceleration performance could be tested. Considering the battery charge acceptance limitations, only a limited and carefully controlled amount of current is allowed to recharge the battery during regenerative phase. Further software imposed limitations means that even when SAGA function requests a deceleration of -1.5 m/s^2, only -0.1 m/s^2 is actually produced at the motor end. Again, since there is no possibility to control the conventional brakes with a programmable actuator (for e.g. like in ABS systems), therefore there is no possibility to evaluate emergency braking or blending braking strategy.

5.4.5 Battery charge acceptance analysis

For typical highway domain deceleration maneuvers, Figure 5.27 shows the current charge loading on the battery. In this model, the eFuture battery is used where it allows a recharge at around 230 V. Even though this is a moderate voltage level compared to high level voltage systems which can go upto 700 V, it is seen that the current characteristics are within the permissible limits allowed by new generation Lithium iron phosphate cells. Although for the eFuture prototype, these current curves are well above the current acceptance limits.

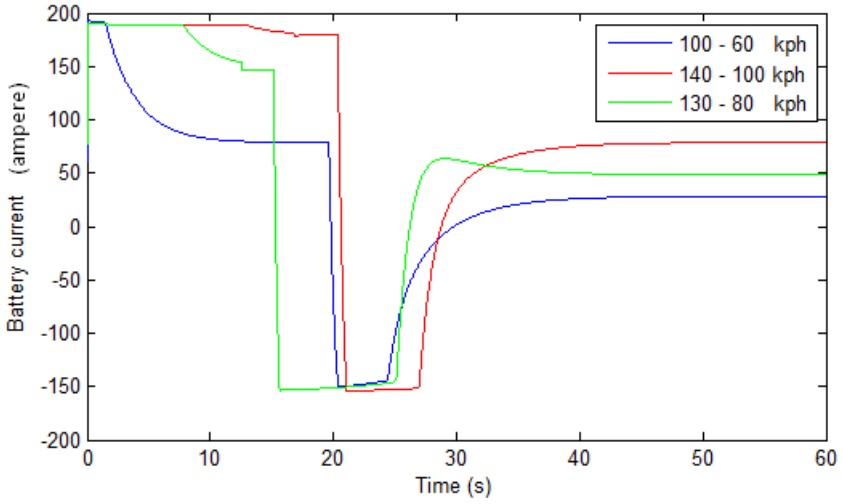


FIGURE 5.27: Current loading on the battery during regenerative braking maneuvers

From various deceleration maneuvers performed at highway speed, it is clear that the deceleration offered by motor does not go lower than -1.5 to -1.7 m/s^2. This limits the negative current into battery at -150 amperes. As discussed earlier in Section 4.1.2, these current characteristics would be well within the acceptance levels for tailored battery packs. It is also imperative to state that for a better performance of regenerative systems, battery packs and motors must be designed to absorb much more than the 30 kW available from the eFuture powertrain if it would be fully utilized.

Conclusion

The most important advantage of BEV over conventional vehicles is it's ability to recuperate energy by absorbing the residual vehicle momentum and storing it back into the battery. As discussed, this advantage of the BEV is heavily compromised due to limitation of the regenerative braking system. The SAGA function attempts to overcome this problem by utilizing beyond horizon information and recovering maximum possible energy while operating within limits of safety and limits of regenerative braking system. Owing to the different traffic characteristics of city and highway domains, specific SAGA functions dedicated to each domain are proposed and evaluated. Thereby an optimum velocity curve with optimum acceleration values is developed and simulated for the city domain. Such a velocity curve not only results in energy savings but also avoids irreversible damage to the expensive electric powertrain. Furthermore, the braking strategies for highway domain are simulated. It is found that constant supervision of safety state of the vehicle is necessary if exclusive motor braking is used. Thereby a optimum blended braking strategy is developed which blends electric and service brakes according to priority for safety or efficiency.

Chapter 6

SAGA as an autonomous controller for HEV/PHEV

This part of the thesis investigates the application of the smart and green adaptive cruise controller to hybrid and plug-in hybrid electric vehicles (HEV and PHEV). For this purpose, it was necessary to develop a model for the HEV/PHEV powertrain management system (PMS) and evaluate the benefits of using SAGA in a HEV/PHEV. To this end, a PMS based on the equivalent consumption minimization strategy (ECMS) is developed and simulated with the HEV and PHEV models to highlight the benefits of using ECMS with SAGA function.

6.1 Bi-layer control concept (ECMS+SAGA)

Unlike the BEV, direct control of the powertrain through SAGA is not possible in the HEV or PHEV as shown in Figure 6.1. In a BEV, the SAGA determines the optimum acceleration or deceleration values (a_{opt}) which can be directly translated into the torque demand (t_{opt}) for the powertrain. This is possible because a single power supply source is being controlled. In HEV or PHEV, even if the SAGA can determine the acceleration and deceleration values i.e. the torque demanded from the powertrain, the powertrain itself is comprised of two power sources. Hence, it is also necessary to control the power-split for the respective power demand.

Thereby, a bi-layered control system is proposed where SAGA acts as a supervisory controller over a core powertrain controller. For a power-split hybrid topology as described in Figure 3.10, the equivalent consumption minimization strategy (ECMS) [PDG+02] is

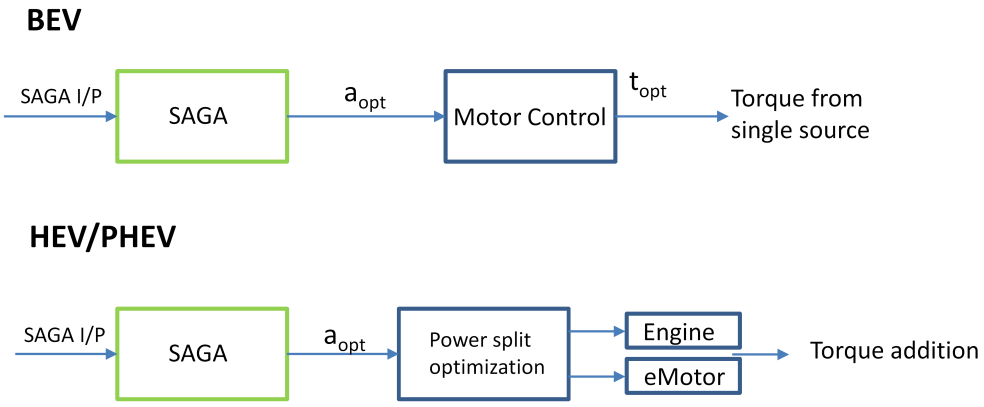


FIGURE 6.1: SAGA as applied to a BEV and a HEV/PHEV

investigated as a core powertrain controller in [AGNH14]. The details of this investigation are elaborated in following sub-sections.

Longitudinal control for a HEV or PHEV must be a bi-layered system wherein the SAGA function and ECMS controller behave in a type of master-slave system. The SAGA function defines the longitudinal motion characteristics. These are passed on to the ECMS controller which further defines the powertrain operation properties. Such a bi-layered control for hybrid powertrain is elaborated in the following.

Figure 6.2 demonstrates a maneuver where the desired set speed is 30 m/s and actual speed is 20 m/s. The front vehicle is 300 m ahead and sensors range is 150 m, so the SAGA function determines an acceleration value in speed control mode. The approximate amount of torque to achieve the specified acceleration is calculated and passed on to the ECMS function. Depending on the system parameters, ECMS determines the power-split, transmission gear and amount of torque to be generated or consumed (stored as electrical energy) for each powertrain component. In short, for the acceleration domain SAGA acts as a surficial command generator whereas ECMS manages the actual powertrain activity.

At headway spacing of 150 m, SAGA senses the front vehicle and shifts into distance control mode. The front vehicle is moving at 10 m/s. SAGA determines if the motor braking capacity is sufficient to achieve the required deceleration within safe headway distance. Otherwise the service brakes are engaged as seen in case of blended braking strategy. ECMS is held dormant during this time and SAGA directly controls the regenerative power components. When the speed of ego vehicle is equalized with front vehicle, the objective is to follow the front vehicle speed. In this operation domain characterized with constant speed and intermittent acceleration, SAGA again performs the supervisory control with ECMS as the active powertrain controller.

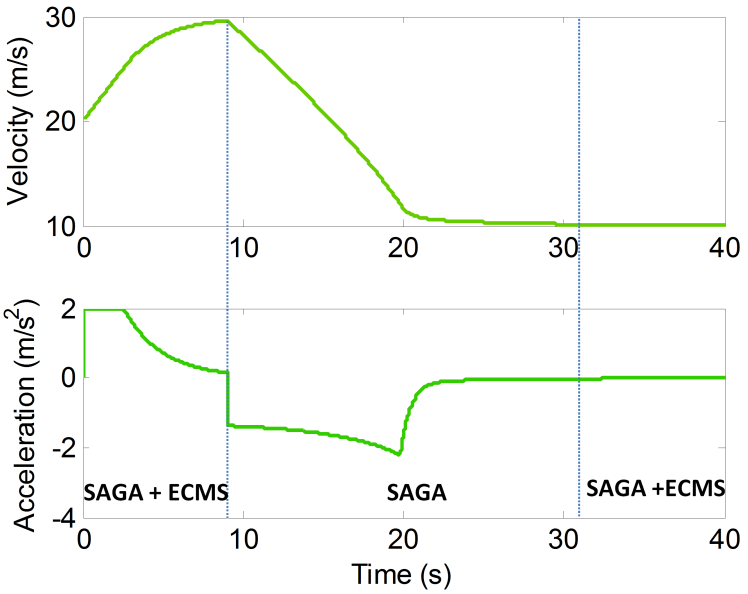


FIGURE 6.2: SAGA as a supervisor for a bi-layered HEV/PHEV control

In order to understand the operation of a SAGA-ECMS bi-layered control and analyze the energy saving impact, it is necessary to understand the ECMS concept. The following sub-sections are dedicated to definition of the ECMS concept. Furthermore, application of ECMS to HEV and PHEV is discussed based on which an ECMS algorithm for control of a TtR (Through the road) hybrid vehicle is developed. The fuel economy values using such a system is compared to a conventional vehicle by simulating models for both systems on standard velocity cycles.

Simulation of SAGA function in relation to deceleration optimization for a regenerative braking system was illustrated in previous chapter. On that basis, it is assumed that SAGA enables an electric vehicle to absorb almost all of the deceleration energy depending on component efficiencies. Thereby, in the following sections the ECMS is designed taking this into consideration that if it is working with a SAGA function then the braking system regains all deceleration energy except component losses.

6.2 Equivalent Consumption Minimization Strategy (ECMS)

6.2.1 ECMS definition through Pontryagin's Minimum Principle

ECMS is a HEV powertrain operation strategy which was pioneered by G. Paganelli et al. in [PDG+02]. In classical engineering application optimization theory, the ECMS concept can trace its roots back to the Pontryagin's Minimum Principle (PMP). The correlation between ECMS and PMP is shown in several research works [SOR09], [SSG+13].

Pontryagin's minimum principle is used in optimal control theory to find the best possible control for taking a dynamical system from one state to another, especially in the presence of constraints for the state or input controls. The Pontryagin's Minimum Principle is defined as follows [Gee07].

For a dynamical system which can be defined by its state x and input u such that,

$$\dot{x} = f(x, u), \quad x(0) = x_0, \quad u(t) \in \mathcal{U}, \quad t \in [0, T]$$

where $\mathcal{U}$ is the set of admissible controls and T is the terminal (i.e., final) time of the system. The control $u \in \mathcal{U}$ must be chosen for all $t \in [0, T]$ to minimize the objective function J which is defined by the application and can be stated as,

$$J = \Psi(x(T)) + \int_0^T L(x(t), u(t))dt \tag{6.1}$$

The constraints on the system dynamics can be adjoined to the Lagrangian L by introducing time-varying Lagrange multiplier vector λ , whose elements are called the co-states of the system. This motivates the construction of the Hamiltonian H defined for all $t \in [0, T]$ by,

$$H(\lambda(t), x(t), u(t), t) = \lambda'(t) f(x(t), u(t)) + L(x(t), u(t) \tag{6.2}$$

where λ' is the transpose of λ.

Pontryagin's minimum principle states that the optimal state trajectory x^* , optimal control u^* , and corresponding Lagrange multiplier vector λ^* must minimize the Hamiltonian H so that,

1. $$H(x^*(t), u^*(t), \lambda^*(t), t) \leq H(x^*(t), u, \lambda^*(t), t)$$

   for all time $t \in [0, T]$ and for all permissible control inputs $u(t) \in \mathcal{U}$. It must also be the case that,

2. $$\Psi_T(x(T)) + H(T) = 0$$

Additionally, the co-state equations,

3. $$-\dot{\lambda}'(t) = H_x(x^*(t), u^*(t), \lambda(t), t) = \lambda'(t) f(x^*(t), u^*(t)) + L_x(x^*(t), u^*(t))$$

must be satisfied.

The principle states informally that the Hamiltonian must be minimized over $\mathcal{U}$,the set of all permissible controls.

Therefore, for a hybrid electric vehicle system where each state can be defined by a scalar value as opposed to the vectors defined in PMP, the state x can be defined as,

$$\dot{x}(t) = f(x, u, t) = \frac{1}{Q_{batt}} \cdot I_{batt}(x, u, t) \tag{6.3}$$

where control variable u is the power-split ratio between the IC engine and eMotor, Q_{batt} is the total charge or energy in the battery and I_{batt} is the current supplied by the battery.

If the Lagrangian L for the hybrid electric system can be interpreted as the instantaneous fuel flow rate expressed in terms of fuel power where the sole aim of optimization is reduction of the fuel consumption then,

$$L(u, t) = P_{fuel}(u, t) = Q_{lhv} \dot{m}_f(u, t) \tag{6.4}$$

Q_{lhv} being the lower heating value (fuel energy density MJ/kg)

subject to constraints,

$$x(0) = x_0$$

$$\dot{x}(t) = f(x, u, t)$$

Instantaneous constraints:

$$u_{min}(t) \leq u_{max}(t) \ \forall t \in [0, T]$$

$$x_{min}(t) \leq x_{max}(t) \ \forall t \in [0, T]$$

Global constraints:

$$x(T) = x_T$$

Then, the Hamiltonian for the HEV system can be defined as

$$H(x, u, t) = P_{fuel}(u, t) - \lambda(t) \cdot \frac{1}{Q_{batt}} \cdot I_{batt}(x, u, t) \tag{6.5}$$

As the PMP suggests, the aim is to minimize the Hamiltonian subject to system constraints.

6.2.2 ECMS concept definition

As the name suggests, the equivalent consumption minimization strategy is based on the concept of equivalent consumption. It was introduced by Paganelli et al. and is recognized as a breakthrough in HEV powertrain control as it paved the way for real-time implementation of optimal control in the hybrid vehicles. The strategy allows for discretization of the global problem into several steps and thereby facilitates local and instantaneous minimization.

The main aim of a hybrid electric vehicle is to help its main power generator (the IC engine) to generate power at best possible efficiencies. Thereby, the secondary power source (eMotor and battery) ensures optimum engine operation by either providing the deficit power or absorbing the excess power which results due to differences in actual demand from vehicle load and supply by the engine at optimum efficiency. In doing so, the battery undergoes a change in its state of charge (SOC) within allowed tolerance range. Therefore, the underlying idea of HEV powertrain operation is,

1. Discharging battery energy and replacing engine power when engine efficiency is at its worst
2. Recharging battery energy when engine efficiency is at its best

The process of charge and discharge of the battery in the HEV is described in Figure 6.3 [PDG+02].

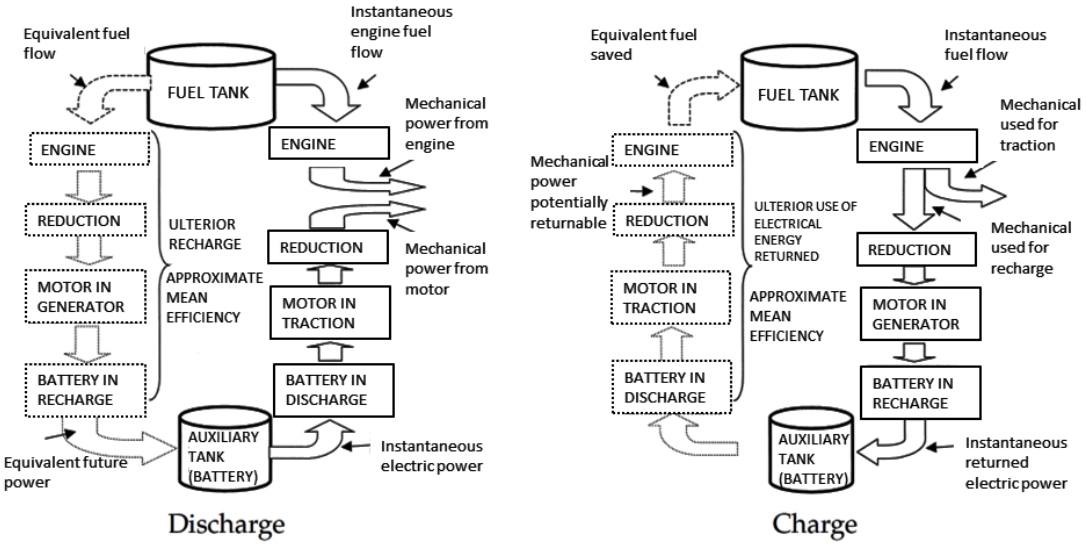


FIGURE 6.3: Charge and discharge process in a HEV

The concept of equivalent fuel can be explained as follows,

1. During the battery discharge, some part or total required power is supplied by the battery thereby reducing the battery SOC and replacing engine power. This in turn reduces the instantaneous fuel flow from the engine side. However in a HEV which has no external refilling of battery (electric) energy, all the energy ultimately comes from fuel being burnt in engine. Even the energy spent by the battery during discharge was earlier charged into the battery by the engine running at a certain efficiency point. Either this, or it must be refilled into the battery at a future instant in time by the engine running at a certain efficiency operating point burning certain amount of fuel. Thus, the battery can be perceived as virtual fuel tank. This fuel deficit being caused by battery discharge, when added to actual fuel consumed by engine is known as total equivalent fuel.

2. On similar lines, when the battery is being charged by the engine at a particular efficiency operating point, this charged energy will be used at a future time instant to replace the engine power, thereby saving the engine power and in turn certain amount of fuel. Hence, this "charge"going into the battery can be perceived as an virtual fuel being pumped into a virtual fuel tank which after subtracting from actual fuel consumed by engine gives the total equivalent fuel.

After the above discussion, one appreciates the importance of charging the battery at best engine efficiency and discharging it at worst engine efficiency. In another view, the same concept can be stated as filling the equivalent fuel into the battery at best engine efficiency and using this equivalent fuel at electrical powertrain efficiency when engine

efficiency is lower at a later instant. However, over the entire operation of the powertrain, it is not possible to attribute an efficiency quality to each amount of equivalent fuel going in/out of the battery depending on the system efficiency characteristics. Since the future load events and powertrain efficiency points are unknown, it is difficult to decide whether the present powertrain state is optimum for charge/discharge of the equivalent fuel. To facilitate this, the concept of an equivalence ratio $s(t)$ was introduced [PDG+02]. The equivalence ratio is a conversion factor between fuel energy and electrical energy which represents a lumped efficiency characteristics of the HEV powertrain over a certain specific load session defined over time. In simple terms, the *equivalence ratio* or *equivalence factor* determines how many units of electrical energy is one unit of fuel worth.

With this ideology the concept of ECMS can be defined as follows. In a HEV the total energy supply at any instant comes from fuel burnt in IC engine and eMotor using battery energy. Therefore,

$$E_{total} = E_{ice} + E_{batt} \tag{6.6}$$

Then, reorganizing Equation 6.6 in terms of power supply or fuel flow rate ($\dot{m}$) considering that,

1. The battery is a virtual fuel tank and its electrical energy flow can be represented as fuel flow using the definition of equivalence ratio $s(t)$ and,
2. The total power consumption can be represented as an equivalent fuel flow ($\dot{m}_{eqv}$) it can be stated that,

$$\dot{m}_{eqv} = \dot{m}_{fuel} = \dot{m}_{ice} + s(t) \cdot \dot{m}_{batt} \tag{6.7}$$

$$\dot{m}_{fuel} = \dot{m}_{ice} + s(t) \cdot \frac{E_{batt}}{Q_{lhv}} \cdot \dot{soc}(t) \tag{6.8}$$

$$\dot{m}_{fuel} = \dot{m}_{ice} + s(t) \cdot \frac{P_{eM}}{Q_{lhv}} \tag{6.9}$$

where $\dot{soc}(t)$ is the change in battery state of charge, m is the fuel mass, P_{eM} is the power supplied by electric motor and Q_{lhv} is the lower heating value of gasoline in MJ/g. The aim is to minimize the cost function J i.e. the total fuel cost m_{fuel} depending on control variables $u(t)$ (power-split ratio) and g_{ice} (IC engine gear ratio) subject to operational constraints as described below.

$$Min\ J = \int_0^T \dot{m}_{fuel}(t, u(t), g_{ice})dt \tag{6.10}$$

subject to,

$$P_{total} = P_{ice} + P_{eM}$$

$$P_{ice.min} \leq P_{ice}(t) \leq P_{ice.max}$$

$$P_{eM.min} \leq P_{eM}(t) \leq P_{eM.max}$$

$$P_{gen.min} \leq P_{gen}(t) \leq P_{gen.max}$$

$$SOC_{batt.min} \leq SOC_{batt}(t) \leq SOC_{batt.max}$$

If we consider the Hamiltonian for ECMS as,

$$H = P_{ice} + s(t) \cdot \frac{E_{batt}}{Q_{lhv}} \cdot \dot{soc}(t) = P_{ice} + s(t) \cdot \frac{E_{batt}}{Q_{lhv}} \cdot \frac{I_{batt}}{Q_{batt}} \tag{6.11}$$

Then comparing it with the Hamiltonian for PMP in Equation 6.5 we get,

$$s(t) = -\lambda(t) \cdot \frac{Q_{lhv}}{E_{batt}} \tag{6.12}$$

i.e. the equivalence ratio can be interpreted as a function of co-state variable in PMP.

For a HEV control, there are two aims for the ECMS,

1. Reduce the fuel consumption by minimizing the cost function as defined in Equation 6.10
2. Sustain the battery SOC within allowable limits

For a known velocity cycle, there is a certain constant value of $s(t)$ which can be termed as a nominal value s_0 for that particular velocity cycle which will satisfy both requirements for HEV control. Such a value for $s(t)$ may be found manually by performing several iterations or by several other methods. One such method is proposed in [SBG04]. Here, the HEV model is simulated using constant power-split ratio over the WLTP-class3 cycle [wlt]. The values of electrical energy and fuel energy required are recorded. Such a process is iterated over the valid power-split range.

The results for the iterations over complete power-split range are represented as shown in Figure 6.4. The slope for the line for negative power-splits is assigned as s_{dis} and for positive power-splits it is assigned as s_{chg}. These values are representatives of the conversion factors between electrical energy and fuel energy depending the electrical energy usage at the end of the driving cycle being positive or negative. These values cannot be directly used in real-time since the future values of electrical energy are unknown. In [MRGS05] , it is shown that only one equivalence factor suffices in ECMS. This $s(t)$ is always located between s_{chg} and s_{dis} values. For simplicity, we take the average of the both. From Figure 6.4, the value of s_{chg} is determined as 1.34 whereas the that of s_{dis} is determined as 4, thus the s_0 is approximated as 2.67 for the WLPT cycle.

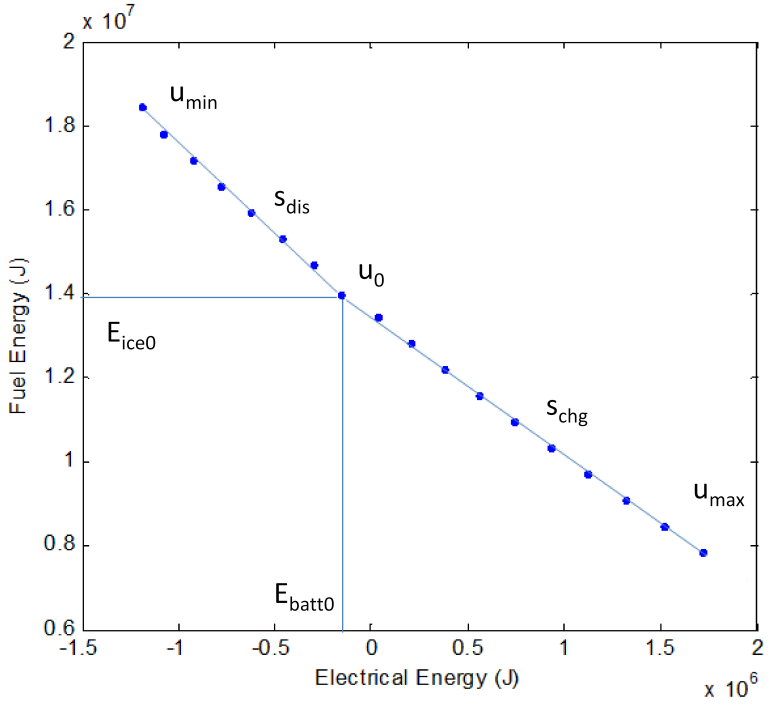


FIGURE 6.4: Approximation of an equivalence factor using energy sweep over the power-split range for a specific cycle

The s_0 can be further pin pointed by several iterations to achieve a perfect charge sustaining operation and optimum fuel consumption for that particular cycle. Thus,

the normal ECMS is an optimal solution which can be only be found if the complete trip velocity values are known a priori. In [MRGS05], it is shown that the control performance of ECMS is very sensitive to the variations in the equivalence factor and that small variations in control factor lead to a non-charge sustaining operation. This makes the ECMS system very hard and rigid to be applied for real-time implementations. Therefore, the concept of Adaptive-ECMS is introduced.

6.2.3 A-ECMS

A-ECMS aims at developing a real-time energy management strategy by enabling the control parameters to relate to the current velocity profile. The main underlying idea is to adapt the equivalence factor according to change in driving conditions in real-time. Thus, the control parameters are refreshed at specific intervals such that they add a compensating effect to the changed load situation to ensure a charge sustaining operation and fuel consumption minimization.

As suggested in [OS11], the early versions of A-ECMS were targeting a system which would adapt the equivalence factor based on predicted information (GPS based). The mission/trip is treated as a short cycle of known length and is optimized for the optimum equivalence factor. Thus, at every interval where the equivalence factor must be updated, the algorithm builds the current mission by combining the past and predicted data and then optimizes the current mission to minimize fuel efficiency and ensure charge sustaining operation. In [OS11], the further development in the field of A-ECMS is classified. A-ECMS was later developed based on the following ideas,

1. Adaptation based on driving cycle prediction
2. Adaptation based on driving pattern recognition
3. Adaptation exclusively based on feedback from SOC

There are also combinations of the above ideas, however for an online real-time implementation the idea must be computationally feasible and robust enough so as not to cause a complete system failure. The most recent and feasible approaches for A-ECMS are based on feedback of the current SOC. While these methods are easy to implement and are low on computation requirement, their performance relies on suitable tuning of parameters.

To evaluate ECMS as a core powertrain controller, the SOC feedback method is chosen given its ease to be formulated into an ECMS algorithm. In this case, there would be

two phenomena at work. The first one ensures the minimization of fuel consumption. This is achieved through the cost function minimization as defined in equation 6.10. Analyzing the structure of the expression, it is clear that if the $s(t)$ is high then the ECMS tries to penalize the use of electrical energy. On the other hand if $s(t)$ is low the use of electrical energy is encouraged. However, in order to ensure the charge sustaining operation, the $s(t)$ must be made dependent on SOC. Here, the second phenomenon is defined where $s(t)$ is updated depending on the SOC deviation. Interestingly, using such a concept highlights the flexibility of ECMS as a controller not only for a charge sustaining pure HEV but also for a charge depleting PHEV configuration. Figure 6.5 represents the SOC characteristics for HEV and PHEV operation.

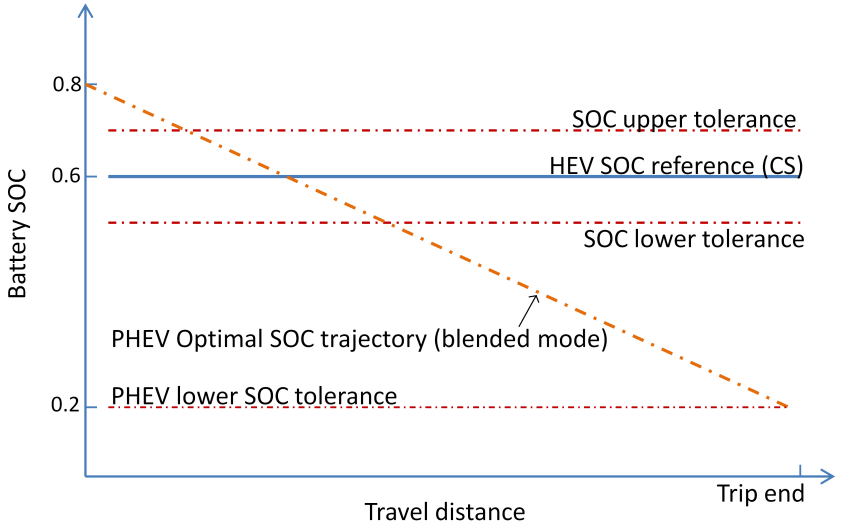


FIGURE 6.5: SOC trajectory setups for charge sustaining HEV operation and PHEV blended mode operation

A HEV operates on charge sustaining mode where over the complete operation range, battery SOC must be maintained within allowable limits and preferably close to the reference SOC level. In contrast, a PHEV operates on a blended mode strategy. The battery for a PHEV usually has higher capacity than that of a HEV and is externally refillable. Therefore, the aim for PHEV operation is not charge sustenance but controlled charge depletion so that it can be replenished externally at the end of the trip. Therefore, depending on the travel distance the blended mode SOC trajectory for a PHEV is determined as shown in Figure 6.5. Based on these SOC operation characteristics, the adaptation for ECMS control parameters is defined as follows. It is based on [FS12].

For HEV

$$s(t) = s_0 + s_0 \cdot K \cdot \tan\left(\frac{soc_{ref} - soc(t)}{2\pi}\right) \tag{6.13}$$

where s_0 is the nominal equivalence factor. Since we know that equivalence factors lie between s_{chg} and s_{dis} the approximation for nominal equivalence factor may be derived as an average of both values. K is a feedback factor, it decides s(t) correction intensity related to the SOC deviation from soc_{ref}. K is manually tuned to obtain an acceptable performance of the system.

For PHEV

The adaptive ECMS (A-ECMS) is implemented and tested for both charge sustaining normal HEV and blended mode Plug-in HEV. While for normal HEV the soc_{ref} does not change, in a PHEV the aim is to use as much battery as possible. Hence the soc_{ref} must be adjusted according to the covered distance.

$$soc_{ref}(t) = \left(\frac{soc_{final} - soc_{init}}{D_{total}}\right) \cdot d(t) + soc_{init} \tag{6.14}$$

where $d(t)$ is the present covered distance value, D_{total} is the final distance value and soc_{init} is the SOC level at the start of the trip.

6.2.4 Simulation Model and Algorithm

Using the above definitions, the A-ECMS using adaptive equivalence factors with SOC feedback is designed as a Matlab function and inserted into the TtR hybrid model using the following schematics and algorithm as shown in Figure 6.6.

A-ECMS Matlab Function Algorithm

Input

Transmission gear ratios (gear_ratio)
IC engine fuel map (g/kWh)
Motor torque speed characteristics
Vehicle velocity (m/s)
Total torque demand (Nm)
Updated Equivalence factor s(t)

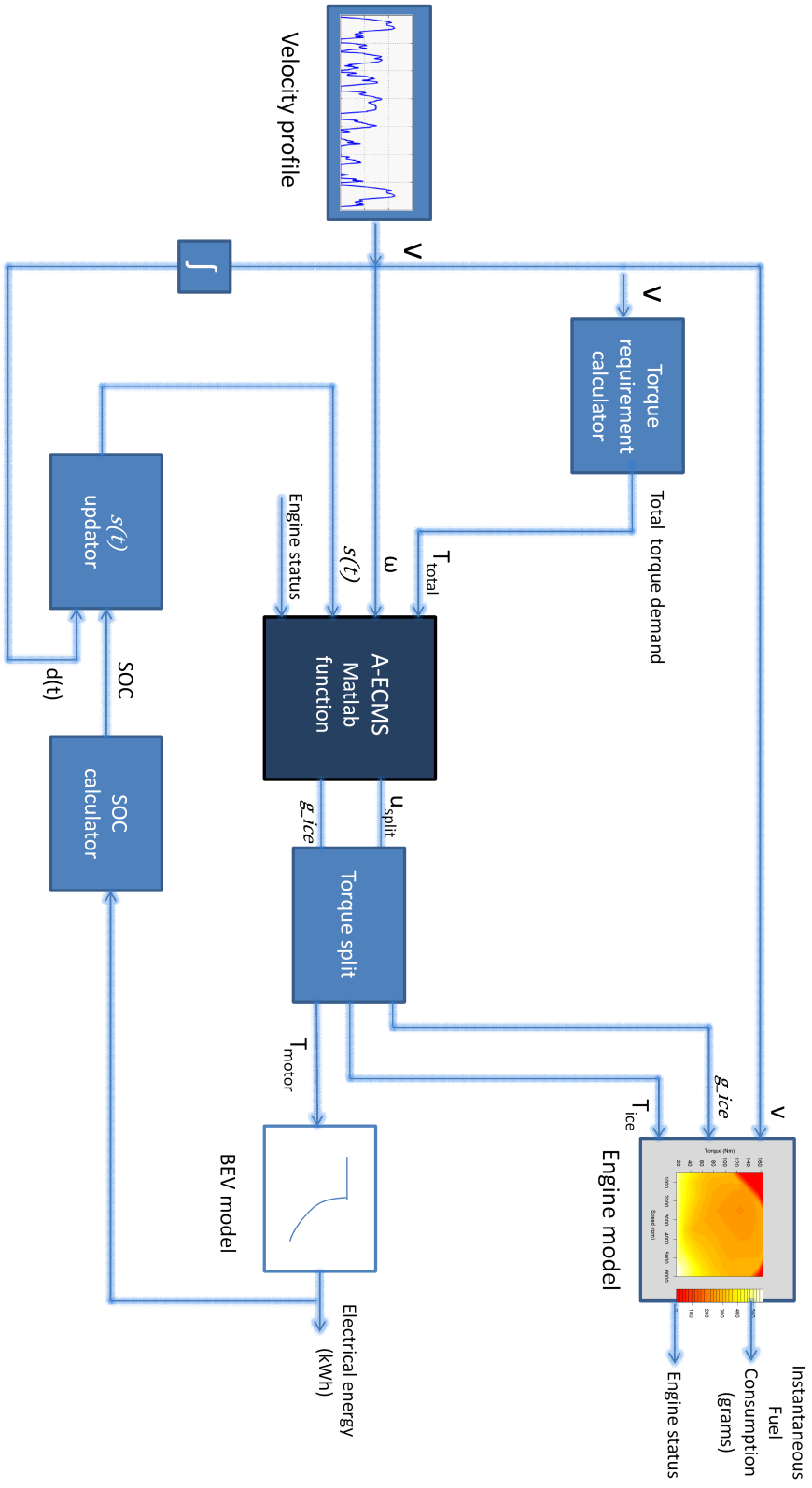


FIGURE 6.6: ECMS simulation model

Engine state (On/off)

Process

for$_1$ (u_{split} = -0.5 to 1 with interval of 0.1)

find demand T_{ice} and T_{motor}

for$_2$ (gear_ratio 1 to 5)
find ω_{ice} and $T_{at.ice}$ with respect to gear
find fuel requirement m_{ice} at the operating point
compare m_{ice} for all gears, find optimum gear and m_{opt} for the required torque
end **for**$_2$

if ($engine_{status}$ = Off)

$m_{opt} = m_{opt}$ + engine start penalty;

else
$m_{opt} = m_{opt}$;

end **if**

Calculate cost function as

$$J(u_{split}, g_{ice}) = m_{opt} + s(t) \cdot \frac{P_{battery}}{Q_{lhv}}$$

end **for**$_1$

compare cost function J for every u_{split} for cost minima.

Output

Optimum power split $u_{split.opt}$
Optimum engine gear $g_{ice.opt}$

6.2.5 Engine Starting Penalty

A very common problem encountered in ECMS development is to align the objectives of fuel consumption minimization by optimum operation of the powertrain to match with the smooth powertrain operating characteristics (for e.g. smooth gear shift, engine start stop). Often to optimize the fuel consumption ECMS attempts to demand power and cut the demand from engine at times within seconds of each other. This phenomenon

causes on one hand the frequent start stop operation for the IC engine which costs energy and destabilizes the smooth powertrain functioning. To avoid this frequent engine starts there is a virtual cost added to the cost function called engine starting penalty. To match this value according to the engine operation domain, it has been tied to the engine speed. Thus this penalty can be defined as,

$$\text{engine start cost} = \frac{250}{\omega^2} \text{ in gram} \tag{6.15}$$

6.3 ECMS simulation results for HEV and PHEV

To validate the benefits of the ECMS strategy in a hybrid electric vehicle, it is directly compared to the performance of a conventional IC engine powered vehicle. To be fair, considering that a hybrid electric vehicle has to account for the increased weight of motor and batteries, the conventional IC engine vehicle is given an advantage of being 200 kg lighter at 1350 kg compared to the 1550 kg for a hybrid vehicle. Furthermore, for a pure IC engine vehicle the fuel consumption is closely related to the driver behavior. For e.g. drivers who do not adjust gears to compensate for the load change according to the vehicle velocity are expected to clock significantly higher fuel consumption values against the drivers who adapt the load to proper gear and maintain the engine in efficient operation region. Considering this, the conventional vehicle is provided with an intelligent gear selection algorithm which will allow it to return its best fuel consumption values to be compared to the performance of an ECMS equipped HEV. Such an algorithm is described in Section 3.2.2 (Figure 3.9). Thus, when a gasoline engine powered conventional vehicle is simulated to run over the WLTP-class3 cycle, Figure 6.7 represents the engine operation behavior over the complete run. In addition, it is assumed that the ECMS hybrid vehicle employs the SAGA function while deceleration. This allows for the consideration that all the deceleration energy is now being absorbed back into the battery subject to component efficiencies.

Running on the WLPT-class3 cycle, the conventional vehicle returns a fuel consumption figure of 6.68 l/100km. As seen in Figure 6.7, the intelligent gear selection algorithm does not allow the engine operation points to go beyond a certain range and forces them into efficient operation region as much as possible. Although this algorithm is not as sophisticated as the one used in a part of ECMS code for gear selection, it does a satisfactory job of emulating a driver biased towards fuel saving. This facilitates a fair comparison between conventional and ECMS based powertrain performances.

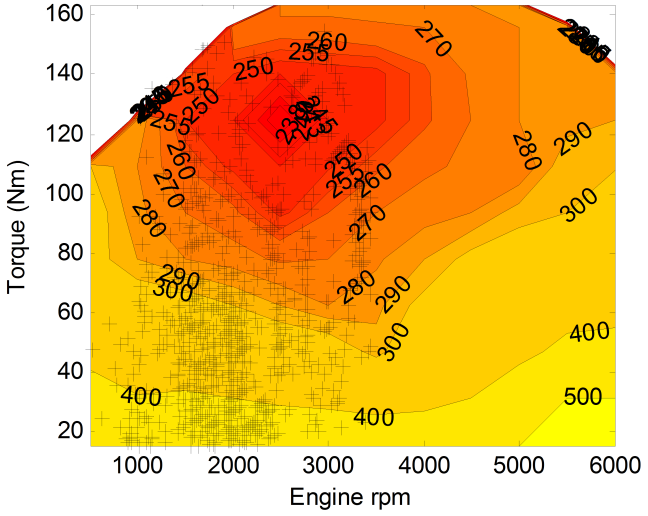


FIGURE 6.7: Engine operation points for conventional vehicle over WLTP-class3 cycle (efficiency map in g/kWh)

6.3.1 Tuning the A-ECMS

As discussed earlier, the nominal equivalence factor s_0 lies between the two values s_{chg} and s_{dis}. To tune the A-ECMS with respect to fuel consumption minimization and charge sustenance characteristics, the first approximation for the s_0 is taken as an average of the two values as 2.67 for the WLTP cycle. Manual tuning for the SOC feedback based A-ECMS is a tedious task and after many permutation and combination for the s_0 and K (SOC feedback gain) values, a pair with optimum performance characteristics is chosen. The Table 6.1 presents some random iteration results for the manual tuning process.

After an initial approximation using s_{chg} and s_{dis} values, the value of s_0 is finally manually tuned to 3.5. The value of K was manually tuned to 0.7. soc_{ref} is fixed at 60%.

6.3.2 Results: HEV (charge sustaining)

This section is dedicated to the A-ECMS performance for charge sustaining HEV. To demonstrate how the ECMS strategy affects the fuel consumption, Figure 6.8 compares the IC engine operation points over a single WLTP-class3 cycle for conventional IC engine vehicle and charge sustaining HEV.

As observed in Figure 6.8, comparison of the engine operating points for ECMS based HEV and pure IC engine powered conventional vehicle clearly demonstrates how ECMS actively relocates points from low engine efficiency region to high efficiency region and at times, completely replaces the inefficient engine operating points by motor power.

Table 6.1: Tuning the A-ECMS with manual iterations

Cycle × 5	**s0**	**k**	**l/100km**	**start cost**	**Type**	***Battery* (Wh)**	*Comments*
WLPT class 3	n/a	n/a	6.68		Conventional		
WLTP class 3	2.3	0.7	5.4	$250/\omega^2$	Hybrid CS	7000	Reference intialization
WLTP class 3	3.3	0.7	5.525	$250/\omega^2$	Hybrid CS	7000	Improved performance with engine starts stops. Implementable since it fits to engine reaction performance. With 7 kWh battery. 116 km.
WLTP class3	3.8	0.7	5.553	$250/\omega^2$	Hybrid CS	7000	Better charge sustenance.
WLTP class 3	3.5	0.7	5.526	$250/\omega^2$	Hybrid CS	7000	Slightly better performance compared to s_0 as 3.8
NEDC	3.5	0.7	0.1974	$250/\omega^2$	Plug-in CD	13000	Almost 97% EV running. Since battery is big the AER is applied for 5 NEDC cycles. If more distance is covered (10 NEDC) then the consumption will increase. But this gives a very good example of control when distance to be traveled is known beforehand.
1 X Arco Mreano ecosm12	3.5	0.7	4.19	$250/\omega^2$	Hybrid CS	7000	Against a conventional I.C. engine simulation consumption of 5.541 l/100 km. End SOC was 56%, reference was 60% . Total distance was 157.8 km.

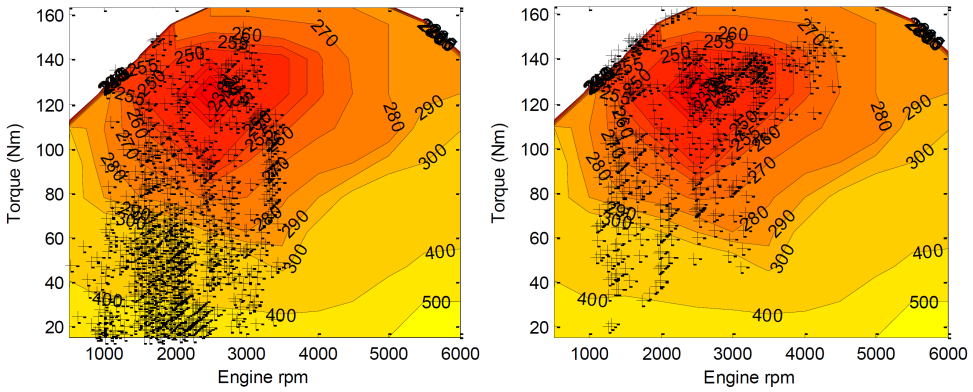


FIGURE 6.8: WLTP class3 cycle engine operating points, conventional ICE (left), TtR ECMS (right)

With the strategy tuned to earlier described specifications, the HEV model was simulated over 5 continuous WLTP-class3 cycles adding to a total of 116 km. The reference SOC was set to 60 % for a Hybrid CS (charge sustaining) operation.

In Figure 6.9, the ECMS controller behavior over an extended cycle distance is simulated. At low speeds, the controller avoids inefficient engine operation and prefers the use of motor power. This discharges the battery and eventually a falling SOC triggers an increased $s(t)$ which makes the cost for using battery energy high. When this cost eventually overcomes the effect of engine starting penalty, the IC engine is brought into operation. The ECMS algorithm takes care that the IC engine operated with optimum efficiency and tries to replace engine power when necessary or overload the engine at times to charge the battery again at best engine efficiency.

Since the s_0 and K are tuned initially, the charge sustaining operation is ensured as shown. The SOC fluctuates within a certain range but is not allowed to excessively deviate from soc_{ref} . Even when the conventional vehicle is given an advantage of being 200 kg lighter than the HEV, the HEV returns a fuel consumption figure of 5.52 l/100km against the 6.68 l/100km for a conventional vehicle. This translates into a direct fuel and CO_2 savings of 17.3%.

6.3.3 Results: PHEV (Blended operation)

The ECMS can be applied as control strategy for PHEVs also just by using a dynamic soc_{ref} Such a concept has already been discussed with equation 6.13. A PHEV has external energy refilling ability and hence unlike the HEV the main ounce is on efficiently using all the refillable energy before its time to again recharge the battery. Therefore, in a control strategy for PHEV it is very important to know beforehand, the trip length or the distance to next possible opportunity for a battery refill. This allows for a

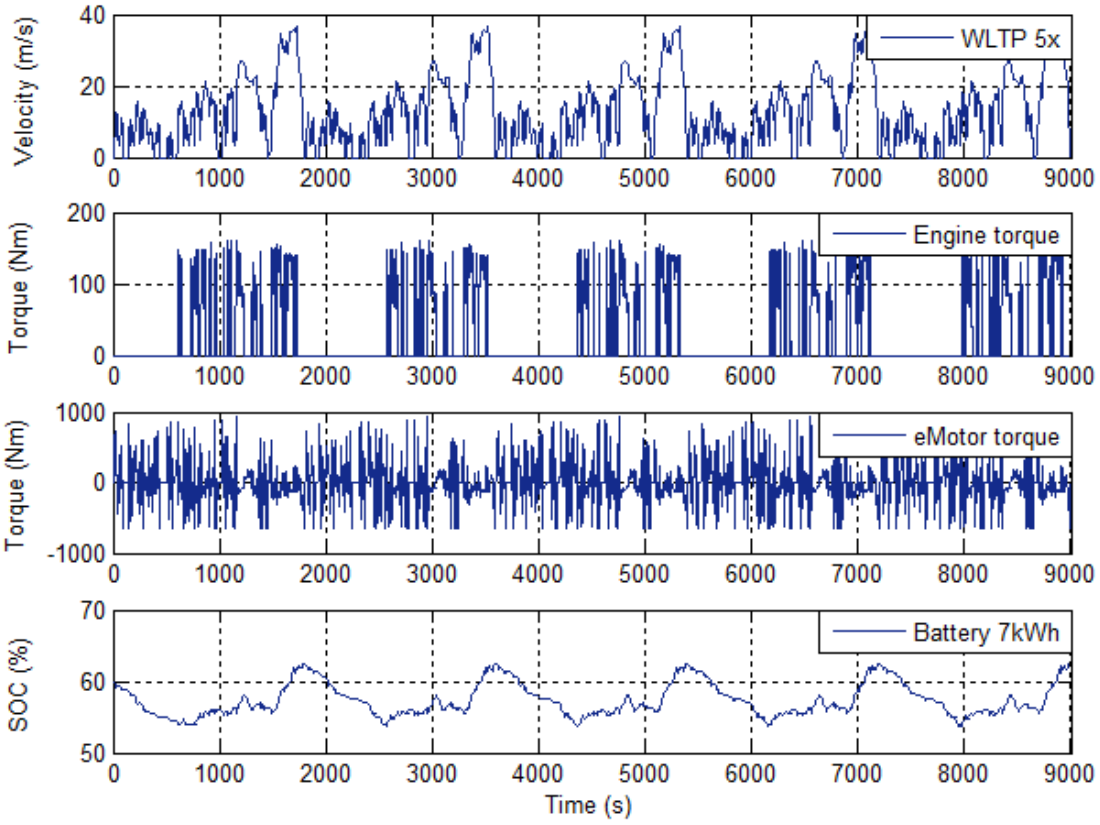


FIGURE 6.9: ECMS controller behavior (charge sustaining HEV, WLTP 116 km, 7 kWh battery)

proper distribution of available electrical energy over the trip duration. To have a better comparison, the PHEV with a 13 kWh battery pack and controlled with ECMS, is simulated as shown in Figure 6.10 exactly with the same conditions and tuning used for HEV ECMS evaluation earlier.

The PHEV is simulated to run 116 km over 5 continuous WLTP-class3 cycles. Assuming that with an all electric range of roughly about 40 - 50 km, the PHEV covers the total distance of 116 km with a fuel consumption performance of 3.23 l/100km which is approximately half that of the conventional vehicle (6.68 l/100km). The battery is charged till 0.8 SOC level and allowed to discharge till the 0.2 SOC level. If calculations are correct, the 0.2 SOC level will be reached at the end of cycle. If it is the case that some distance remains to be covered, then the PHEV must revert to charge sustaining operation. In comparison to HEV operation, the reduced engine operation is clearly noticeable in the engine torque graph.

Since the PHEV uses externally refillable energy, it does not make sense to calculate the fuel savings and attribute them to the control strategy benefits though there are definitely instances during PHEV operation where ECMS has ensured optimum engine operation and reduced fuel consumption. However, a large part of the fuel savings

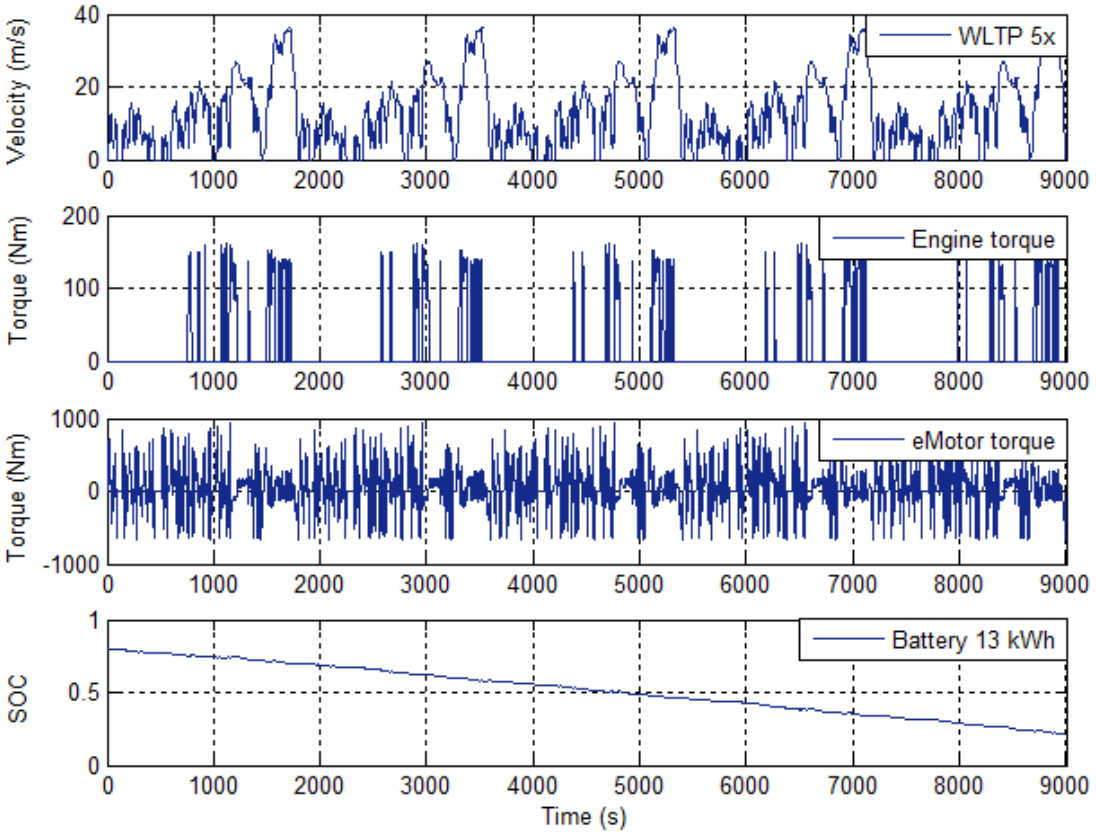


FIGURE 6.10: ECMS controller behavior (blended Plug-in HEV, WLTP 116 km, 13 kWh battery)

would have to be attributed to the reduction in the battery SOC. Nonetheless, using such a powertrain would then result in direct fuel and CO_2 savings of about 52% for the given trip. It is however interesting to notice that, as the trip length increases the fuel savings would start dropping till they eventually reach the level of HEV as discussed earlier in Figure 2.12. Then one can put a case forward stating that the PHEVs (with configuration as stated in this work) would be highly effective in city driving (within AER), very effective for trips of about 100 km, fairly effective for 200 km and lose all advantage over normal HEV if they have to be continuously driven for about 300 km unless the battery size is increased which will in turn increase their weight.

6.3.4 Real world cycle evaluation

To evaluate the effect of HEV using the ECMS controller, it was simulated to run on 5 WLTP-class3 cycles where the nominal equivalence factor s_0 was manually tuned to fit the cycle energy dynamics. Since, it is earlier claimed that the ECMS strategy adapts itself to the changes in load conditions to actively reduce fuel consumption and sustain the SOC level, it is necessary to test the algorithm on a random velocity test

mission which is actually not a cycle. This means that the system tuned to WLTP-class3 cycle must adapt itself to control the powertrain running on a complete random trip parameters.

For this purpose, a velocity data set of recorded velocity is chosen based on [ARC] known as Arco Merano or (A_M). The HEV with CS operation strategy is simulated over the complete run of 157 km.

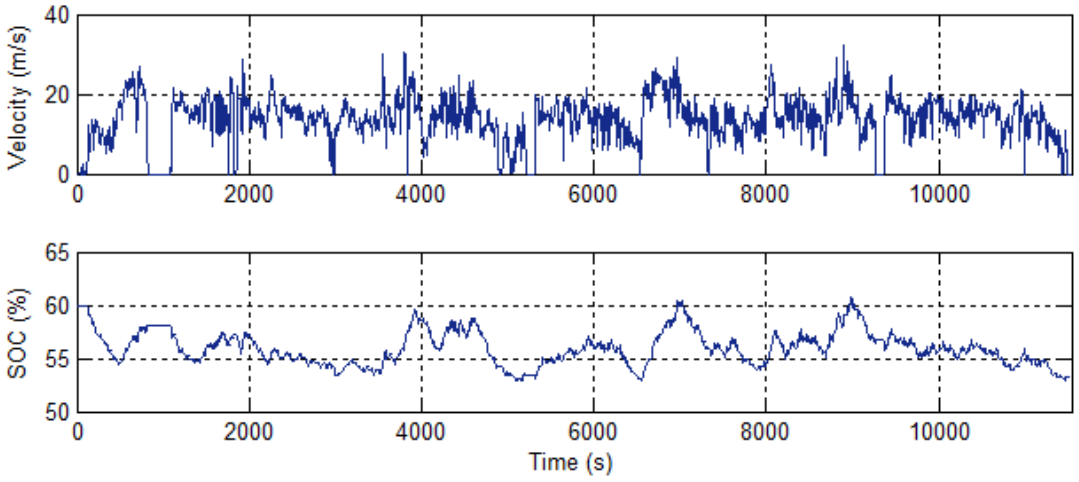


FIGURE 6.11: ECMS controller behavior on a real world recorded velocity session (A_M)

Figure 6.11 strongly suggests a departure from the repetitive SOC patterns as opposed to the 5 WLTP cycles simulation seen in Figure 6.10. The test results reflect a drive of about 3 hrs with 157 km and indicate that even though the SOC remains mostly in the lower side of the reference, it is never allowed to fall uncontrollably and is steered back to the reference level at many instances. Thus the A-ECMS successfully adapts the control parameters using its SOC feedback loop and maintains the SOC within tolerable limits. In this run, the HEV returns a fuel consumption performance of 4.19 l/100km as compared to the conventional vehicle returning a 5.54 l/100km thereby saving fuel and CO_2 to the tune of 24.3 %. Interestingly, given the low velocity characteristics of the A_M velocity drive the PHEV returns a value of 1.96 l/100km which is a classic example of increasing the vehicle range by reducing the average trip velocity and acceleration-deceleration dynamics.

The overall simulation results are compiled in the Table 6.2 for a direct comparison.

Conclusion

The ECMS successfully controls the HEV and PHEV powertrain to find the best power-split between eMotor and IC engine and manipulates the powertrain to find best overall

TABLE 6.2: Fuel consumption comparison for various powertrain configurations

Velocity cycle	***Powertrain***	***Consumption(l/100km)***
WLTP class3 (5x)	Conventional ICE	6.68
WLTP class3 (5x)	Pure HEV (CS)	5.52
WLTP class3 (5x)	Plug-in HEV (Blended)	3.23
Real world (A_M)	Conventional ICE	5.54
Real world (A_M)	Pure HEV (CS)	4.19
Real world (A_M)	Plug-in HEV (Blended)	1.96

operating efficiency. However, it must be noted that ECMS can afford to replace inefficient engine operating points only if there is enough charge in battery which will allow such an operation. Hence, irrespective of the powertrain control strategy, a major portion of overall improvement in the powertrain operation efficiency can be attributed to the energy which is recuperated during deceleration by the regenerative braking system. As discussed earlier, present regenerative braking systems are severely compromised due to battery and motor performance limitations. Therefore, not all of the available deceleration energy is absorbed into the battery which in turn allows less flexibility for ECMS to replace inefficient engine operation points. On the other hand, SAGA takes into consideration the limitations of regenerative braking system beforehand and attempts to recuperate almost all the the available deceleration energy. As simulated earlier in Chapter 5, SAGA enables the regenerative braking system to absorb deceleration energy at 80% efficiency. Hence, when the HEV/PHEV models are simulated for fuel economy as shown in Table 6.2, it is possible to assume that majority of the energy during braking maneuvers is recuperated subject to operational efficiencies of the regenerative braking system components.

Thereby, it is argued that using SAGA in combination with ECMS would allow for substantial gains in fuel economy and reduction of CO_2 as compared to those HEVs which do not use SAGA and will not be able to regenerate comparable amount of deceleration energy to allow flexibility to it's PMS to aggressively replace the inefficient engine operation points.

Chapter 7

Conclusion

7.1 Conclusion and summary

Recently, an EU research committee [KR08] predicted that ITS has the potential to reduce fuel consumption and thereby, cut CO_2 emission by 15% each year till 2020. This dissertation investigated the basic aspects of how ITS could widen the opportunities for fuel savings by evaluating the scenarios where the performance and efficiency of vehicle powertrain and regenerative system could be enhanced using the information provided by ITS. In this context, an eco-longitudinal motion controller was developed called Smart and Green ACC, which actively balances the efficiency and safety while maximizing the deceleration energy regeneration.

The literature search section is mainly dedicated towards presenting the state of art in the fields which will be most influential in shaping the energy efficiency factor in transportation segment. The advent of autonomously driven vehicle disassociates the dependency of powertrain efficiency on individual driving style. Moreover, the automation of lateral and longitudinal control helps in increasing the effectiveness of ITS data utilization to control vehicle motion in a way that is conducive for achieving optimum powertrain efficiency. Furthermore, the various powertrain configuration and their characteristics are described along with the developments in powertrain control strategies. This is followed with a ITS relevant information on data communication.

It was aimed to evaluate the effect of a eco-longitudinal motion controller with respect to each of the different electric vehicle powertrain configurations in various traffic scenarios. In Chapter 3, the modeling of these vehicle configurations, namely, BEV, HEV and PHEV is described. To compare the increased efficiency, the conventional vehicle was modeled as a benchmark. All models use the same eFuture vehicle prototype

as a base which is then modified based on the powertrain configurations. The models are based in Matlab-Simulink platform and were verified based on energy calculation comparison between energy model and test track measured values in case of BEV. For conventional vehicle, the fuel economy values for similar weighted vehicles was compared to validate the model. The HEV and PHEV model was generated combining the BEV with conventional vehicle model.

Chapter 4 defines the Smart and Green ACC as a vehicle longitudinal motion controller which balances safety and efficiency. The basic idea behind such an ACC was to save energy either from the supply side or by enhancing the regenerative system performance. On these lines, a safety envelope concept was developed which defines the safety state of the vehicle by marking the regenerative braking capacity with respect to front vehicle characteristics. Apart from this the SAGA function is also constrained by the ISO ACC guidelines. Various possible concepts for the development of SAGA function are described namely, exclusive braking, threshold braking and blended optimized braking. Figure 4.15 presents application area map for the SAGA function.

The application of the SAGA function to a BEV is presented in Chapter 5. It was observed that "one system fits all"approach was not possible given the different characteristics of city and highway traffic domains. The highly dynamic city traffic domain has a low average speed and frequent start stops where the velocity often performs cycles between 0 - 50 kph. Figure 5.1 gives an idea about the position of city domain in the efficiency map of the e-motor. Considering the large difference between powertrain efficiency range in the city domain, a dynamic programming based algorithm was developed to find the optimum velocity trajectory for the BEV during the acceleration phase. By using motor torque as the control variable, the algorithm returns optimum acceleration value corresponding to the present velocity by simulating the entire BEV energy model using the "greedy algorithm"type of dynamic programming. This part of development can be identified as the energy saving through supply side. To realize energy saving through regeneration side, another algorithm was proposed which considers the regenerative braking system limitations and tries to adjust the total braking distance in city domain so as to allow enough tolerance for the regenerative system to absorb maximum deceleration energy in specific braking scenarios (e.g. traffic signal approach). When these two algorithms for city domain are combined and simulated with a BEV energy model over a specific city velocity cycle, an overall saving of 9% was realized as compared to an aggressive human driver model. This figure will vary depending on the instances of accelerations and decelerations over the trip. One important point is that this algorithm, which forms a part of SAGA function for city domain, affects drivability in terms of allowable acceleration and hence, at times may require some extra time to reach destination as compared to normal driving style. At present this situation may be

unacceptable to some drivers who prefer a sporty performance against efficiency. However, in future, when autonomous driving becomes a reality, these algorithms will come in handy to smoothly move platoons of vehicles as traffic segments between one traffic signal to another, thus optimizing energy consumption of not one but a whole fleet of vehicles.

The highway traffic domain is a high speed and low acceleration area. On the e-motor efficiency map (Figure 5.1) it is observed that in this domain the efficiency range does not vary as much as in city domain. Therefore, the only energy saving potential from the supply side is to save on the high air drag energy by reducing the average trip velocity. However, such a measure is not feasible because it would increase the time to destination by several minutes which is absolutely undesirable. Nonetheless, the high velocity of the highway domain presents a excellent opportunity to save energy from the regeneration side. Owing to the motor power and battery charge acceptance constraints, regenerative systems offered very limited performance. However, the latest state of art automotive traction battery cells offer much better performance and hence it is proposed to design the battery pack to cater to the complete deceleration energy absorption requirements. In this context, the SAGA function for the highway domain proposes maximum/exclusive use of motor braking for all deceleration maneuvers in the highway scenarios. Simulations show that for the eFuture project prototype which uses a 30 kW motor, exclusive motor braking proved sufficient for most highway braking requirements where deceleration demand is not too high e.g. deceleration from 130 kph to 80 kph where a 150 m headway was present. In certain demanding situations (130 - 60 kph), it was not wise to just rely on exclusive motor braking blindly. A control system was proposed which uses either a threshold emergency control or an optimized brake blending using motor and service brakes. It was observed that even though the threshold braking was functionally safe, it proved ergonomically unsatisfactory for the passengers owing to its high deceleration maneuvers. The blended braking shows acceptable performance since it continuously monitors the vehicle safety state and rectifies the deviation from reference within time and in a ergonomically smooth manner. Table 5.1 lists the regenerated energy values for different braking maneuvers. A fixed energy saving comparison is not possible for such scenarios, however, it can be concluded that every successfully implemented highway deceleration (slow moving front vehicle/ speed limit etc) maneuver for SAGA system will yield substantially more regenerative energy as compared to present ACC systems which do not optimize vehicle longitudinal dynamics to suit the performance of their regenerative braking systems.

SAGA as applied to a TtR hybrid vehicle is discussed in Chapter 6. In case of HEV, a master-slave set-up is proposed where the SAGA function acts as a longitudinal motion controller and generates commands for acceleration/deceleration. The ECMS control

algorithm was modeled to act as a core powertrain manager. This SOC feedback based energy management strategy is tuned by taking into consideration that 80% of deceleration energy can be regenerated if SAGA function is used. ECMS works in a two sided effect where from one side it actively reduces the fuel consumption and on other side tries to maintain the battery SOC within a tolerable range. Simulations were performed on a WLTP-class3 cycle for TtR pure charge sustaining hybrid, plug-in hybrid and compared with the performance of the conventional vehicle. For the five continuous WLTP-class3 cycles, the charge sustaining HEV running on ECMS returned a 17.3% reduction in fuel consumption and CO_2 emission whereas a plug-in hybrid realized a 52% decrease which however is a variable figure since plug-in hybrids run on externally refillable energy. To evaluate whether the ECMs tuning held good for missions other than WLTP-class3, all the simulations were retested using velocity values from a random recorded trip. The 157 km trip was successfully managed by the ECMS controller where the SOC was maintained in a tolerance band (charge sustaining operation) and fuel consumption reduced by 24.3%.

Finally, the concept of SAGA function using ITS information to actively balance the safety and efficiency and control the longitudinal motion of an electric vehicle is elaborated by defining a system architecture for an autonomously driven vehicle. The ITS infrastructure, communication protocols and international standardizations of green traffic management are still in an embryonic stage. It will take certain incubation time for the complete commercial functional system of autonomous vehicles to hit the road and hence most of the present research efforts are concentrated in this direction. Once such a system is in place which can reliably exchange data within its nodes where vehicle will then be guided to their destination fully on V2I basis, the next step would be to control vehicle longitudinal motion to enhance the safety and efficiency performance in order to save fuel and reduce environmentally harmful emissions. The development of function like the Smart and Green ACC is the first step in this direction.

7.2 Future work possibilities

Most of the work in this thesis is focused on developing the SAGA function based on intensive simulations. Although a primitive version of the SAGA function was field tested on the eFuture vehicle prototype Section 5.4.4, it was not possible to implement and test the fully functional exclusive motor braking/blended braking concepts owing to the extensive limitation on the eFuture vehicle battery charge acceptance characteristics where, the battery pack would permit no more than 100 amperes of incoming current.

Furthermore, the e-motor was capable of 30 kW which, according to simulations, is certainly underpowered in some cases of the required regenerative braking performance. To test the full capabilities of SAGA function it is first necessary to build regenerative system to specifications which will fulfill the deceleration energy absorption requirements. To this end, a sufficiently powered motor with tailored battery pack (xxS-xxP) must be developed.

The application of SAGA to a HEV is conceptualized in a way that the SAGA function mostly optimizes the regeneration phase. During the energy supply phase, the SAGA function acts as a normal ACC where the demanded torque is later split between the two power sources through ECMS optimization for enhanced fuel economy. It is possible to evaluate further, if controlling the longitudinal vehicle dynamics during the acceleration phase can reduce the fuel consumption. Furthermore, the SOC feedback based ECMS algorithm which is applied to TtR in this thesis is especially easy to implement on an actual vehicle considering its simplicity when compared to the complex powertrain management strategies applied to the planetary gear based hybrids.

It is elaborated how the SAGA function would make use of the ITS data to adapt the constraints of the vehicle regenerative system with longitudinal motion control requirements to optimize safety and efficiency. The next step is to standardize a protocol with respect to which information would be received/transmitted, interpreted and processed to form a set of data, to be fed as input to SAGA function at each interval. In short, it deals with the development of the data fusion and pre-processing layers (Figure 7.1) which generate a vehicle state definition for the SAGA function. This is further explained in the following section. Although there is progress in development of automotive communication protocol standardization, it is something which will have to be done on an international scale with involvement of various national governments, research institutes, automotive OEMs and electronics OEMs and hence it will take time. Till such a time, functions like SAGA will have to be constantly re-adapted to new standards.

Finally, the overall evaluation for feasibility of implementation of a safe and efficient automated/autonomous vehicle longitudinal motion controller leads to identification of new requirements in a vehicle control architecture. These are further discussed in the following section.

7.3 An architecture for co-operative lateral and longitudinal control of Autonomous vehicles

Any system can be divided in the form of a generic representation which consists of sensing, processing and actuation layers. Figure 7.1 shows a schematic representation of an autonomously driven vehicle control system architecture. It specifically addresses the need for an architecture which caters to the ever developing field of various scattered eDAS (eco. Driver Assistance Systems) which in the near future, will be combined on a single platform to realize the full concept of ITS (Intelligent Transportation Systems). More importantly it helps to locate the SAGA function in the chain of control systems. The SAGA function has been developed as a eco-longitudinal vehicle motion control function which is not programmed to take into account the needs for lateral motion control. The architecture described in Figure 7.1, tries to address this part where the SAGA function must filter its output in consultation with the vehicle lateral control. In addition, the architecture also throws light on the complications in the systems when the autonomous vehicle concept is applied to a hybrid electric vehicle.

The **sensing layer** consists of the sensors relevant for the vehicle environment sensing as well as vehicle motion and powertrain state feedback. The stereo and mono cameras provide data feed to determine the lane markings and determine lateral position of vehicle in the lane. This data can also be combined with the LIDAR sensor data to form a 3D map of the vehicle environment. Both RADAR and LIDAR can be used to sense obstacles or front vehicles and calculate relevant characteristics. The GPS system provides the coarse vehicle position. Various other sensor may be used to further ascertain the vehicle position, motion and powertrain state.

In such modern sensing layers a lot of data is generated which need to be analyzed to make an accurate vehicle state definition. Most autonomous vehicle architectures use a **data fusion layer** where data from all the sensors is compared/combined to have a reliable solution. However, for implementation of ITS, this layer must be further expanded to absorb the data from various external sources or systems such as traffic data from V2V/V2I communications, horizon data from the DSRC transmitters, curve warning speed an acceleration restrictions and speed limit data which will help form a comprehensive horizon environment definition. When all these information is fused, a complete vehicle state definition is generated which provides the constraints for present and future vehicle states. This state constraint data set is then passed as an input to the control/processing layer.

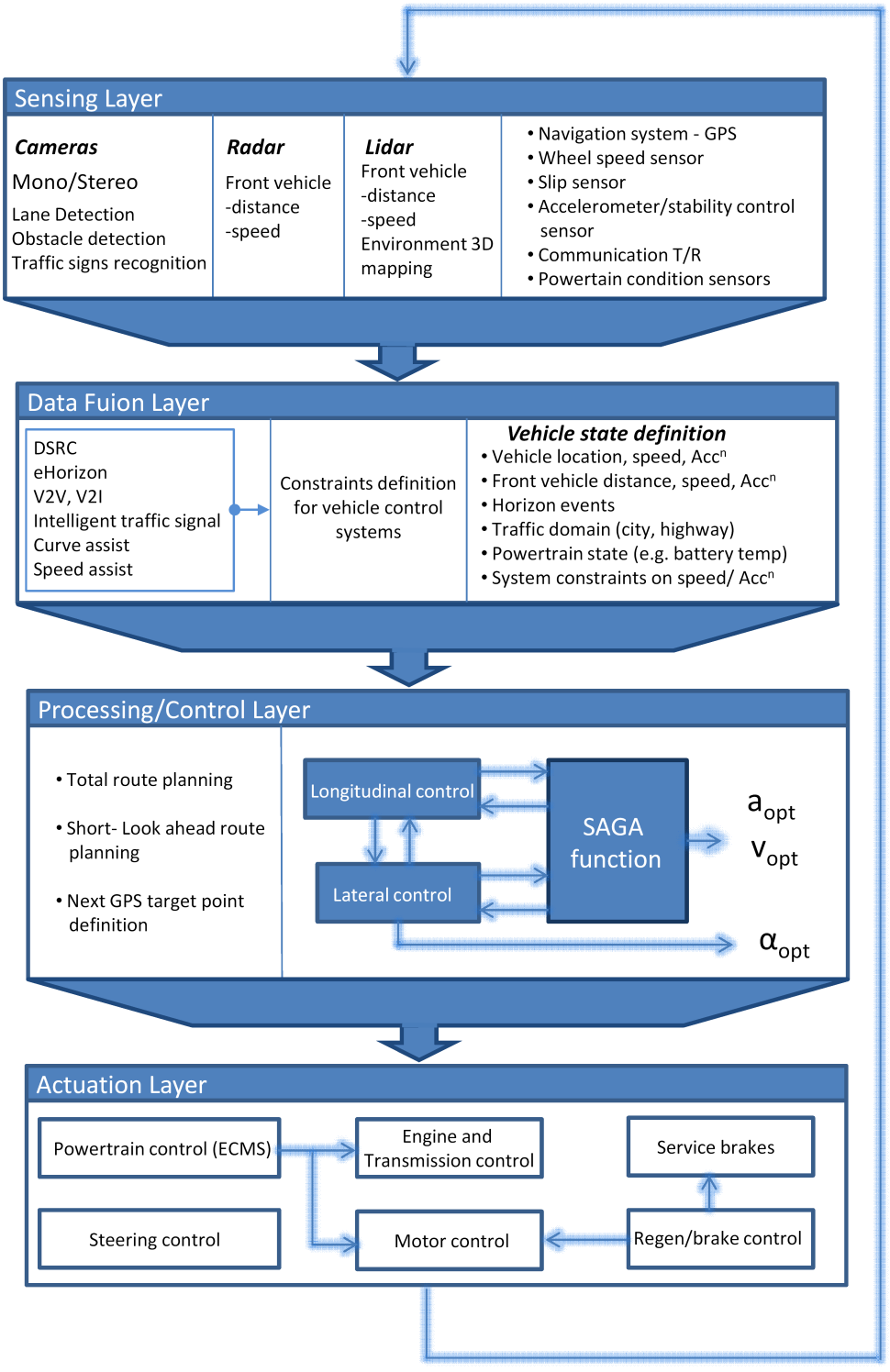


FIGURE 7.1: A generic architecture for a hybrid autonomous vehicle using SAGA function

In this case, the **control/processing layer** receives a pre-processed set of data which is conditioned to be directly used in the relevant processing algorithms. These algorithm include a navigation system which is responsible for the long term and short term route planning. The main aim for the autonomously driven vehicle is to find its next target GPS co-ordinate and steer the vehicle in between the lane markings avoiding the obstacles and adapting the longitudinal speed. Corresponding to the described tasks, once the next target GPS point is defined it is up to the longitudinal and lateral control systems move the vehicle till that point, however, how it is done is extremely important from the safety and energy point of view. Hence, there must be co-operative consultations between the lateral and longitudinal systems. For e.g. the ACC allows for a 2 m/s^2 acceleration. This is acceptable if the vehicle is to move in a straight line. However, during a turn or during a turn on a signal from standstill such high acceleration is unsafe. Apart from this, longitudinal movement of the vehicle is the main energy consumer. The SAGA function optimizes the powertrain and motion characteristics to find a optimum solution for motion control. This solution, must also be consulted through the lateral control so as not to allow unsafe vehicle maneuvers. Furthermore, the systems like intelligent traffic signal information, curve warning systems, horizon traffic data, V2V emergency braking messages form a set of constraints which are transferred from fusion layer and must be respected by the control systems. These numerous demands make the architecture for the modern energy efficient autonomous vehicle increasingly complicated.

The **actuation layer** specifically portrays the schematics for a hybrid electric vehicle. Optimized motion requests must be transformed into power and torque values. For a hybrid vehicle the ECMS strategy is discussed earlier further optimizes the requires power by splitting it between the two power sources depending on the powertrain state (e.g. battery SOC etc). This suffices for the positive power demand. For the negative power demand, normally the SAGA function already optimizes the motor and service brakes distribution. At times however, it may be possible due to an adverse battery state (e.g. high temperature, high SOC etc) that the distribution needs to be reworked or overridden for only service brake operation. Translation of requested steering angle into physical vehicle deviation taking into consideration vehicle stability and road conditions is a topic of ongoing research. Finally the actuators provide a feedback of their actions which also serve as a input for sensing layer if need be for a corrective action.

Appendix A

BEV Powertrain Modelling and Validation

The BEV model is developed with an aim to calculate the energy consumption and mainly takes into account the forward longitudinal movement of the vehicle. The Simulink based model can be described in two parts which are here referred to as separate model levels. The higher level or the level 1 consists of the main energy calculation system whereas the lower level or level 2 consists of the main components of the BEV and is itself a subsystem of level 1. In the following, the BEV model is described in detail with help of Figure A.1 and Figure A.2.

The Figure A.1 represents the level 2 diagram in Simulink. It consists of four main subsystems namely, the e-motor, the energy storage system (ESS) or battery, the vehicle acceleration calculator (Force) and the vehicle resistance calculator. The e-motor and the ESS has been already described in detail in previous sub-sections. The motor model is supplied with speed (ω), torque request and battery voltage as inputs. Taking the valid torque request as mechanical output torque at the speed (ω), the electrical power can be calculated by adding the losses. Since the voltage is known the current requirement for this torque request is calculated. The calculated current is supplied as an input to the battery (ESS) block. The vehicle resistance calculator is an important subsystem in the energy modeling. Different forces act on the vehicle while it is in motion. The torque supplied by the motors provides the force in the forward direction responsible for the acceleration of the vehicle. The brakes provide a torque in the opposite direction. Apart from the above forces, three other significant forces namely, air drag, rolling resistance and gradient force also must be taken into account. Table A.1 lists the notations that have been used to define the formulae for the forces and their corresponding energies.

The following ideology is used.

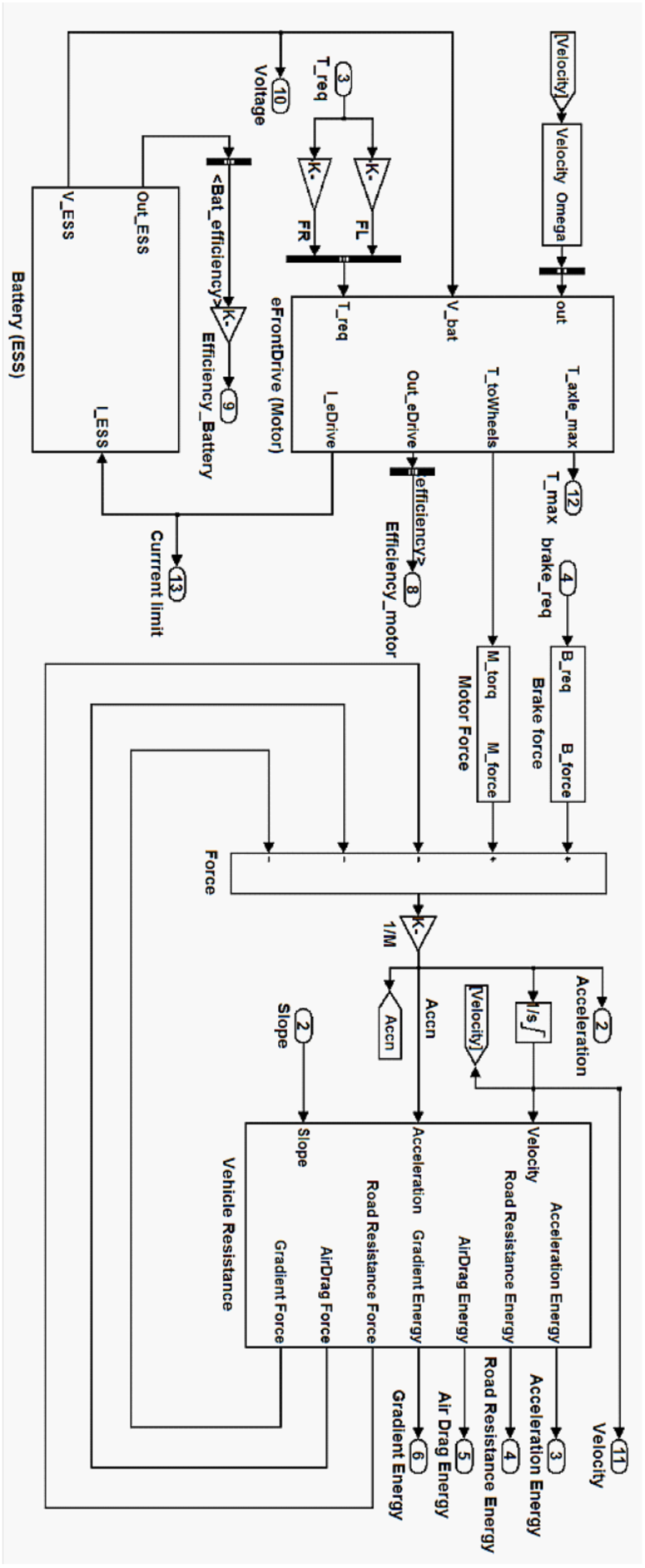


FIGURE A.1: Vehicle model subsystem (level 2)

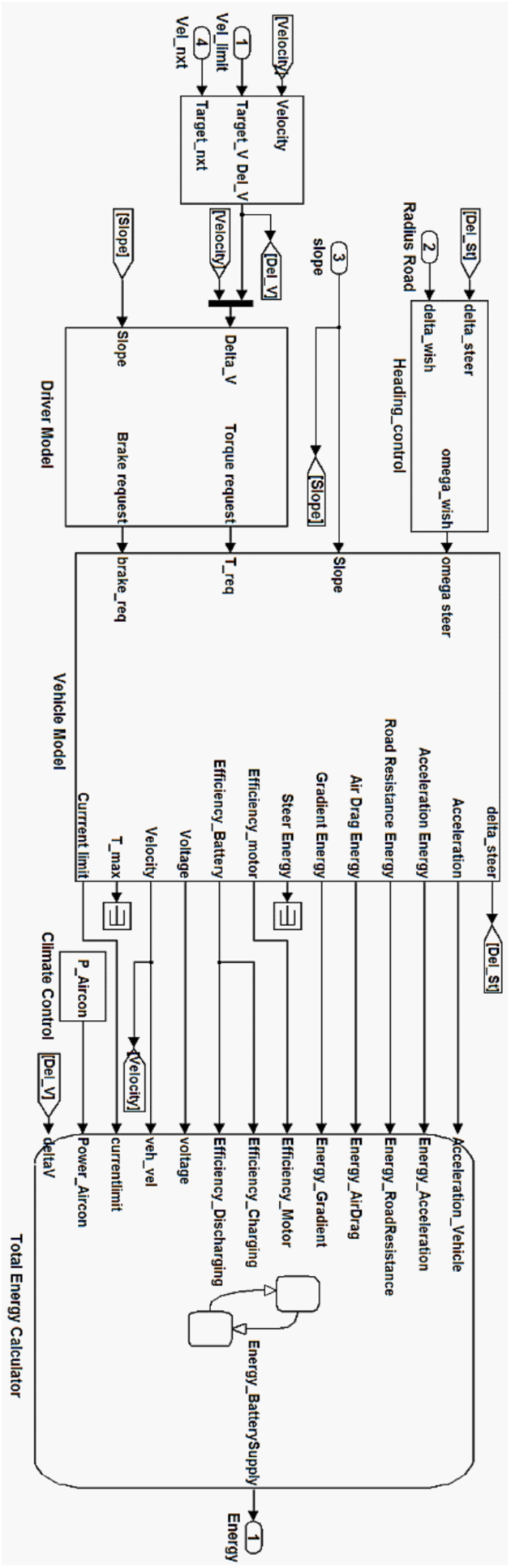


FIGURE A.2: BEV energy consumption model (level 1)

Vehicle mass	M	kg
Front area	A	m^2
Drag coefficient	C_w	-
Wheel radius	r	m
Co-efficient of rolling resistance	f_r	-
Vehicle acceleration	a	m/s^2
Vehicle veolcity	v_x	m/s
Energy	E_x	J
Force	F_x	N
Power	P	W
Air density	ρ	kg/m^3

TABLE A.1: Terminology

$$E_x = \int P_x \, dt \tag{A.1}$$

$$P_x = F_x \times v \tag{A.2}$$

The expressions for respective energies are derived as follows

$$F_{drag} = \frac{C_w \times \rho \times A \times v^2}{2} \tag{A.3}$$

$$E_{drag} = \frac{C_w \times \rho \times A \times \left(\frac{v_{initial} + v_{final}}{2}\right)^3 \times t}{2} \tag{A.4}$$

$$F_{roll} = M \times g \times f_r \tag{A.5}$$

$$E_{roll} = \frac{M \times g \times f_r \times (v_{initial} + v_{final}) \times t}{2} \tag{A.6}$$

$$F_{gradient} = M \times g \times \sin\beta \tag{A.7}$$

$$E_{gradient} = \frac{M \times g \times \sin\beta \times (v_{initial} + v_{final}) \times t}{2} \tag{A.8}$$

where, $v_{initial}$ and v_{final} are the velocities at the start and end of the sample time. This is done to reduce the error in integration.

The resultant force acting on the vehicle is the summation of the above forces. It is calculated in the block named "Force" in Figure A.1. Once the resultant force is known the acceleration of the vehicle and acceleration energy is calculated using the following formula.

$$F = m \times a \tag{A.9}$$

The level 1 or the higher level contains the main energy calculation. Figure A.2 represents the Simulink block diagram for level 1 where the main subsystems are the driver, the vehicle model (level 2) and the total energy calculator. The climate control subsystem calculates power required for heating or cooling depending on the cabin temperature of the vehicle as shown in Figure A.3. It is based on research paper from US Department of Energy on the climate control system power requirement of electric vehicles [ACI94].

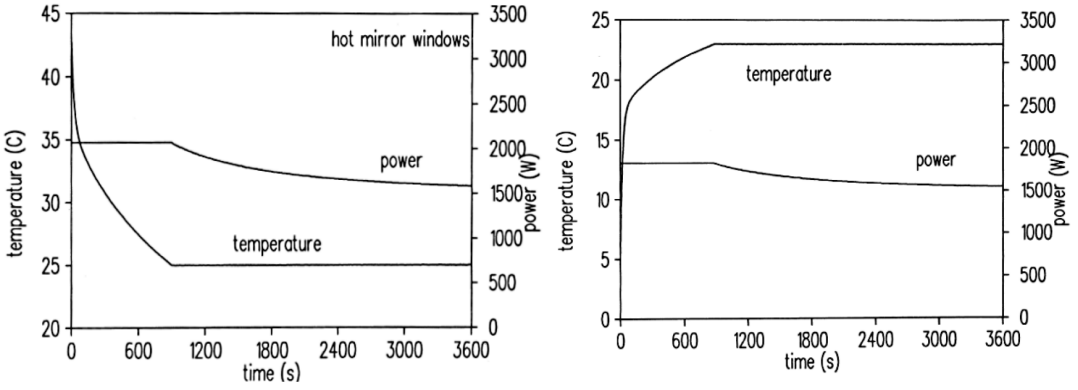


FIGURE A.3: Temperature-Power-time characteristics for cooling and heating

The driver model generates a torque or brake request depending on the velocity difference between the present and target velocity (δV). It also contains the regenerative braking

unit which is modeled according to the actual measurement values of the regenerative brakes of eFuture prototype. The motor is requested a minimum negative torque of -260 Nm depending on the δV and the present velocity (eFuture prototype settings). As the braking effect takes place and the velocity decreases, the regenerative brake request is also decreased gradually and at velocity values lower than 3 m/s no more negative torque is provided. The regenerative characteristics are adjusted as partial or full motor braking as per the simulation requirements. The driver model receives a set of distance dependent velocity limits and slope values. It generates torque and brake requests which are then supplied as input to e-motor in level 2. The vehicle model which was briefly discussed earlier, supplies various energy consumption values to the Stateflow block named "Total energy calculator". As the name suggests, the main function of this block is to calculate the final energy consumption of the vehicle taking into account all the different energies and the efficiencies at which they are being supplied as well as the power consumption of accessories. This block must differentiate between three states of the vehicle namely; acceleration or constant velocity, deceleration state where recuperation is possible and a unique state of deceleration where no recuperation is possible since the inertia of the vehicle is fully compensated by the negative forces from air drag, rolling resistance.

The BEV energy consumption model can calculate the energy requirement in kWh for a defined driving distance where velocity limits and slope values are specified. To validate this model, the simulation results were compared with the actual measurement of energy consumption values from the TATA eVista BEV which was the base for eFuture prototype. For this purpose real time values for velocity, battery current and voltage were measured during a test run. The BEV model was modified to directly accept time dependent velocity values as input instead of distance dependent velocity limits (backward looking model). The measured velocity values from the test run were supplied to the BEV model. The energy consumption values were compared as shown in Figure A.4. The measured and simulated curves considerably match, thus validating the model. Owing to several factors like exact air velocity at test track, battery temperature and state or even repeatability of measuring system a higher level of tolerance must be considered in energy consumption simulations.

Figure A.5 represents the simulation results for the BEV energy consumption model. For the purpose of further evaluation of a SAGA function, a non-standard urban velocity limit pattern is defined as seen in the first (topmost) plot in Figure A.5.

The velocity limits fluctuate between 50 kph to 30 kph corresponding to the speed limits of residential and built-up areas. The dotted line represents how the driver model follows the velocity limit. The corresponding torque supplied by the e-motor model is as shown in the second graph. The torque characteristics reflect the acceleration and recuperation

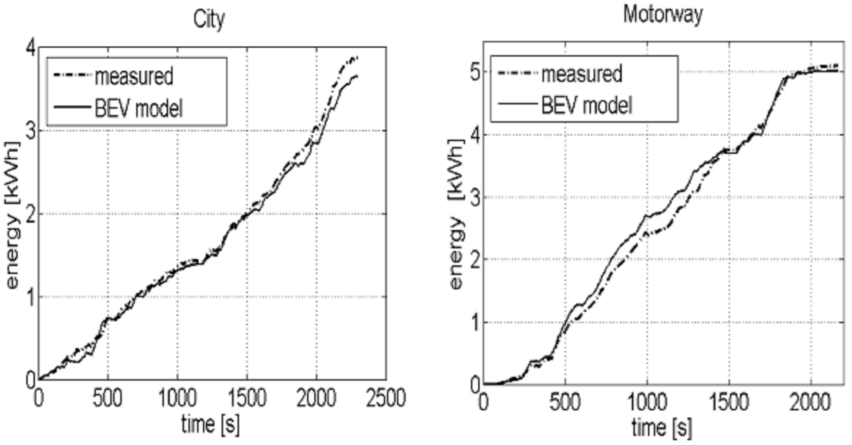


FIGURE A.4: BEV model validation results

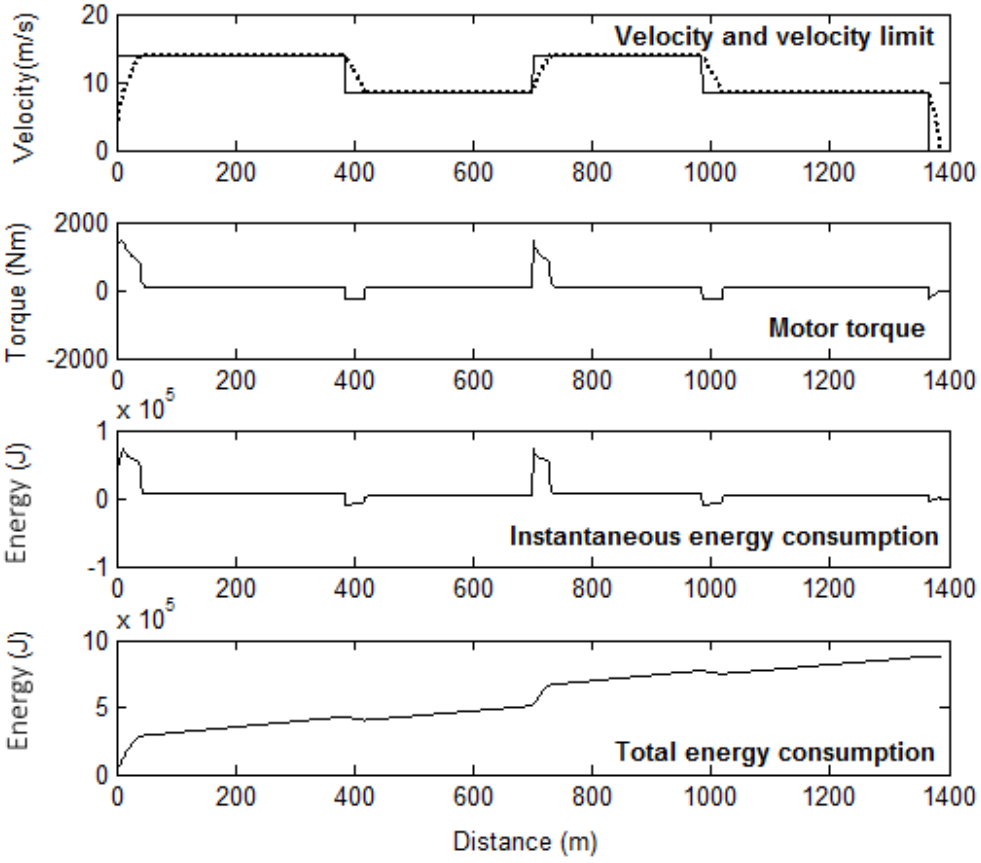


FIGURE A.5: BEV energy calculation simulation

phases where negative torque up to -260 Nm is applied by the e-motor. The remaining brake force is supplied by the brake model making total braking torque of -750 Nm. The total energy consumption is calculated by summation of the instantaneous energy consumption which is calculated in a particular sample time chosen by Simulink solver. These two values can be observed in the remaining graphs in the figure. Finally for a 1400 m distance, the model returns an energy consumption value of approximately 8.7 $\times 10^5$ J i.e. 0.24 kWh. If a 24 kWh battery is considered then this shall result in a driving range of almost 140 km. It is however notable that the range of a BEV is drastically affected by usage of climate control system and type of drive profile. In case of normal temperatures and constant 40 kph driving the range may cross 160 km whereas in case of an extreme hot/cold day with high speed or high acceleration/deceleration driving range may not exceed 120 km.

Bibliography

[A12] A123 Systems, Inc. *Nanophosphate® High Power Lithium Ion Cell AHR32113 M1 UltraB.*

[ACC10] *Intelligent transport systems – Adaptive Cruise Control systems – Performance requirements and test procedures*, iso 15622:2010 edition, 2010.

[ACI94] Salvador M Aceves and WJ Comfort III. Load calculation and system evaluation for electric vehicle climate control. In *Presented at the Society of Automotive Engineers International Congress and Exposition, Detroit, MI, 27 Feb.-2 Mar. 1995*, volume 1, 1994.

[AGNH13] Sagar Akhegaonkar, Sebastien Glaser, Lydie Nouveliere, and Frederic Holzmann. Smart and green acc series: A city and highway specific approach towards a safe and efficient edas. In *EVS-27, Barcelona, Spain, November 17-20*, 2013.

[AGNH14] Sagar Akhegaonkar, Sebastien Glaser, Lydie Nouveliere, and Frederic Holzmann. Smart and green acc: As applied to a through the road hybrid electric vehicle. In *Advanced Microsystems for Automotive Applications 2014*, pages 15–27. Springer, 2014.

[air] Audi Sport air tunnel Retrieved 2014-10-24. Available at http://galerie.designnation.de/bild/35106.

[Akh11] Sagar Akhegaonkar. Energy management of battery electric vehicles. Master's thesis, Institut für Kraftfahrzeuge, RWTH Aachen University, 2011.

[And04] Michel André. The artemis european driving cycles for measuring car pollutant emissions. *Science of the total Environment*, 334:73–84, 2004.

[ANP+12] Sagar Akhegaonkar, Lydie Nouvelière, Roman Potarusov, Volker Scheuch, Frédéric Holzmann, and Sébastien Glaser. Modeling and simulation of battery electric vehicle to develop an energy optimization algorithm. AVEC, 2012.

[ARC] Ecosm12, ArcoMerano matfile, Retrieved 2014-01-21. Available at http://www.ecosm12.org/node/21.

[bata] HEV Vehicle Battery Types. Retrieved 2014-03-25. Available at http://www.thermoanalytics.com/support/publications/batterytypesdoc.html.

[batb] Nissan Leaf Forum. Retrieved 2014-08-13. Available at http://www.mynissanleaf.com/viewtopic.php?f=27&t=12781&sid=6f66355df77d847f50aa8234a6b222f2.

[batc] Nissan Leaf Forum. Retrieved 2014-08-13. Available at http://www.mynissanleaf.com/viewtopic.php?f=4&t=17168.

[batd] Nissan OEM Prices and Equipment. Retrieved 2014-08-13. Available at http://www.nissan.de/DE/de/vehicle/electric-vehicles/leaf/prices-and-equipment/prices-and-specifications.html.

[BCM99] S. Burch, M. Cuddy, and T. Markel. *ADVISOR 2.1 Documentation*. Nat. Renewable Lab., 1999.

[Bel54] Richard Bellman. The theory of dynamic programming. Technical report, DTIC Document, 1954.

[BG+10] Kamil Cagatay Bayindir, Mehmet Ali Gözükücük, et al. A comprehensive overview of hybrid electric vehicle: Powertrain configurations, powertrain control techniques and electronic control units. *Energy Conversion and Management*, 52:1305–1313, October 2010.

[BM+12] Bertozzi, Massimo, et al. Equipment and capabilities of the vehicles for the VisLab intercontinental autonomous challenge. In *Proc. GIRPR*, 2012.

[BS98] WD BECK and J Speer. Der aktuelle bundeseinheitliche verwarnungs-und bußgeldkatalog mit erläuterungen. 8. *Auflage, ADAC-Verlag, München*, 1998.

[BWGR00] B. M. Baumann, G. Washington, B. C. Glenn, and G. Rizzoni. Mechatronic design and control of hybrid electric vehicles,. *EEE/ASME Trans. Mechatronics,*, 5(1):58–71, March 2000.

[BZP13] Danijela Barić, Goran Zovak, and Marko Periša. Effects of eco-drive education on the reduction of fuel consumption and co2 emissions. *PROMET-Traffic&Transportation*, 25(3):265–272, 2013.

[CCS08] Man-Feng Chang, Jyh-Shin Chen, and Mutasim A Salman. Predictive energy management system for hybrid electric vehicles, April 22 2008. US Patent 7,360,615.

[DAB14] J. Dickmann, N. Appenrodt, and C. Brenk. Making bertha. *Spectrum, IEEE*, 51(8):44–49, August 2014.

[Def08] Kenneth S. Deffeyes. *Hubbert's Peak: The Impending World Oil Shortage (New Edition)*. Princeton University Press, 2008.

[DGR02] Sebastien Delprat, Thierry-Marie Guerra, and Janette Rimaux. Optimal control of a parallel powertrain: from global optimization to real time control strategy. In *Vehicular Technology Conference, 2002. VTC Spring 2002. IEEE 55th*, volume 4, pages 2082–2088. IEEE, 2002.

[Dij59] Edsger W Dijkstra. A note on two problems in connexion with graphs. *Numerische mathematik*, 1(1):269–271, 1959.

[dJvKK13] Bram de Jager, Thijs van Keulen, and John Kessels. *Optimal control of hybrid vehicles*. Springer, 2013.

[DLGR04] Sebastien Delprat, Jimmy Lauber, Thierry-Marie Guerra, and Janette Rimaux. Control of a parallel hybrid powertrain: optimal control. *Vehicular Technology, IEEE Transactions on*, 53(3):872–881, 2004.

[DZ87] Ernst Dieter Dickmanns and Alfred Zapp. A curvature-based scheme for improving road vehicle guidance by computer vision. In *Cambridge Symposium_Intelligent Robotics Systems*, pages 161–168. International Society for Optics and Photonics, 1987.

[ecoa] "ecoDriver Project" official website. Retrieved 2014-03-25. Available at http://www.ecodriver-project.eu.

[ecob] "eCoMove Project" official website. Retrieved 2014-03-25. Available at http://www.ecomove-project.eu.

[efu] "eFuture Project" official website. Retrieved 2014-03-25. Available at http://www.efuture-eu.org/.

[EHZM06] B Eckardt, A Hofmann, S Zeltner, and M Maerz. Automotive powertrain dc/dc converter with 25kw/dm (exp3) by using sic diodes. In *Integrated Power Systems (CIPS), 2006 4th International Conference on*, pages 1–6. VDE, 2006.

[eur] "EUREKA Project E45 PROMETHEUS". EUREKA website. Retrieved 2014-03-25. Available at [1]"EUREKAProjectE45PROMETHEUS". EUREKAwebsite.

[FS12] Henrik Fridén and Hanna Sahlin. Energy management strategies for plug-in hybrid electric vehicles. 2012.

[ftNTES06] National Research Council (US). Transportation Research Board. Committee for the National Tire Efficiency Study. *Tires and Passenger Vehicle Fuel Economy: Informing Consumers, Improving Performance*, volume 286. Transportation Research Board, 2006.

[GAI09] GAIA Advanced Lithium Battery Systems, Nordhausen Germany. *HP 601300 LFP 18Ah/58 Wh Lithium Ion Cell*, August 2009. Available at http://www.gaia-akku.com/fileadmin/user_upload/downloads/Handhabungshinweis_HP601300LFP-18Ah.58Wh.pdf.

[GAO+13] Sebastien Glaser, Sagar Akhegaonkar, Olivier Orfila, Lydie Nouveliere, Volker Scheuch, and Frederic Holzmann. Smart and green acc, safety and efficiency for a longitudinal driving assistance. In *Advanced Microsystems for Automotive Applications 2013*, pages 123–133. Springer, 2013.

[Gee07] Hans P Geering. *Optimal control with engineering applications*. Springer, 2007.

[GHG11] The contribution of transport to ghg emissions. Technical report, EU Transport GHG: Routes to 2050 project, 2011. Available at http://www.eutransportghg2050.eu/cms/the-contribution-of-transport-to-ghg-emissions/.

[GHG13] Global greenhouse gas emissions data. Technical report, United States Environmental Protection Agency, 2013. Available at http://www.epa.gov/climatechange/ghgemissions/global.html.

[GRO12] JENS GROOT. *State-of-Health Estimation of Li-ion Batteries: Cycle Life Test Methods*. PhD thesis, Department of Energy and Environment, CHALMERS UNIVERSITY OF TECHNOLOGY, Göteborg, Sweden, 2012.

[IEO14] International energy outlook 2014: World petroleum and other liquid fuels with projections to 2040. Technical Report DOE/EIA-0484(2014), U.S. Energy Information Administration, September 2014. Available at http://www.eia.gov/forecasts/ieo/pdf/0484(2014).pdf.

[JWR00] V. H. Johnson, K. B. Wipke, and D. J. Rausen. Hev control strategy for realtime optimization off uel economy and emissions. *SAE paper*, (1543), 2000.

[Kam] Raj Kishore Kamalanathsharma. Acceleration and Deceleration Characteristics of Vehicles at Intersections – A Literature Review Retrieved 2014-10-24. Available at http://filebox.vt.edu/users/rkishore/pdf/resources/AccelDecelTable.pdf.

[KDN+07] MC Knauff, Chris J Dafis, Dagmar Niebur, Harry G Kwatny, and CO Nwankpa. Simulink model for hybrid power system test-bed. In *Electric Ship Technologies Symposium, 2007. ESTS'07. IEEE*, pages 421–427. IEEE, 2007.

[Klu94] Karl Kluge. Extracting road curvature and orientation from image edge points without perceptual grouping into features. In *Intelligent Vehicles' 94 Symposium, Proceedings of the*, pages 109–114. IEEE, 1994.

[KR08] Paul Kompfner and Wolfgang Reinhardt. ICT for clean and efficient mobility, final report. Technical report, ERTICO-ITS Europe and ACEA, November 2008. Brussels.

[KTSH07] Arne Kesting, Martin Treiber, Martin Schönhof, and Dirk Helbing. Extending adaptive cruise control to adaptive driving strategies. *Transportation Research Record: Journal of the Transportation Research Board*, 2000(1):16–24, 2007.

[LA+11] J. Levinson, J. Askeland, et al. Towards fully autonomous driving: Systems and algorithms. In *Proc. IEEE Intelligent Vehicles Symposium (IV)*, page 163–168, 2011.

[LH+08] John Leonard, Jonathan How, et al. A perception-driven autonomous urban vehicle. *Journal of Field Robotics*, pages 1–48, 2008.

[LNM10] Hong Tu Luu, Lydie Nouveliere, and Saïd Mammar. Ecological and safe driving assistance system: Design and strategy. In *Intelligent Vehicles Symposium (IV), 2010 IEEE*, pages 129–134. IEEE, 2010.

[LPG04] Chan-Chiao Lin, Huei Peng, and JW Grizzle. A stochastic control strategy for hybrid electric vehicles. In *American Control Conference, 2004. Proceedings of the 2004*, volume 5, pages 4710–4715. IEEE, 2004.

[LPGK03] Chan-Chiao Lin, Huei Peng, Jessy W Grizzle, and Jun-Mo Kang. Power management strategy for a parallel hybrid electric truck. *Control Systems Technology, IEEE Transactions on*, 11(6):839–849, 2003.

[LS98] H.-D. Lee and S.-K. Sul. Fuzzy-logic-based torque control strategy for parallel-type hybrid electric vehicle. *IEEE Trans. Ind. Electron*, 45(4):625–632, August 1998.

[MB12] Akhilesh Kumar Maurya and Prashant Shridhar Bokare. Study of deceleration behaviour of different vehicle types. *International Journal for Traffic and Transport Engineering*, 2(3):253–270, 2012.

[MBI] Mercedes Benz Intelligent Drive System, Retrieved 2015-01-21. Available at http://http://www.mercedes-benz-intelligent-drive.com.

[MMB01] Greg Marsden, Mike McDonald, and Mark Brackstone. Towards an understanding of adaptive cruise control. *Transportation Research Part C: Emerging Technologies*, 9(1):33–51, 2001.

[MMY09] Seungwuk Moon, Ilki Moon, and Kyongsu Yi. Design, tuning, and evaluation of a full-range adaptive cruise control system with collision avoidance. *Control Engineering Practice*, 17(4):442–455, 2009.

[MRGS05] Cristian Musardo, Giorgio Rizzoni, Yann Guezennec, and Benedetto Staccia. A-ecms: An adaptive algorithm for hybrid electric vehicle energy management. *European Journal of Control*, 11(4):509–524, 2005.

[NSC+10] Christopher Nowakowski, Steven E Shladover, Delphine Cody, Fanping Bu, Jessica O'Connell, John Spring, Susan Dickey, and David Nelson. *Cooperative Adaptive Cruise Control: Testing Drivers' Choices of Following Distances*. California PATH Program, Institute of Transportation Studies, University of California at Berkeley, 2010.

[NSW09] Magnus Neuman, Henrik Sandberg, and Bo Wahlberg. Rule-based control of series hevs derived from deterministic dynamic programming. In *Submitted to American Control Conference*, 2009.

[NVP+09] Gerrit Naus, René Vugts, Jeroen Ploeg, René van de Molengraft, and Maarten Steinbuch. Cooperative adaptive cruise control. In *IEEE automotive engineering symposium Eindhoven, The Netherlands*, volume 6, 2009.

[OS11] Simona Onori and Lorenzo Serrao. On adaptive-ecms strategies for hybrid electric vehicles. In *Proceedings of the International Scientific Conference on Hybrid and Electric Vehicles, Malmaison, France*, pages 6–7, 2011.

[Pac69] SJ Pachernegg. A closer look at the willans-line. Technical report, SAE Technical Paper, 1969.

[PDG+02] Gino Paganelli, Sebastien Delprat, Thierry-Marie Guerra, Janette Rimaux, and Jean-Jacques Santin. Equivalent consumption minimization strategy for parallel hybrid powertrains. In *Vehicular Technology Conference, 2002. VTC Spring 2002. IEEE 55th*, volume 4, pages 2076–2081. IEEE, 2002.

[PKR05] Pierluigi Pisu, Kerem Koprubasi, and Giorgio Rizzoni. Energy management and drivability control problems for hybrid electric vehicles. In *Decision and Control, 2005 and 2005 European Control Conference. CDC-ECC'05. 44th IEEE Conference on*, pages 1824–1830. IEEE, 2005.

[PSRS03] Pierluigi Pisu, Enrico Silani, Giorgio Rizzoni, and Sergio M Savaresi. A lmi-based supervisory robust control for hybrid vehicles. In *American Control Conference, 2003. Proceedings of the 2003*, volume 6, pages 4681–4686. IEEE, 2003.

[RWRG03] A. Rajagopalan, G. Washington, G. Rizzoni, and Y. Guezennec. Development of fuzzy logic control and advanced emissions modelling for parallel hybrid vehicles. Technical Report NREL/SR-540-32919, NREL Tech. Rep, December 2003.

[S+10] Paul Sankey et al. The end of the oil age 2011 and beyond: a reality check. Technical report, Deutsche Bank, December 2010. Available at http://http://bioage.typepad.com/files/1223fm-05.pdf.

[SAE14] SAE. Automated driving: Levels of driving automation, sae international standard j3016. 2014.

[Sal07] Farzad Rajaei Salmasi. Control strategies for hybrid electric vehicles: Evolution, classification, comparison, and future trends. *IEEE TRANSACTIONS ON VEHICULAR TECHNOLOGY*, 56(5), 2007.

[SBG04] Antonio Sciarretta, Michael Back, and Lino Guzzella. Optimal control of parallel hybrid electric vehicles. *Control Systems Technology, IEEE Transactions on*, 12(3):352–363, 2004.

[SE] Roman Staszewski and Hannes Estl. "Making cars safer through technology innovation. Retrieved 2014-03-25. Available at http://www.ti.com/lit/wp/sszy009/sszy009.pdf.

[SOR09] Lorenzo Serrao, Simona Onori, and Giorgio Rizzoni. Ecms as a realization of pontryagin's minimum principle for hev control. In *Proceedings of the 2009 conference on American Control Conference*, pages 3964–3969. IEEE Press, 2009.

[SSG+13] Lorenzo Serrao, Antonio Sciarretta, Olivier Grondin, Alexandre Chasse, Yann Creff, Domenico Di Domenico, Philippe Pognant-Gros, Carole Querel, and Laurent Thibault. Open issues in supervisory control of hybrid electric vehicles: a unified approach using optimal control methods. *Oil & Gas Science and Technology–Revue d'IFP Energies nouvelles*, 68(1):23–33, 2013.

[TB00] Edward D Tate and Stephen P Boyd. Finding ultimate limits of performance for hybrid electric vehicles. Technical report, SAE Technical Paper, 2000.

[VAvDV06] Bart Van Arem, Cornelie JG van Driel, and Ruben Visser. The impact of cooperative adaptive cruise control on traffic-flow characteristics. *Intelligent Transportation Systems, IEEE Transactions on*, 7(4):429–436, 2006.

[vda] Automated driving, Retrieved 2014-01-21. Available at https://www.vda.de/en/topics/innovation-and-technology/automated-driving.html.

[VE03] Ardalan Vahidi and Azim Eskandarian. Research advances in intelligent collision avoidance and adaptive cruise control. *Intelligent Transportation Systems, IEEE Transactions on*, 4(3):143–153, 2003.

[vol13] European accident research and safety report 2013. Technical report, Volvo Trucks, 2013. Available at http://www.pvst.com.br/wp-content/uploads/2014/04/ARTreport2013.pdf.

[Whe] Tire Rolling Resistance Retrieved 2014-10-24. Available at http://www.rouesartisanales.com/article-1503651.html.

[wlt] Worldwide harmonized Light vehicles Test Procedure Retrieved 2014-10-24. Available at http://www.unece.org.

[YAS] YASA motors. *YASA-250*. Available at http://www.yasamotors.com/products/yasa-250/.